

PHASE TRANSFORMATION AND HEAT TREATMENT

**SUBJECT CODE: MTPC2005
COURSE: B. TECH
SEMESTER: 4th**



***LECTURES NOTE BY:
Mr. Rahul Ranjan Mohanta
(Assistant Professor)***

**DEPARTMENT OF METALLURGICAL AND MATERIALS ENGINEERING
PARALA MAHARAJA ENGINEERING COLLEGE, BERHAMPUR**

DISCLAIMER

This document does not claim originality and cannot be used as a substitute for prescribed textbooks. The information presented here is merely a collection by the author for their respective teaching assignments as an additional tool for the teaching-learning process. Various sources as mentioned in the document's reference and freely available material from the internet were consulted for preparing this document. The ownership of the information lies with the respective author or institution. Further, this document is not intended to be used for commercial purposes and the faculty is not accountable for any legal or otherwise issues arising from this document's use. The committee faculty members make no representations or warranties with respect to the accuracy or completeness of the contents of this document and specifically disclaim any implied warranties of merchantability or fitness for a particular purpose.

MTPC2005 PHASE TRANSFORMATION AND HEAT TREATMENT OF METALS (3-0-0)

Course Objective:

1. To provide students with a comprehensive understanding of the thermodynamic and kinetic principles governing phase transformations in materials, including nucleation, growth, and the role of phase diagrams in predicting microstructural evolution.
2. To equip students with the knowledge and practical skills required to design and apply heat treatment techniques, such as annealing, quenching, tempering, and surface hardening, to achieve desired mechanical and microstructural properties in metals and alloys.

Module I (6 Hrs)

Introduction: Definition and types of Phase transformations, Free Energy for Ideal solution and regular solution, free energy composition diagrams, Spinodal decomposition, Miscibility gap; Ternary Phase Diagram.

Module-II (6 Hrs)

Order-disorder Transformation examples of ordered structures, long range and short range order. influence of ordering on properties. Crystal interfaces and microstructure. Microstructure evolution including recrystallization and grain growth.

Module III (6 Hrs)

Review of Iron-carbon alloy system, Graphitization, Importance of Austenite Grain size. Formation of Austenite, Pearlitic, Bainitic and Martensitic Transformations (Mechanisms, Kinetics and Morphologies)

Module IV (6 Hrs)

Heat treatment of steels: TTT and CCT diagrams, conventional heat treatment processes – annealing, normalizing, hardening and tempering. Hardenability, Factors influencing hardenability, Methodology.

Module V (6 Hrs)

Surface heat Treatment Process: Heat treatment of non-ferrous alloys (Al-Cu, brass, Ti alloys, Ni alloys), Heat treatment of special steel(maraging steel, HSLA)

Course Outcome:

- CO1: Students will be able to explain the fundamental concepts of phase transformations, interpret free energy diagrams, and analyze spinodal decomposition, miscibility gaps, and ternary phase diagrams.
- CO2: Students will understand order-disorder transformations, evaluate their influence on material properties, and analyze microstructure evolution processes such as recrystallization and grain growth.
- CO3: Students will demonstrate the ability to analyze the iron-carbon system, understand graphitization, and describe pearlitic, bainitic, and martensitic transformations in terms of mechanisms, kinetics, and morphologies.
- CO4: Students will gain the skills to interpret TTT and CCT diagrams, design conventional heat treatment processes, and evaluate factors influencing the hardenability of steels.
- CO5: Students will be able to apply surface heat treatment processes, understand heat treatment techniques for non-ferrous alloys, and analyze the treatment of special

steels like maraging steel and HSLA.

Text Books:

1. "Phase Transformations in Metals and Alloys" by David A. Porter, Kenneth E. Easterling, and Mohamed Sherif
2. "Heat Treatment: Principles and Techniques" by T.V. Rajan, C.P. Sharma, and Ashok Sharma

Reference Books:

1. "Physical Metallurgy Principles" by Robert E. Reed-Hill and Reza Abbaschian
2. "Introduction to Materials Science for Engineers" by James F. Shackelford
3. "Solid State Phase Transformations" by Raghavan, PHI

LESSON PLAN : PHASE TRANSFORMATION & HEAT TREATMENT (PTHT)

Module I	Lecture 1	Introduction: Thermodynamics of phase equilibrium and phase changes
	Lecture 2	Thermodynamics of phase equilibrium and phase changes (continued...)
	Lecture 3	Definition, utility, order and classification of phase transformations.
	Lecture 4	Diffusion, Definition of Fick's law on steady and non-steady state diffusion
	Lecture 5	Solutions to Ficks second law of diffusion; Mechanism of diffusion in solids.
	Lecture 6	Chemical diffusion- Kirkendall effect, Darken's analysis
	Lecture 7	Effect of pressure and temperature on diffusivity
	Lecture 8	Nucleation and growth: Formation of nucleus; Homogeneous and Heterogeneous nucleation
	Lecture 9	Mechanism and kinetics of thermally activated growth; Interface controlled growth
	Lecture 10	Mechanism and kinetics of diffusion control growth regimes
	Lecture 11	Phase equilibrium and phase diagrams: Important phase changes in unary and binary systems, Isomorphous and eutectic Systems
	Lecture 12	Types and interpretation of phase diagram; Utility of phase diagrams; Important phase diagrams in metallic and ceramic systems
	Lecture 13	Lever rule, Free energy Composition diagrams,
	Lecture 14	Ternary phase diagrams .
Module II	Lecture 15	Liquid-solid transformation: Solidification, nucleation and growth mechanisms and kinetics
	Lecture 16	Alloy solidification – cellular and dendritic morphology
	Lecture 17	Eutectic and peritectic solidification. Application of solidification
	Lecture 18	Solid state diffusive transformation: Classification of solid-solid transformations; Nucleation in solids,
	Lecture 19	Precipitate growth; Age hardening
	Lecture 20	Spinodal decomposition; Precipitate coarsening
	Lecture 21	Order-disorder change, polymorphic change
	Lecture 22	Recovery, Recrystallization
	Lecture 23	Grain growth
	Lecture 24	Eutectoid transformation. Application of solid state precipitation
	Lecture 25	Pearlitic and bainitic transformations in steel;
	Lecture 26	Martensite and martensitic changes in ferrous materials.

Module III	Lecture 27	Review of Iron-carbon alloy system: Iron-cementite and iron-graphite phase diagrams
	Lecture 28	Cooling of hypo-eutectoid, eutectoid and hyper-eutectoid steels
	Lecture 29	Cooling of hypo-eutectic, eutectic and hyper-eutectic cast irons, nucleation and growth of pearlite
	Lecture 30	Heat treatment of steels: TTT and CCT diagrams
	Lecture 31	Conventional heat treatment processes – annealing, normalizing
	Lecture 32	Hardening and Tempering
	Lecture 33	Hardenability, role of alloying elements in steels
	Lecture 34	Surface hardening in steels
	Lecture 35	Chemical treatment in steels
	Lecture 36	Thermo-mechanical treatment of steels; High temperature and low temperature Thermo-Mechanical treatment
	Lecture 37	Heat treatment of some Cu, Al and Ti based alloys.
	Lecture 38	Heat treatment of some Cu, Al and Ti based alloys (continued...)

→ Atoms move only over one or two inter atomic distances from parent phase to product phase across an interface.

2) Long range diffusion:

→ Compositional changes

→ Atoms move through several thousands of inter atomic distances.

Two basic mechanisms of Phase Transformations:

1) ***Nucleation and Growth mechanism:*** A tiny particle identical in structure and composition to the product phase nucleates and then grows in size.

2) ***Spinodal Decomposition:*** Compositional fluctuations occur in parent phase and then grow in intensity with time, until two discrete phases corresponding to equilibrium compositions form.

Nucleation may be:

- 1) Homogenous Nucleation
- 2) Heterogenous Nucleation.

(To be covered later in detail in other chapter.)

Gibb's Phase Rule : $F = C - P + 2$

(Applicable only to systems under conditions of true equilibrium)

Where,

C → number of components in system

P → no. of phases in equilibrium

F → Degrees of Freedom → the maximum no. of variables that may be independently varied without changing no. of phases in equilibrium.

When $F = 0$, $P = C + 2$ → maximum no. of phases that can be simultaneously present in equilibrium in a system.

$F = C - P + 1$ → Condensed Phase Rule for binary systems at fixed pressure of 1 atm.

Thermodynamic order of Transformations:

Transformations can be classified as 1st order, 2nd order.... etc. depending on how Gibbs Free Energy G changes with external parameters of temperature and pressure.

1) First – order Transformations:

Here, Gibbs free energy changes continuously through a phase transformation at equilibrium temperature T_0 and Pressure P_0 for an $\alpha \rightarrow \beta$ transformation.

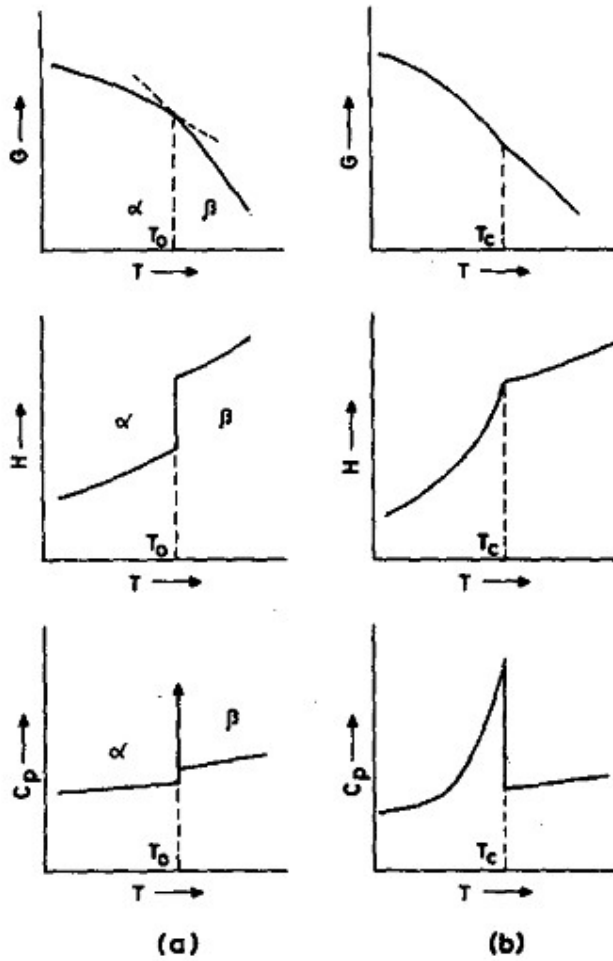


Fig. Variation of Gibb's free energy (G), enthalpy (H) and specific heat (C_p) in vicinity of transition temperature for a (a) first order and (b) second order transformation

Free energy curve changes slope abruptly at T_0 or P_0 i.e. first derivatives of G w.r.t Temperature and Pressure have discontinuities.

First derivatives of Gibbs Energy are :

$$\left(\frac{\partial G}{\partial T}\right)_P = -S \quad \text{or} \quad \left(\frac{\partial(G/T)}{\partial(1/T)}\right)_P = H$$

$$\left(\frac{\partial G}{\partial P}\right)_T = V$$

Lecture 2

Necessary criterion for any Phase transformation is:

Free energy change, $\Delta G = G_2 - G_1 < 0$

Where, $G_1, G_2 \rightarrow$ free energies of initial and final states.

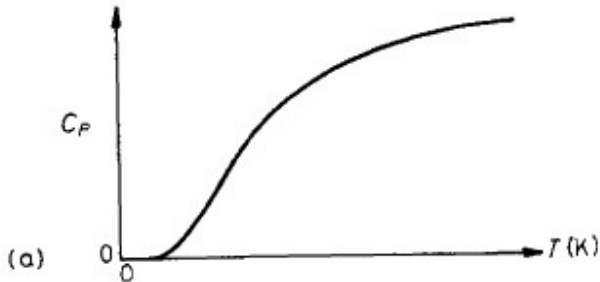
Single Component System:

Phase change in single component system by change in temperature at fixed pressure = 1 atm.

1. Calculate variation of Gibbs free energy G with temperature T:

$$C_P = \left(\frac{\partial H}{\partial T} \right)_P \text{----- (1)}$$

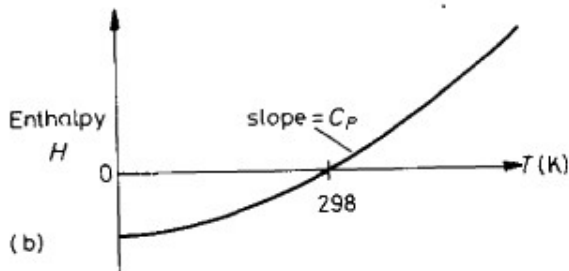
Where, $C_p \rightarrow$ specific heat at constant pressure.



Variation of Enthalpy H with T is given by,

Integrating eqn (1) we get,

$$H = \int_{298}^T C_P dT \text{----- (2)}$$



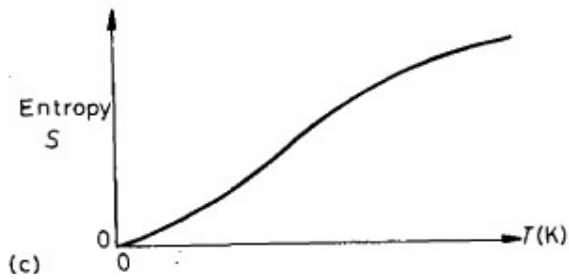
Variation of Entropy with Temperature is given by,

$$\frac{C_p}{T} = \left(\frac{dS}{dT} \right)_p \quad \text{----- (3)}$$

Entropy at Absolute zero i.e. 0 K = 0

Integrating eqn (3) we get,

$$S = \int_0^T \frac{C_p}{T} dT \quad \text{----- (4)}$$



Variation of G with temperature is given by combining fig. (b) & (c)

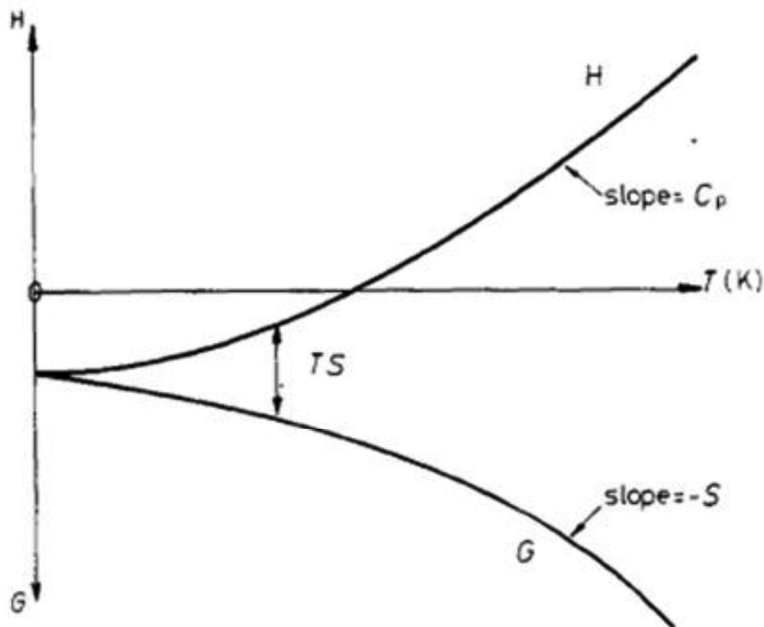


Fig. Variation of Gibb's free energy with temperature

For a Fixed mass & Composition at variable Temperature & Pressure,

Maxwell's Relation:

$$dG = -SdT + VdP \quad \text{----- (5)}$$

At constant P, $dP = 0$,

$$\left(\frac{\partial G}{\partial T}\right)_P = -S \quad \text{----- (6)}$$

=> G decreases with increasing T at a rate given by $-S$.

Gibbs free energy of liquid decreases more rapidly with increasing temperature than that of solid.

At T_m (Equilibrium melting temperature) both phase (solid & liquid) have same value of G & both solid and liquid can exist in equilibrium.

2. Pressure Effects:

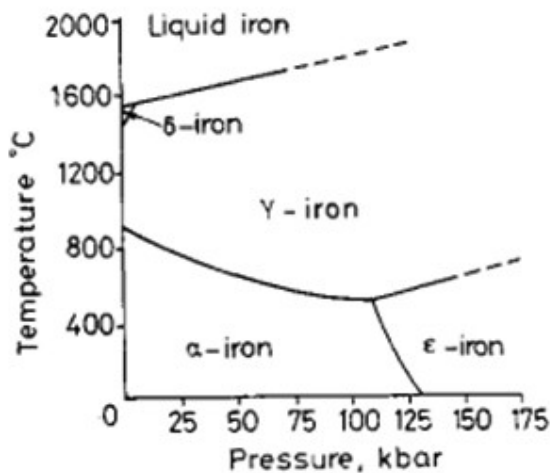


Fig. Effect of pressure on the equilibrium phase diagram of pure iron

Increasing pressure decreases α/γ equilibrium temperature and raises equilibrium melting temperature. At very high pressure hcp ϵ -Fe becomes stable.

At constant T, free energy of phase increases with Pressure,

$$\left(\frac{\partial G}{\partial P}\right)_T = V \quad \text{----- (7)}$$

If two phases in equilibrium are α and β , then apply eqn (5) to 1 mole of both α and β gives,

$$\begin{aligned} dG^\alpha &= V_m^\alpha dP - S^\alpha dT \\ dG^\beta &= V_m^\beta dP - S^\beta dT \end{aligned} \quad \text{----- (8)}$$

For equilibrium, $G^\beta = G^\alpha$, $\Delta G = 0$, and $\Delta H - T\Delta S = 0$, so

$$\left(\frac{dP}{dT}\right)_{eq} = \frac{S^\beta - S^\alpha}{V_m^\beta - V_m^\alpha} = \frac{\Delta S}{\Delta V} \quad \text{----- (9)}$$

We know,

$$\begin{aligned} G^\alpha &= H^\alpha - TS^\alpha \\ G^\beta &= H^\beta - TS^\beta \end{aligned}$$

putting $\Delta G = G^\beta - G^\alpha$ etc. gives

$$\Delta G = \Delta H - T\Delta S \quad \text{----- (10)}$$

But since at equilibrium $G^\beta = G^\alpha$, $\Delta G = 0$, and

$$\Delta H - T\Delta S = 0$$

$$\left(\frac{dP}{dT_{eq}}\right) = \frac{\Delta H}{T_{eq}\Delta V} \quad \text{----- (11)}$$

Clausius- Clapeyron Equation

Gives rate of change of Transformation temperature as a function of Pressure.

γ -Fe has smaller molar volume than α -Fe. So

$$\Delta \bar{V} = V_m^\gamma - V_m^\alpha < 0 \quad \text{but}$$

$$\Delta H = H^\gamma - H^\alpha > 0 \quad (\text{since liquid has higher enthalpy than solid})$$

So,

(dP/dT) is negative.

Thus increase in Pressure lowers equilibrium transition temperature.

But the δ/L equilibrium temperature is raised with increasing Pressure due to larger molar volume of liquid phase.

Lecture 3

Thermodynamics of phase equilibrium and phase changes (continued...)

Binary Solutions:

Here three variables: Composition, Temperature, Pressure is present

$$X_A + X_B = 1$$

$$G_1 = X_A G_A + X_B G_B \quad \text{J mol}^{-1}$$

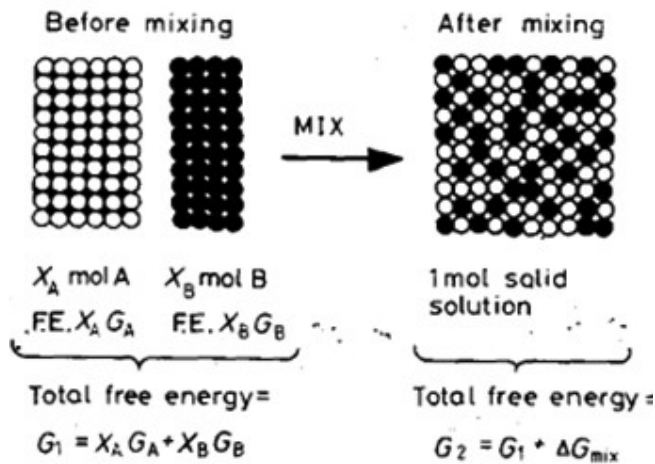


Fig. Free energy of mixing

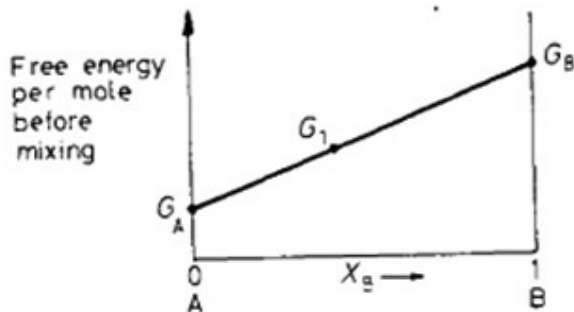


Fig. 1 Variation of G_1 (Gibb's free energy before mixing) with alloy composition X_A or X_B

$$G_2 = G_1 - \Delta G_{\text{mix}}$$

$$G_1 = H_1 - TS_1$$

$$G_2 = H_2 - TS_2$$

$$\Delta H_{\text{mix}} = H_2 - H_1$$

$$\Delta S_{\text{mix}} = S_2 - S_1$$

$$\Delta G_{\text{mix}} = \Delta H_{\text{mix}} - T \Delta S_{\text{mix}}$$

$$\Delta G_{\text{mix}} = -T \Delta S_{\text{mix}}$$

$$S = k \ln w$$

$$N_A = X_A N_a$$

$$N_B = X_B N_a$$

$$\Delta S_{\text{mix}} = -R (X_A \ln X_A + X_B \ln X_B)$$

$$\Delta G_{\text{mix}} = RT (X_A \ln X_A + X_B \ln X_B)$$

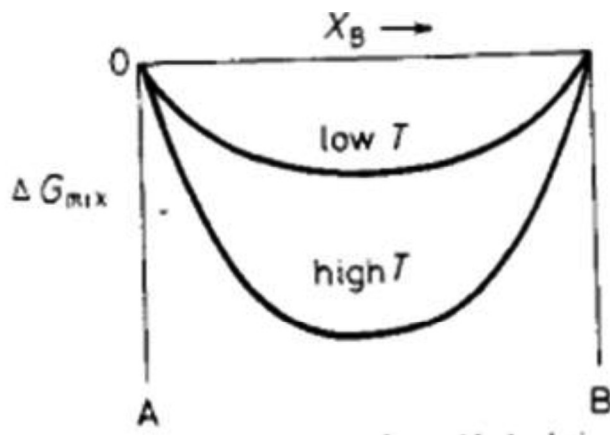


Fig. 2 Free energy of mixing for an ideal solution

$$G = G_2 = X_A G_A + X_B G_B + RT (X_A \ln X_A + X_B \ln X_B)$$

Free energy of Regular solution is given by,

$$\Delta G_{\text{mix}} = \Omega X_A X_B + RT (X_A \ln X_A + X_B \ln X_B)$$

Actual free energy of alloy,

$$G = X_A G_A + X_B G_B + \Omega X_A X_B + RT (X_A \ln X_A + X_B \ln X_B)$$

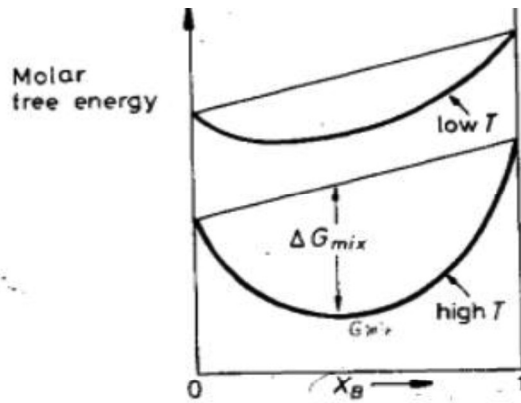


Fig. The molar free energy (free energy per mole of solution) for an ideal solid solution A, combination of fig. 1 and 2.

Lecture 4

Diffusion, Definition of Fick's law on steady and non-steady state diffusion

Diffusion: Defined as the mass flow process by which atoms/molecules change their neighbours within a phase under the influence of thermal energy and gradient (which may be concentration gradient, pressure gradient, temperature gradient, stress, electric field or gravitational field gradient).

Diffusion depends on temperature:

$$D(T) = D_0 \exp \left[-\frac{Q}{RT} \right]$$

With increase in temperature, diffusion increases.

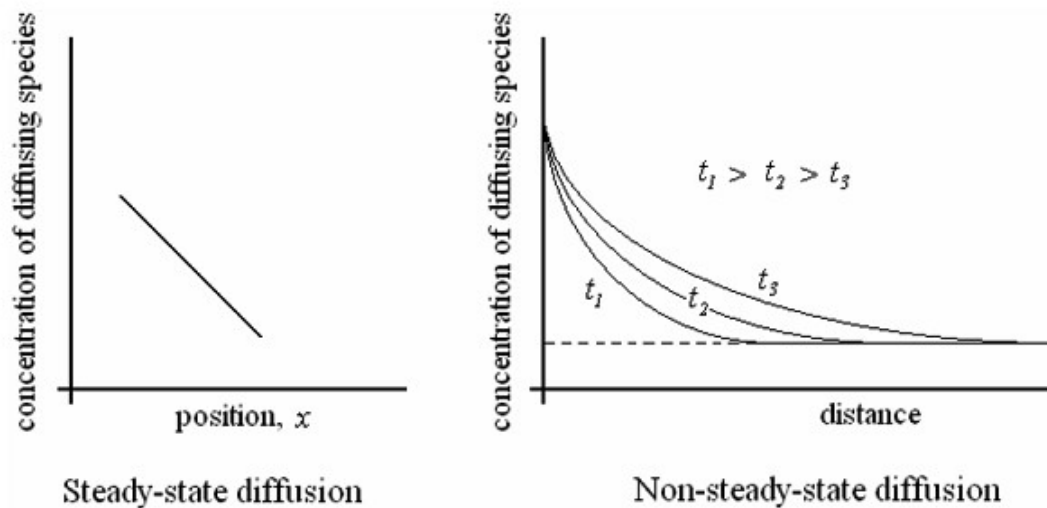


Fig. Steady state and non-steady state diffusion processes

Diffusion may be:

- Steady state: Fick's first law- independent of time- flux remains constant
- Non- steady state: Fick's second law- depends on time- flux varies.

Fick's first law of diffusion:

Let us consider a stable (or metastable) binary solution phase with concentration gradient only in x direction. Now consider two adjacent lattice planes, 1 and 2 normal to x-axis separated by inter-planar distance α . Concentration of diffusing species is then uniform within a plane but different in the two adjacent planes due to concentration gradient x direction. Let planes 1 and 2 contain n_1 and n_2 number of diffusing species per unit area, respectively.

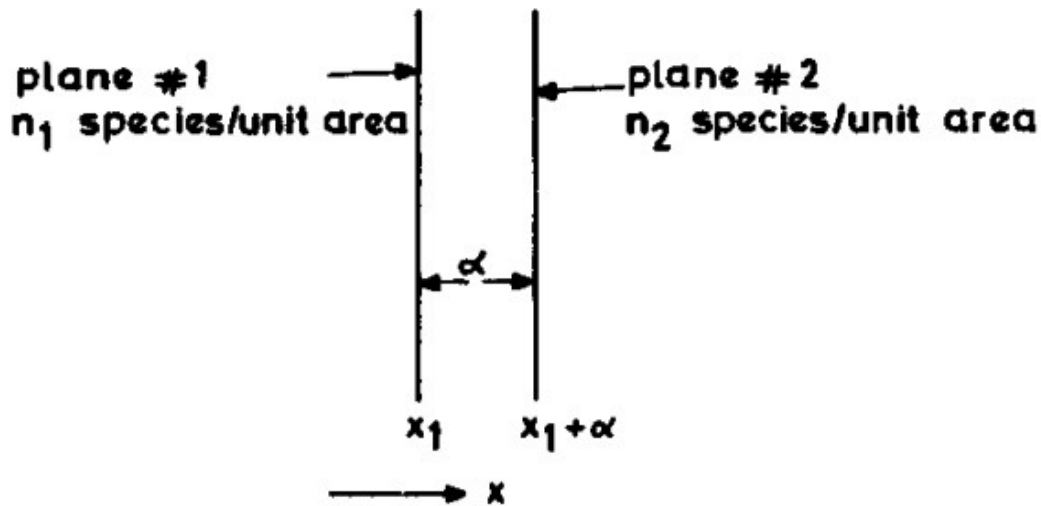


Fig. 1 One dimensional diffusion

It is assumed that diffusing species randomly jump in the material with equal probability in all three directions with a jump frequency Γ and jump distance α . Jump frequency Γ_x in x direction is then $\Gamma/3$. Number of diffusing species jumping from plane 1 to 2 in x direction, N_{x+} and from plane 2 to 1 in $-x$ direction, N_{x-} , per unit area in time δt .

$$N_{x+} = n_1 (\Gamma_x / 2) \delta t = \frac{1}{6} n_1 \Gamma \delta t \dots\dots\dots (1)$$

$$N_{x-} = n_2 (\Gamma_x / 2) \delta t = \frac{1}{6} n_2 \Gamma \delta t \dots\dots\dots (2)$$

Species jump with equal probability in $+x$ and $-x$ directions. Hence average jump frequency in either direction is $\Gamma_x / 2$ or $\Gamma/6$. From Eq.1 and 2 net transfer of diffusing species per unit area from plane 1 to plane 2 in $+x$ direction in time δt is then given by:

$$N_{1 \rightarrow 2} = N_{x+} - N_{x-} = \frac{1}{6} (n_1 - n_2) \Gamma \delta t \dots\dots\dots (3)$$

Their flux J_x in x direction is,

$$J_x = N_{1 \rightarrow 2} / dt = \frac{1}{6}(n_1 - n_2) \Gamma \dots\dots\dots (4)$$

Concentrations of diffusing species per unit volume at planes 1 and 2 are given by $C_1 = n_1/\alpha$ and $C_2 = n_2/\alpha$. Now concentration C_2 in plane 2 may be written as Taylor series expansion around concentration C_1 in plane 1 as:

$$C_2 = C_1 + \alpha(\partial C / \partial x)_1 + \text{higher order terms} \dots\dots\dots(5)$$

α is very small, higher order terms in the Taylor series may be ignored. Substituting for n_1 and n_2 in Eq.4 In terms of concentrations C_1 and C_2 and using Eq.5.

$$\text{We get } J_x = -\frac{1}{6} \Gamma \alpha^2 \left(\frac{\partial C}{\partial x} \right) = -D(\partial C / \partial x) \dots\dots\dots (6)$$

Where, D is given by: is called diffusion coefficient. Eq.6 represents Fick's first law of diffusion in one dimension.

$$D = \frac{1}{6} \Gamma \alpha^2 \dots\dots\dots (7)$$

Eq. 6 can be generalised for three dimensional diffusion to give by:

$$J = - D \cdot \nabla C \dots\dots\dots (8)$$

STEADY-STATE DIFFUSION

For diffusion flux J Eq. 6 and 8 can be solved and concentration as a function of distance already state conditions. Let us consider one dimensional diffusion across a slab of thickness X where different concentration of the species, C_1 and C_2 are maintained at all times at opposite faces of the slab at $x=0$ and $x=X$, respectively which shown in Fig.2. After an initial transient period, steady state conditions would be obtained in the slab and diffusion flux across any plane normal to x-axis would be given by:

$$J_x = - D_{C'}(\partial C / \partial x)_{x'} = - D_{C''}(\partial C / \partial x)_{x''}$$

where C' and C'' are concentrations at any two points x' and x'' , respectively, between $x = 0$ and $x = X$ and $D_{C'}$ and $D_{C''}$ are diffusion coefficients at C' and C'' . When diffusion coefficient is independent of concentration, concentration gradient is same at all points in the slab. Concentration then varies from C_2 at $x = 0$ to C_1 at $x = X$

$$J_x = - D_C \left(\frac{C_2 - C_1}{X} \right)$$

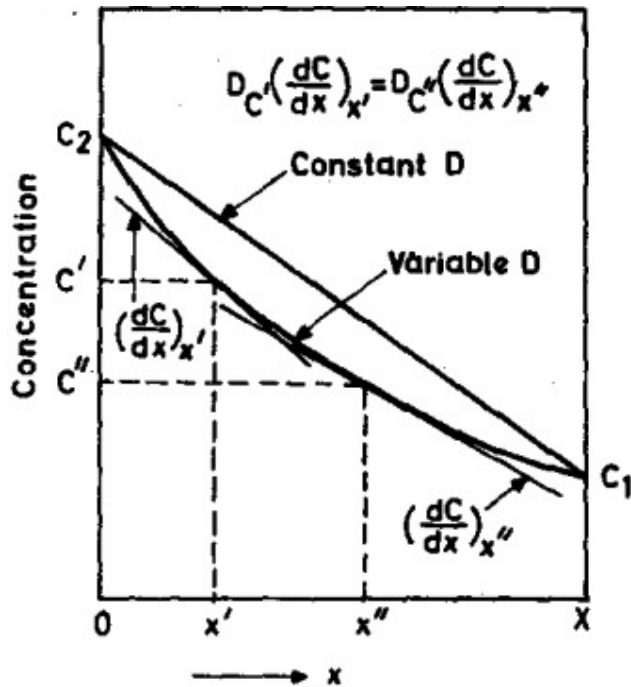


Fig. 2 Concentration profile during one dimensional steady state diffusion

Example of steady state diffusion : Permeation of hydrogen atoms through a sheet of palladium with different imposed hydrogen gas pressures on either side of slab.

Fick's second law of Diffusion:

Fick's 2nd law is an extension of the first law to non-steady state flow.

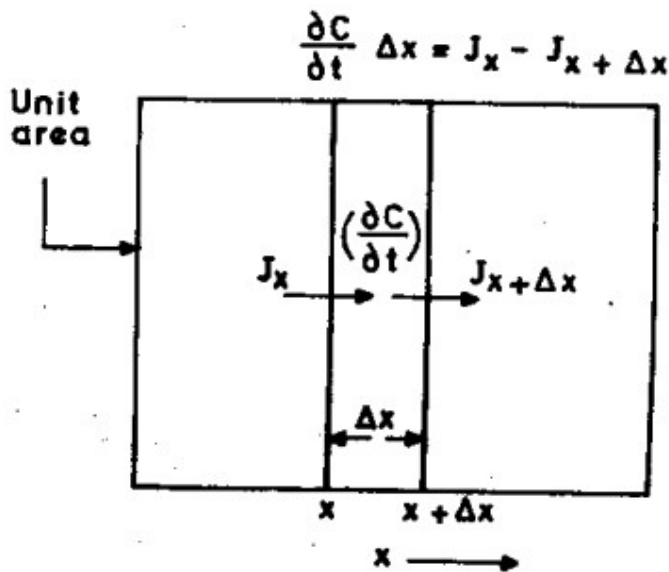


Fig. Non steady state diffusion

Here, at a given instant, flux is not the same at different cross-sectional planes along the diffusion direction x . Also, flux at a given cross-section is a function of time.

Derivation of Fick's 2nd law of diffusion :

Consider an elemental volume of length Δx along the diffusion distance x & of unit cross-sectional area (perpendicular to the diffusion distance).

Volume of such an element Δx

Rate of accumulation of diffusing species within this elemental volume ,

$$(\partial C / \partial t) \Delta x = J_x - J_{x+\Delta x} \quad \text{----- (1)}$$

$$J_{x+\Delta x} = J_x + (\partial J / \partial x)_x \Delta x$$

We know, $J = -Ddc/dx$

$$\frac{\partial C}{\partial t} = \frac{\partial}{\partial x} \left(D \frac{\partial C}{\partial x} \right) \quad \text{----- Fick's 2nd law of diffusion in 1-D for unidirectional flow under non-steady state conditions.}$$

----- (2)

$$\frac{\partial C}{\partial t} = \nabla(D \cdot \nabla C) \quad \text{----- (3)}$$

When diffusion coefficient is isotropic & independent of concentration,

$$\frac{\partial C}{\partial t} = D \frac{\partial^2 C}{\partial x^2}$$

$$\frac{\partial C}{\partial t} = D \cdot \nabla^2 C$$

N.B. -

D - diffusivity or diffusion coefficient

D depends on (i) nature of diffusing species (ii) composition of medium in which diffusion occurs (iii) temperature at which diffusion occurs.

Unit of D: $m^2 s^{-1}$

Lecture 5

Solutions to Fick’s second law of diffusion; Mechanism of diffusion in solids.

1) Thin Film Solution

This solution uses the simplified form of Fick’s the second law. It can be used to determine the diffusion coefficient D experimentally. A thin disc or film of material rich in the diffusing specie(concentration c_2) is welded as a sandwich between two rods or thick discs containing a low(or zero) concentration c_1 of the diffusing species. The thickness of the sandwiched film is much smaller than the diffusion distance to be encountered in the experiment. Under such condition, the concentration-distance curves obtained after different diffusion times constitute a set of symmetrical Gaussian distribution curves, centered at the middle of the thin discs .

Assume D of solute is independent of concentration.

Diffusion process is governed by:

$$\frac{\partial C}{\partial t} = D \frac{\partial^2 C}{\partial x^2} \text{----- (1)}$$

The corresponding solution to Eq.1 is

$$c(x,t) - c_1 = \frac{\alpha}{2\sqrt{\pi Dt}} \exp\left(-\frac{x^2}{4Dt}\right) \dots\dots\dots(2)$$

Where $\alpha = (c_2 - c_1)a$

$$= \int_{-\infty}^{+\infty} (c - c_1) dx \dots\dots\dots(3)$$

By differentiating Eq. 2, it is seen that Eq.1 is obtained, showing that Eq. 2 is one of the possible solutions

The initial conditions of this set up are

1. $t=0, x=0, c = \infty$; and
2. $t=0, x \neq 0, c=c_1$

Condition 1 results, because it is assumed that all the diffusing specie in the initial thin film is concentrated on a plane of zero thickness. The boundary conditions are

3. $t > 0, x \pm \infty, c=c_1$; and

4. $t = \infty$, for all x ,

Condition 4 results from the fact that the volume of the thin film is negligible compared to the volume of the entire set-up.

After the diffusion anneal, the concentration c can be determined as a function of the diffusion distance x , by means of careful sectioning and chemical analysis. The experimental data are plotted as $\log(c-c_1)$ versus x^2 . This should yield a straight line, from the slope of which D can be determined using Eq.2.

2) Grube solution (Infinite diffusion couple/infinite diffusion in composite) :

The experimental set-up here consists of a diffusion couple, i.e. two long bars welded face to face the concentration of the diffusing specie in one, c_2 being higher than that in the other c_1 . The concentration-distance profiles after lengths of diffusion annealing time are shown in Fig. 2.

Fig.2

The Grube solution is simply a assumption of a large number of thin film solution. Consider a thin strip dk at a distance k from the origin. If only this strip were present, the thin film solution would yield:

$$c(x,t) - c_1 = \frac{(c_2 - c_1)dk}{2\sqrt{\pi Dt}} \exp\left\{-\frac{(x-k)^2}{4Dt}\right\} \dots \dots \dots (4)$$

For the entire crystal, the solution is then given by

$$c(x,t) - c_1 = \frac{(c_2 - c_1)dk}{2\sqrt{\pi Dt}} \int_{-\infty}^0 \exp\left\{-\frac{(x-k)^2}{4Dt}\right\} dk \dots \dots \dots (5)$$

Let $(x-k)/2\sqrt{Dt} = \eta$, then, $-2\sqrt{Dt} d\eta = dk$. Using these relationships in Eq. 5, we have

$$c(x,t) - c_1 = \frac{(c_2 - c_1)}{\sqrt{\pi}} \left[- \int_{-\infty}^0 \exp(-\eta^2) d\eta - \int_0^{x/2\sqrt{Dt}} \exp(-\eta^2) d\eta \right]$$

$$= \frac{c_2 - c_1}{2} \left[1 - \operatorname{erf}\left(\frac{x}{2\sqrt{Dt}}\right) \right] \dots \dots \dots (6)$$

The term erf in Eq.6 stands for error function. By definition,

$$\operatorname{erf}\left(\frac{x}{2\sqrt{Dt}}\right) = \frac{2}{\sqrt{\pi}} \int_0^{x/2\sqrt{Dt}} \exp(-\eta^2) d\eta \dots \dots \dots (7)$$

where η is an interaction variable. In Fig.3, η is plotted against $\exp(-\eta^2)$.

From $\eta = 0$ to $\eta = +\infty$ is $+\sqrt{\pi}/2$;

From $\eta = 0$ to $\eta = -\infty$ is $-\sqrt{\pi}/2$;

So we have the following results relating to the error function:

1. $\text{erf}(\infty) = 2/\sqrt{\pi} \times \sqrt{\pi}/2 = 1$
2. $\text{erf}(-\infty) = 2/\sqrt{\pi} \times -\sqrt{\pi}/2 = -1$
3. $\text{erf}(0) = 0$
4. $\text{erf}\left(-\frac{x}{2\sqrt{Dt}}\right) = -\text{erf}\left(\frac{x}{2\sqrt{Dt}}\right)$

The initial and boundary conditions of the diffusion couple set-up are:

1. At $t=0$, for all x , $c = \frac{c_1+c_2}{2} = \bar{c}$
2. $t = 0, x < 0, c = c_2$
3. $t = 0, x > 0, c = c_1$
4. $t > 0, x = -\infty, c = c_2$
5. $t > 0, x = +\infty, c = c_1$
6. $t = \infty$, for all x , $c = \frac{c_1+c_2}{2} = \bar{c}$

For determining the diffusion coefficient D , the diffusion couple is annealed at a given temperature for a known time t . Then the concentration c is measured as a function of the diffusion distance x with the origin being taken at the cross-over point. The concentration at a given position after the diffusion annealed $c(x,t)$ and the initial concentration c_1 and c_2 will yield the value of the error function from Eq.6. From the error function table with x and t known, D can be measured.

3. The Matano-Boltzmann Solution

This solution takes into account the dependence of D on concentration. Therefore, it starts with the more general form of the Fick's second law

$$\frac{\partial c}{\partial t} = D \frac{\partial^2 c}{\partial x^2} \dots\dots\dots (1)$$

Boltzmann showed that, if c is a function of a single variable such as $\lambda = x/\sqrt{t}$, Eq. 1 can be transferred into an ordinary homogeneous differential equation:

$$-\frac{\lambda}{2} \frac{dc}{d\lambda} = \frac{d}{d\lambda} \left(D \frac{dc}{d\lambda} \right) \dots\dots\dots (8)$$

By introducing the initial and boundary conditions for a diffusion couple:

1. $t = 0, x < 0, c = c_2$,
2. $t = 0, x > 0, c = c_1$, and
3. $t > 0, x = \pm \infty, \frac{\partial c}{\partial x} = 0$,

for a fixed annealing time t , the solution of Eq. 8 is:

$$D = -\frac{1}{2t} \left(\frac{dx}{dc} \right) \int_{c_1}^c xdc$$

Subject to the condition that

$$\int_{c_1}^{c_2} xdc = 0$$

This condition is realised by choosing the origin $x=0$ such that the hatched areas A1 and A2 in Fig. 4 are equal. The cross-sectional plane corresponding to $x = 0$ is called Matano interface. From the experimental data, $c(x)$ is known, so that D can be determined graphically.

Mechanisms of Diffusion in solids:

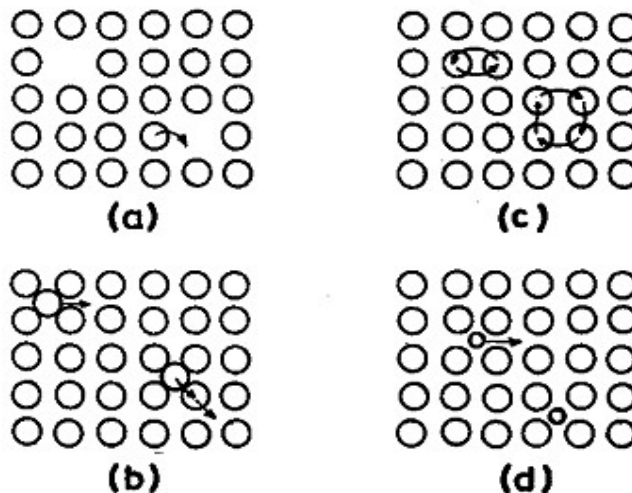


Fig. Diffusion mechanisms in crystalline solids (a) vacancy mechanism, (b) interstitial and interstitialcy mechanism (c) interchange and ring mechanisms (d) interstitial diffusion

a) Vacancy mechanism:

An atom next to a vacant site/ vacancy can diffuse by interchanging positions with a neighbouring vacant site, giving rise to vacancy mechanism of diffusion. In this process vacancy moves in opposite direction.

b) Interstitial mechanism:

Atoms which are small enough to occupy interstitial sites diffuse by jumping from one interstitial site to a neighbouring interstitial site. This is known as Interstitial mechanism of diffusion.

Interstitialcy mechanism:

An interstitial atom may move to a normal lattice site next to it and pushes the atom present on that site to an adjacent interstitial position.

c) Ring mechanism:

In this mechanism three or more atoms may rotate together as a ring, thereby exchanging their position (square/round shape ring).

d) Interstitial diffusion (depends on temperature). This is generally faster than vacancy diffusion because there are many more interstitial sites than vacancy sites to jump to. Requires small impurity atoms (e.g. C, H, O) to fit into interstices in host.

Lecture 6

Chemical diffusion - Kirkendall effect

In a binary solid solution of A & B the rate at which A & B diffuse are not necessarily the same. The lower melting component diffuses faster than the other component. This leads to Kirkendall effect where non-diffusive mass transfer takes place in a diffusion couple.

Let us consider diffusion in a binary solution with a concentration gradient in direction X.

$$C_1 + C_2 = C = \text{constant}$$

and

$$\partial C_1 / \partial x = -\partial C_2 / \partial x$$

During one dimensional diffusion in a binary solution, mass flux of the components at any point is given by Fick's first law of diffusion as,

$$J_2 = -D(C) \frac{\partial C_2}{\partial x} = D(C) \frac{\partial C_1}{\partial x} = -J_1$$

Where J_1 is mass flux of components 1 and J_2 that of component 2, and $D(C)$ is diffusion coefficient at that point (or concentration). Hence, two components in a binary solution may have different intrinsic diffusivities, D_1 and D_2 of components 1 and 2, respectively; still a single chemical diffusion composition $D(C)$ is sufficient to completely describes the diffusion process. $D(C)$ must then be some function of D_1 and D_2 . To reconcile different intrinsic diffusivities of the components with single chemical diffusion coefficient in a binary solution, some non-diffusive mass transfer must also occur during diffusion under concentration gradient. Non-diffusive mass transfer in a diffusion couple experiment was first observed by Sigmore and Kirkendall and is known as Kirkendall effect. Their experiment is briefly describe below.

Experiment:

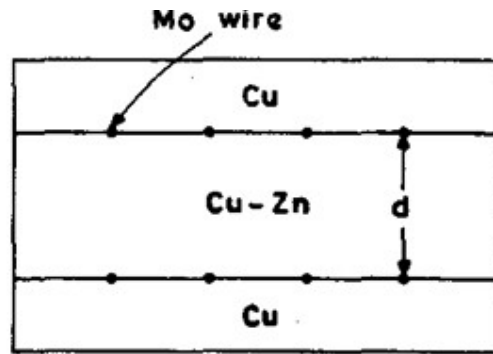


Fig. Kirkendall effect in Cu/Cu-Zn diffusion couple

Inert markers (high melting point, insoluble metals such as Mo and W) were rapped around a slab of 70 Cu – 30 Zn brass of thickness d & then a thick layers of pure Cu were deposited on both opposite sides of the slab.

The assembly was then heated to a high temperature where diffusion could occur at reasonable rates.

After cooling to room temperature and sectioning, it was observed that distance d between the markers continuously decreased with increasing diffusion time.

Hence, it can be concluded that during diffusion, flux of Zn past the markers was greater than that of Cu in opposite direction, i.e. a net mass flow past the markers had occurred in the direction of slower-moving species (Cu).

Reason:

Melting point of Cu > Melting point of Zn.

So rate of diffusion of Zn is more than that of Cu, i.e. Cu diffuses slowly to inside & Zn diffuses faster towards outside so that final composition of Cu and Zn changes. It is no more 70 Cu- 30 Zn.

So the interface moves/shifts in that direction in which diffusion is slow.

Since Cu diffuses slowly inwards so interface moves inwards i.e. in direction where slow diffusion occurs.

Example of Kirkendall effect :

Let hydrogen & Argon at the same pressure be kept in two chambers inter connected through a tube. A frictionless piston in the tube separates the gases. On opening an orifice in the piston, the gases inter diffuse. The lighter gas (hydrogen) will diffuse faster, resulting in pressure difference that will tend to shift the piston in the direction in which slower diffusing argon is moving.

Numerical problems:

1) Consider the surface treatment of steel with C at 950°C. The initial concentration of C in the steel is 0.25 wt% and the surface concentration during treatment is 1.2 wt%. How long will it take to reach 0.8 wt% C at a position of 0.5 mm below the surface?

Given: $D=1.6 \times 10^{-11}$ m²/s .

2) Consider the gas carburizing of steel at 927°C. The diffusion coefficient of carbon in steel at this temperature is 1.28×10^{-11} m²/s. The carbon content at the surface is 0.90% and the initial carbon content is 0.20%. Calculate the carbon content 0.50 mm below the surface after 5 hours of carburizing time.

3) Consider the impurity diffusion of gallium into a silicon wafer at 1100°C. Prior to commencement of diffusion the wafer was free of gallium. At time = 0 the surface concentration is changed to 1024 atoms/m³. Find the depth below the surface at which the concentration will be 1022 atoms/m³ after 3 hours.

Given: $D=7.0 \times 10^{-17}$ m²/s.

4) In alclad, 20 mm thick duralumin sheets are covered on either side with 0.2mm thick pure aluminium sheets. For retaining the corrosion resistance, Cu concentration at a depth of 0.1 mm from the outer surface should not exceed 0.4 %

How long can the material be kept at 550° C, without damaging the corrosion resistance ?

5) At 950° C , a 0.8 % carbon steel is getting decarburized for a duration of 4 hr in an atmosphere equivalent to 0 % carbon at the surface of steel.

Determine the minimum depth upto which post-machining is to be done, if the carbon content at the surface after- machining should not be below 0.6 %.

Darken’s analysis

Darken derived a relationship between \tilde{D} , D_A and D_B using the following assumptions:

1. The molar volume of the solid solutions is independent of concentration,
2. Porosity developed during diffusion is negligible and
3. The bulk flow is perpendicular to the croo-sectional [pplane that is no lateral dimensional changes occur.

Relative to the position of the weld interface or the Matano interface, the net flux of atoms is zero. That is,

$$J_A + J_B = 0 \dots\dots\dots (1)$$

$$\left(-\tilde{D} \frac{dc_A}{dx}\right) + \left(-\tilde{D} \frac{dc_B}{dx}\right) = 0 \dots\dots\dots (2)$$

The fluxes of A and B are due to their intrinsic diffusivities as well as to the bulk flow. Therefore, we can write

$$\left(-\tilde{D} \frac{dc_A}{dx} + v c_A\right) + \left(-\tilde{D} \frac{dc_B}{dx} + v c_B\right) = 0 \dots\dots\dots (3)$$

Where v is the velocity of the markers, placed at the original weld. Rearranging Eq. 3 we have

$$v = \frac{D_B(dc_B/dx) + D_A(dc_A/dx)}{c_A + c_B} \dots\dots\dots (4)$$

As c_A and c_B are concentrations expressed in mol/m³, $c_A + c_B = 1/V$ where V is the molar volume

$$v = (D_B - D_A) \frac{dX_B}{dx} \dots\dots\dots (5)$$

Where X_B is the mole fraction of B equal to V_{cB} and $X_A = 1 - X_B$.

Since:

$$-\tilde{D} \frac{dc_B}{dx} = -D_B \frac{dc_B}{dx} + v c_B \dots\dots\dots (6)$$

$$-\tilde{D} \frac{dX_B}{dx} = -D_B \frac{dX_B}{dx} + v X_B \dots\dots\dots (7)$$

Substituting for $\frac{dX_B}{dx}$ from Eq. 7 into Eq. 5, we get

$$v = (D_B - D_A) \frac{v X_B}{D_B - \tilde{D}} \dots\dots\dots (8)$$

$$D_B - \tilde{D} = (D_B - D_A) X_B \dots\dots\dots (9)$$

$$\tilde{D} = D_A X_B + D_B X_A \dots\dots\dots (10)$$

which is the relation between the inter-diffusion coefficient and the intrinsic diffusivities derived by Darken.

Lecture 7

Effect of pressure and temperature on diffusivity

EFFECT OF TEMPERATURE

For a substitutional atom diffusing via the vacancy mechanism, we have to consider the availability of a neighbouring vacant site for the atom to jump. The probability that the diffusing atom will find a particular neighbouring site to be vacant is equal to $\exp(-\Delta G_f/RT)$, where ΔG_f is the free energy of formation of a mole of vacancies. The number of successful jump attempts is given by $\nu \exp(-\Delta G_m/RT)$, where ν is the lattice vibration frequency and ΔG_m is the free energy of motion of vacancy. The frequency ν' with which an atom exchanges position with any of the neighbouring sites is then given by

$$\nu' = Z\nu \exp(-\Delta G_m/RT) \exp(-\Delta G_f/RT)$$

Where Z is the coordination number.

From Fick's First Law from the Atomic Model the probability of jumps in three mutually perpendicular directions, $D = 1/6(\delta^2 \nu')$

$$D = \frac{1}{6} \delta^2 Z \nu \exp\left[-\left(\frac{\Delta G_m + \Delta G_f}{RT}\right)\right]$$

In simple cubic, FCC and BCC crystals

$$\frac{1}{6} \delta^2 Z = a_0^2$$

where a_0 is the lattice parameter of the cubic crystals.

$$D = a_0^2 \nu \exp\left[-\left(\frac{\Delta G_m + \Delta G_f}{RT}\right)\right]$$

Using $\Delta G = \Delta H - T\Delta S$

$$D = a_0^2 \nu \exp\left[-\left(\frac{\Delta G_m + \Delta G_f}{RT}\right)\right] \exp\left[-\left(\frac{\Delta H_m + \Delta H_f}{RT}\right)\right]$$

Experimental data show that

$$D = D_0 \exp\left(-\frac{Q}{RT}\right)$$

D_0 is called frequency factor and Q is called activation energy for diffusion.

A plot of $\ln D$ versus $1/T$ yields a straight line

The slope of the line is equal to $-\frac{Q}{R}$ and the intercept of the y axis is $\ln D_0$

Effect of Pressure on Diffusion :

In addition to temperature, pressure also affects diffusivity in materials to some extent. Diffusion coefficient in general may also be written as

$$D = \frac{1}{6} \Gamma \alpha^2 = A \exp\left(-\frac{\Delta G_D}{RT}\right) \dots\dots\dots \text{equn(1)}$$

Where A is a constant and ΔG_D is activation Gibbs energy of diffusion. When diffusion occurs by vacancy mechanism $\Delta G_D = \Delta G_v + \Delta G_m$, where ΔG_v and ΔG_m are Gibbs energies of formation and movement of vacancies, respectively. For interstitial diffusion $\Delta G_v = \Delta G_m$, where, ΔG_m is activation Gibbs energy for movement of interstitials. Taking logarithm of both sides of equa(1) and differentiating with respect to pressure, we get:

$$\left[\frac{\partial \ln(D/A)}{\partial P} \right]_T = -\frac{1}{RT} \left[\frac{\partial(\Delta G_D)}{\partial P} \right]_T = -\frac{\Delta V_D}{RT}$$

.....equn(2)

where ΔG_D is called activation volume of diffusion. For diffusion by vacancy mechanism,

$$\Delta V_D = \left[\frac{\partial(\Delta G_D)}{\partial P} \right]_T = \left[\frac{\partial(\Delta G_v)}{\partial P} \right]_T + \left[\frac{\partial(\Delta G_m)}{\partial P} \right]_T = \Delta V_v + \Delta V_m$$

Where, ΔV_v is molar volume of vacancies and ΔV_m is activation volume for the movement of vacancies. If no relaxation of atoms occurs around vacancies in the lattice, then ΔV_v would be equal to molar volume of the material. Relaxation of atoms around vacancies reduces ΔV_v in metals to about 0.5 to 0.7 of their molar volume. Activation volume for movement of vacancies, ΔV_m (the change in volume when an atom moves from its normal site to activated position during its movement) is expected to be positive, but small. Therefore, when diffusion occurs by vacancy mechanism, ΔV_D is positive and is of the order of 0.5 to 0.7 of molar volume of the material. Hence, diffusivity decreases with increasing pressure in accordance with eqn (2).

For interstitial diffusion, and substitutional diffusion by interstitialcy mechanism, $\Delta G_D = \Delta G_m$ and hence ΔV_D is given by:

$$\Delta V_D = \left[\frac{\partial(\Delta G_D)}{\partial P} \right]_T = \left[\frac{\partial(\Delta G_m)}{\partial P} \right]_T = \Delta V_m$$

.....equn (4)

Hence, ΔV_D in these cases is quite small, equal to activation volume for movement interstitial atoms only, and hence, diffusivity not affected much by pressure. ΔV_D in liquids is also very small, of the order of about 5% of molar volume and therefore diffusivity in liquids also remains relatively unaffected by pressure.

Lecture 8

Nucleation and growth: Formation of nucleus; Homogeneous and Heterogeneous nucleation

Formation of nucleation:

In case of first order phase transformations, where a metastable phase transform to a more stable phase (or phases) occur by nucleation and growth. Phenomenon of nucleation and growth are fundamentally different from each other.

Nucleation: it is the formation of small stable particles of solid metal from liquid metal, called nuclei.

Growth: it is the increase in size of these stable nuclei particles by atoms joining them from liquid metal.

Nucleation:

Nucleation is of two types, Such as:

1. Homogeneous nucleation
2. Heterogeneous nucleation

Homogeneous nucleation:

When the probability of nucleation is same everywhere within the volume of liquid phase, it is called as homogeneous nucleation. The energy difference between the liquid & the solid is the volume free energy, ΔG_V per unit volume. This energy is negative (below T_m) and is the driving force for solidification. Let solid nucleus formed is a sphere of radius r & nucleation is controlled by two factors:

- i. Volume free energy change = $4/3 \pi r^3 \Delta G_V$
- ii. Surface energy of new solid formed = $4\pi r^2 \gamma^{SL}$

ΔG_V = volume free energy per unit volume (-ve)

γ^{SL} = surface energy per unit area (+ve)

This term is always positive & inhibits the process of nucleation.

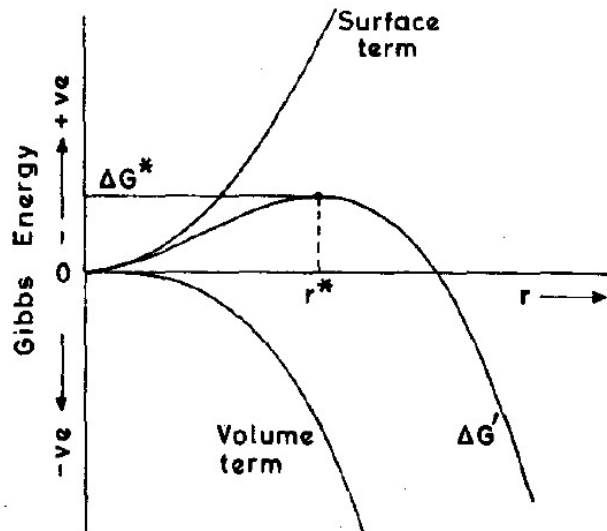


Fig. 1 Gibbs energy of a spherical embryo as a function of its size

Fig. 1 shows that $\Delta G'$ as a function of r when ΔG_V is negative, $\Delta G'$ initially increases, goes through a maximum critical radius size r^* and then continuously decreases.

For a spherical nucleus with radius r

$$\Delta G' = -\frac{4}{3}\pi r^3 \Delta G_V + 4\pi r^2 \gamma^{SL}$$

At the temperature ($< T_m$) for which the curve has been drawn, the critical radius, r^* is the value of r corresponding to the maximum of ΔG^* . The value of r^* is therefore obtained by equating to zero the derivative of $\Delta G'$ with respect to radius, r , thus,

$$\Delta G^{*'} = -4\pi r^2 \Delta G_V + 8\pi r \gamma^{SL}$$

$$r^* = \frac{2 \gamma^{SL}}{\Delta G_V} \quad \Delta G^* = \frac{16\pi (\gamma^{SL})^3}{3(\Delta G_V)^2}$$

The difference between the Gibbs free energy of liquid and solid (also called the driving force for the phase transformation) is proportional to the undercooling below the melting temperature, $\Delta T = T_m - T$

$$\Delta G_V = \frac{\Delta H_m \Delta T}{T_m}$$

where H_m is the latent heat of melting or fusion

$$r^* = \left(\frac{2 \gamma^{SL} T_m}{\Delta H_m} \right) \frac{1}{\Delta T}$$

$$\Delta G^* = \left(\frac{16 \pi (\gamma^{SL})^3 T_m^2}{3(\Delta H_m)^2} \right) \frac{1}{(\Delta T)^2}$$

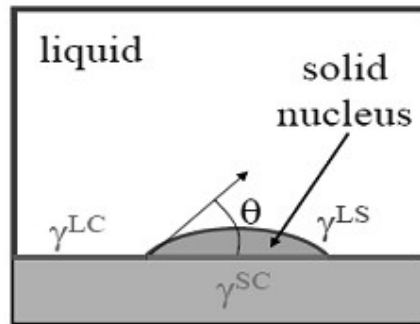
Both r^* and G^* decrease with increase in under cooling.

HETEROGENEOUS NUCEATION:

Here, the probability of nucleation is much higher at certain preferred sites such as mold wall, inclusions, grain boundaries, compared to rest of the parent phase.

Example - Solidification of a liquid on an inclusion surface

Heterogeneous Nucleation



The formation of the nucleus leads to a Gibbs free energy change of $\Delta G_r^{\text{het}} = -V_s \Delta G_v + A^{\text{SL}} \gamma^{\text{SL}} + A^{\text{SC}} \gamma^{\text{SC}} - A^{\text{SC}} \gamma^{\text{LC}}$

$$V_s = \pi r^3 (2 + \cos(\theta)) (1 - \cos(\theta))^2 / 3$$

$$A^{\text{SL}} = 2\pi r^2 (1 - \cos(\theta)) \quad \text{and} \quad A^{\text{SC}} = \pi r^2 \sin^2(\theta)$$

One can show that

$$\Delta G_r^{\text{het}} = \left\{ -\frac{4}{3} \pi r^3 \Delta G_v + 4\pi r^2 \gamma^{\text{SL}} \right\} S(\theta) = \Delta G_r^{\text{hom}} S(\theta)$$

$$S(\theta) = (2 + \cos \theta)(1 - \cos \theta)^2 / 4$$

$$\Delta G_r^{\text{het}} = \left\{ -\frac{4}{3} \pi r^3 \Delta G_v + 4\pi r^2 \gamma^{\text{SL}} \right\} S(\theta) = \Delta G_r^{\text{hom}} S(\theta)$$

$$\text{where } S(\theta) = (2 + \cos \theta)(1 - \cos \theta)^2 / 4 \leq 1$$

$$\text{At } r = r^* \quad \frac{d\Delta G_r}{dr} = (-4\pi r^2 \Delta G_v + 8\pi r \gamma^{\text{SL}}) S(\theta) = 0$$

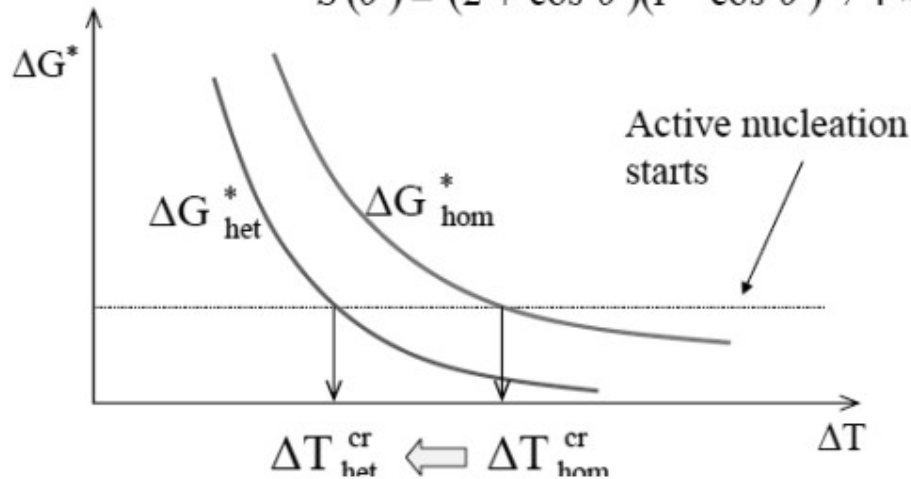
$$r^* = \frac{2 \gamma^{\text{SL}}}{\Delta G_v}$$

- same as for homogeneous nucleation

$$\Delta G_{\text{het}}^* = S(\theta) \frac{16 \pi (\gamma^{\text{SL}})^3}{3 (\Delta G_v)^2} = S(\theta) \Delta G_{\text{hom}}^*$$

$S(\theta)$ can be small \Rightarrow if $\theta = 10^\circ$

$$S(\theta) = (2 + \cos \theta)(1 - \cos \theta)^2 / 4 \approx 10^{-4}$$



By comparing the free energy terms for homogeneous nucleation process for various contact conditions:

- When product particle makes only a point contact with the foreign surface i.e. $\theta = 180^\circ$, the foreign particle does not play a role in the nucleation process $\rightarrow \Delta f^*_{het} = \Delta f^*_{hom}$
- If the product particle completely wets the foreign surface i.e. $\theta = 0^\circ$, there is no barrier for heterogeneous nucleation $\rightarrow \Delta f^*_{het} = 0$
- In the intermediate conditions such as where the product particle attains hemispherical shape, $\theta = 90^\circ \rightarrow \Delta f^*_{het} = 1/2 \Delta f^*_{hom}$

Lecture 9

Mechanism and kinetics of thermally activated growth; Interface controlled growth

Thermally Activated growth: occurs by random individual movement of atoms (i.e. diffusion) to and across the parent/ product interfaces.

Thermally activated growth is of 2 types:

- ➔ **Interface controlled growth**
- ➔ **Diffusion controlled growth**

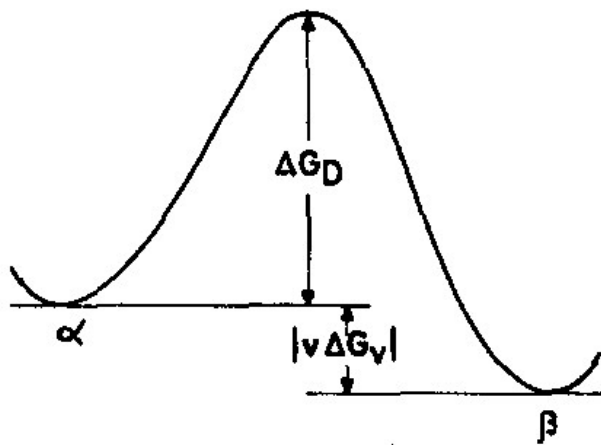
Interface controlled growth	Diffusion controlled growth
1) When there is no change in composition during the transformation, growth is controlled by short-range movement of atoms across the interface and is called Interface-controlled growth. (Some transformations with compositional changes can also be interface-controlled.)	1) When composition of product phase is different is different than that of parent phase, long range diffusion of one of the component atoms/solute is required for growth to occur. This is called Diffusion-controlled growth.
2) Example: Recrystallization, Grain growth, Polymorphic transformation, Massive transformation.	2) Example: Eutectoid reaction, Discontinuous precipitation.

INTERFACE - CONTROLLED GROWTH:

Growth rate at constant temperature :

$\alpha \rightarrow \beta$ transformation occurs.

Parent phase product phase



If β phase has same composition as α , then β -phase may grow by thermally activated movement of atoms across α/β interface.

Assume: Incoherent interface.

Free energy barrier for atom jump across the interface during growth.

Where, ΔG_D is activation energy required for an atom to jump from α to β across the interface.

v is volume of β per atom.

ΔG_v is Gibbs energy of transformation per unit volume of β

$|v\Delta G_v|$ is change in chemical free energy per atom in $\alpha \rightarrow \beta$ transformation .

$\Delta G_D + |v\Delta G_v|$ is activation energy required for an atom to jump from β to α across the interface.

$$\Delta G_D + |v\Delta G_v| > \Delta G_D$$

Rate of transfer of atoms from α to β per unit area of interface,

$$\frac{dn_{\alpha \rightarrow \beta}}{dt} = s_\alpha v_\alpha \exp\left(-\frac{\Delta G_D}{kT}\right) \dots \dots \dots (1)$$

Where, s_α and v_α are no. of atoms per unit area at interface in α & lattice vibration frequency respectively.

k is Boltzmann's constant, T is temperature (in $^\circ K$).

Similarly, rate of transfer of atoms from β to α per unit area of interface is given by,

$$\frac{dn_{\alpha \rightarrow \beta}}{dt} = s_\beta v_\beta \exp\left(-\frac{\Delta G_D + |v\Delta G_v|}{kT}\right) \dots \dots \dots (2)$$

Where, s_β and v_β are no. of atoms per unit area at interface in β & characteristic/lattice vibrational frequency.

Assume, $s_\alpha = s_\beta = s$ and $v_\alpha = v_\beta = v$ then

Net flow of atoms from α to β per unit area of interface is obtained from eqn (1) & (2) as,

$$\left(\frac{dn}{dt}\right)_{\alpha \rightarrow \beta} = \frac{dn_{\alpha \rightarrow \beta}}{dt} - \frac{dn_{\beta \rightarrow \alpha}}{dt} = sv \exp\left(-\frac{\Delta G_D}{kT}\right) \left[1 - \exp\left(-\frac{|v\Delta G_V|}{kT}\right)\right] \dots \dots \dots (3)$$

Growth rate of α/β interface, U (m/sec) = rate of increase in volume of β -phase per unit area of interface.

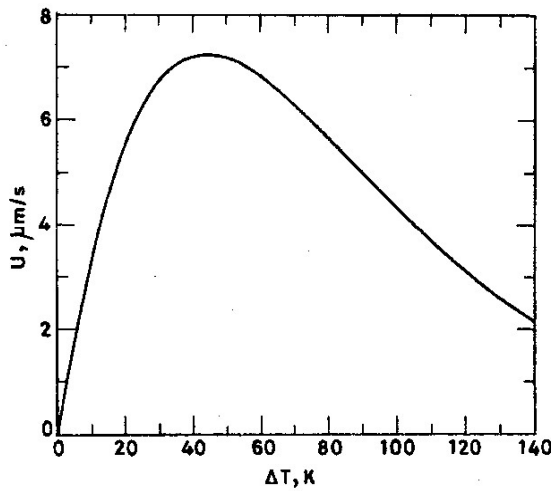
$$U = v \left(\frac{dn}{dt}\right)_{\alpha \rightarrow \beta} = vsv \exp\left(-\frac{\Delta G_D}{kT}\right) \left[1 - \exp\left(-\frac{|v\Delta G_V|}{kT}\right)\right]$$

$$\text{Or } U = \lambda_j v \exp\left(-\frac{\Delta G_D}{kT}\right) \left[1 - \exp\left(-\frac{|v\Delta G_V|}{kT}\right)\right] \dots \dots \dots (4)$$

Where, U is growth rate of interface

v is volume per atom in β phase

$\lambda_j = vs$ is jump distance across the interface.



Variation of Growth rate as a function of temperature ΔT

Diffusion coefficient through an incoherent interface is given as,

$$D_b = \lambda_j^2 v \exp\left(-\frac{\Delta G_D}{kT}\right) \dots \dots \dots (5)$$

$$U = \frac{D_b}{\lambda_j} \left[1 - \exp\left(-\frac{|v\Delta G_V|}{kT}\right)\right] \dots \dots \dots (6)$$

Kinetics for Interface-controlled growth:

Johnson – Mehl Model:

→ Assumptions:

- 1) Nucleation rate I is equal to $1/(1-x) dN_v/dt$
- 2) Growth rate $U(= dr/dt)$ is independent of X & t.
- 3) Nucleation occurs randomly in the untransformed phase but not applied in Segregation/coring of foreign particles & inclusion of grain boundaries.
- 4) Product phase particles grow as spheres until impingement occurs. i.e $U_x = U_y = U_z \rightarrow$ Growth rate is independent of crystal direction.

→ At any time, τ ($\tau < t$) if product phase spherically nucleates, then

$$\text{Volume fraction} = 4/3\pi U^3 (t - \tau)$$

No. of particles nucleated per unit volume of alloy in time $dT = I dT$

So, volume of all these particles at time $t =$ corresponding volume fraction transformed \times no. of nucleation particles.

$$dX_{\text{ext}} = 4/3\pi U^3 (t - \tau) I d\tau \text{ ----- (1)}$$

$$dX_{\text{ext}} (1-X) = dx \text{ (corrected for impingement) ----- (2)}$$

Combining eqn (1) & (2),

$$\frac{dX}{(1-X)} = 4/3\pi U^3 (t - \tau) I d\tau$$

Integrating both sides between 0 to X, we get

$$\int_0^X \frac{dX}{(1-X)} = \int_{\tau=0}^{\tau=t} 4/3\pi U^3 (t - \tau) I d\tau$$

Solving we get, $X = 1 - \exp\left(-\frac{\pi}{3} I U^3 t^4\right) \dots \dots \dots (3)$ **Johnson-Mehl Equation.**

$$X = 1 - \exp[-(Kt)^n] \text{ ----- (4)}$$

Comparing eqn (3) & (4) we get,

$K = \frac{\pi}{3}IU^3t^4$ when $n=4$ indicates that the volume of the transformation product increases (1) with the first power of time due to the constant rate of nucleation and (2) with the third power of time due to constant linear growth rate, dr/dt , as volume is proportional to r^3 . A plot of X versus t for typical values of I and U has the sigmoidal shape which is shown in the Fig.

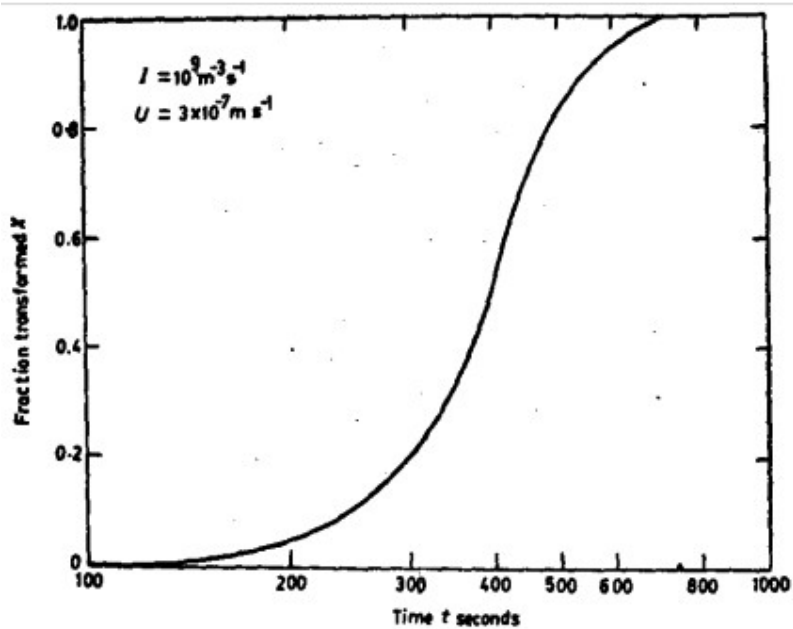


Fig. Fraction transformed X as a function of reaction time t for typical values of nucleation rate I and growth rate U . It has sigmoidal shape.

The Avrami Model

Avrami assume that there are N_v preferred sites per unit volume and they decrease exponentially with time on nucleation:

$$N_t = N_v \exp(-wt) \dots \dots \dots (5)$$

Where N_t is the number of preferred nucleation sites left over at time t and w is a frequency factor characteristic of a particular system. If w is very large, even for small t , $\exp(-wt) \sim 0$, so that all sites are nucleated at the start of the transformation process. Under such conditions, the fraction transformed X varies with time t as follows:

$$X = 1 - \exp\left[-\frac{\pi}{3}N_vU^3t^3\right] \dots \dots \dots (6)$$

Note that the time exponent here turns out to be three arising from a constant linear growth rate, the nucleation rate I being 0.

If w is small a decreasing rate of nucleation is observed during the transformation.

Lecture 10

Mechanism and kinetics of diffusion control growth regimes

General expression for Growth rate (spherical particles):

Consider continuous precipitation of β phase particles from supersaturated solid solution of α in a binary system of A & B.

α - supersaturated \rightarrow α -saturated + β -precipitate

Let us consider growth of spherical β precipitates of composition C_β from a metastable

A phase of composition C_0 ($C_\beta > C_0$) during a $\alpha \rightarrow \beta$ transformation at temperature T in a binary system shown in Fig.1

It is assumed that α/β interface is coherent

Diffusion is controlled by diffusion of solute in α -matrix.

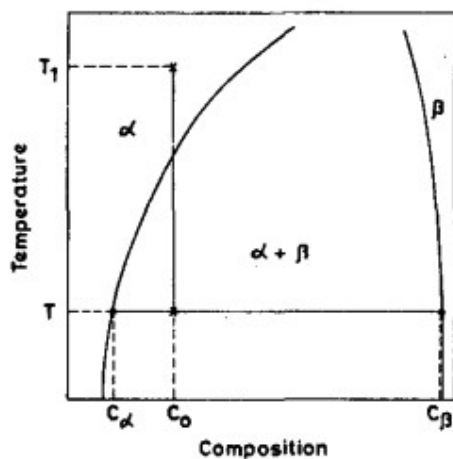


Fig. 1 Precipitation of β phase from supersaturated α phase

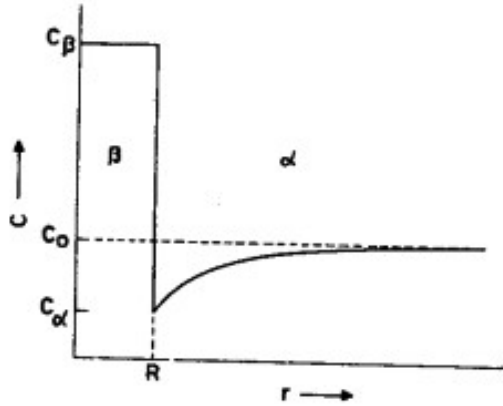


Fig 2. Solute concentration profile during growth of an isolate spherical β precipitate from supersaturated α phase in fig. 1

At temperature T_0 , α -solid solution of composition C_0 is just saturated. On cooling to temperature T , solid solution becomes supersaturated w.r.t. B-component atoms. β -particles being rich in B composition (of matrix) changes to C- α . Diffusion is governed by Fick's law which in spherical coordinates is,

$$\frac{\partial C}{\partial t} = D \left(\frac{\partial^2 C}{\partial r^2} + \frac{2}{r} \frac{\partial C}{\partial r} \right) \quad \text{----- (1)}$$

Where D is diffusion coefficient of solute in α , C is concentration of solute in α , r is radial distance from the center of β particle and t is time. The boundary conditions for this problem are: $C=C_\alpha$ at $r=R$ and $C=C_0$ at $r=\infty$ at any time $t>0$, and $R=0$ at $t=0$. Diffusion distance under these conditions is proportional to $(Dt)^{1/2}$. Therefore, let us introduce a dimensionless parameter s , equal to $r/(Dt)^{1/2}$, such that C is a function of s only. In terms of parameter s .

Equation (1) can be written as :

$$\frac{d^2 C}{ds^2} = - \left(\frac{s}{2} + \frac{2}{s} \right) \frac{dC}{ds} \quad \text{----- (2)}$$

boundary conditions become, $C=C_\alpha$ at $s=R/(Dt)^{1/2}$, and $C=C_0$ at $s=\infty$.

Equation (2) has solution,

$$\frac{dC}{ds} = - \frac{A}{s^2} \exp\left(-\frac{s^2}{4}\right) \quad \text{----- (3)}$$

Integrating above equation from any value of s to s = ∞,

$$C(s) - C_0 = A \int_s^{\infty} \frac{\exp(-u^2/4)}{u^2} du = A\Phi(s)$$

where,

$$\Phi(s) = \int_s^{\infty} \frac{\exp(-u^2/4)}{u^2} du \quad \text{----- (4)}$$

Integrating above equation by parts we get ,

$$\Phi(s) = \frac{\exp(-s^2/4)}{s} - \frac{\sqrt{\pi}}{2} \operatorname{erfc}(s/2) \quad \text{----- (5)}$$

At the surface of growing β particle, r=R and C=C_α we get

$$A = \frac{C_\alpha - C_0}{\Phi(S)} \quad \text{----- (6)}$$

where, S is equal to R/(Dt)^{1/2}.

$$(C_\beta - C_\alpha) \frac{dR}{dt} = -J_{r=R} = D \left(\frac{\partial C}{\partial r} \right)_{r=R} \quad \text{----- (7)}$$

Where dR/dt is growth velocity of the interface and -J_{r=R} is diffusion flux of solute interface.

$$\left(\frac{\partial C}{\partial r} \right)_{r=R} = \left(\frac{dC}{ds} \right)_{r=R} \left(\frac{\partial s}{\partial r} \right)_{r=R} = -\frac{A}{S^2 \sqrt{Dt}} \exp\left(-\frac{S^2}{4}\right) \quad \text{----- (8)}$$

s=r/(Dt)^{1/2} and at r=R, s=S.

Substituting eqn (8) & (6) in eqn (7),

$$S^3 = 2 \left(\frac{C_o - C_\alpha}{C_\beta - C_\alpha} \right) \left(\frac{\exp(-S^2/4)}{\Phi(S)} \right) = 2\xi \left(\frac{\exp(-S^2/4)}{\Phi(S)} \right) \quad \text{----- (9)}$$

where, $\xi = [(C_o - C_\alpha)/(C_\beta - C_\alpha)]$ is relative supersaturation and,

$$\Phi(S) = \frac{\exp(-S^2/4)}{S} - \frac{\sqrt{\pi}}{2} \text{erfc}(S/2) \quad \text{----- (10)}$$

Once S is known, radius R of β particle & its Growth rate U is given by,

$$R = S\sqrt{Dt} \quad \text{and} \quad U = \frac{dR}{dt} = \frac{S}{2} \sqrt{\frac{D}{t}}$$

- ⇒ Particle radius R proportional to $t^{1/2}$
- ⇒ Growth velocity U is inversely proportional to $t^{1/2}$

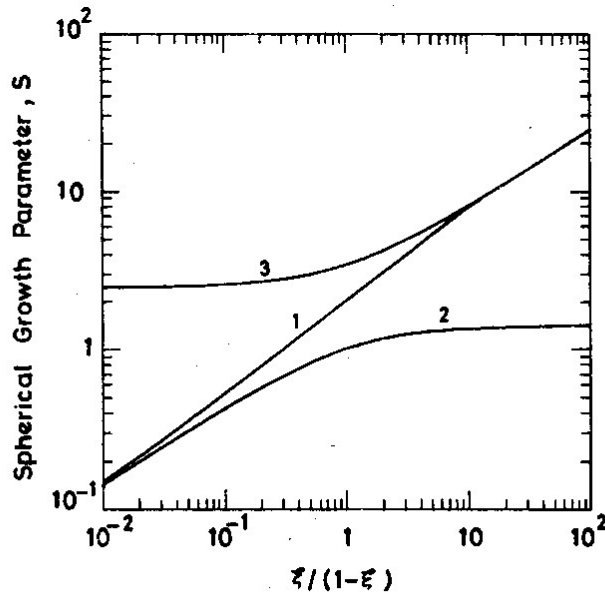


Fig. 6.5: Spherical growth rate parameter S as a function of relative supersaturation ξ from, (1) eq.(6.19), (2) eq.(6.23) and (3) eq.(6.26).

Kinetics of Diffusion-controlled Growth :

$$\alpha_{\text{supersat}} \rightarrow \alpha_{\text{sat}} + \beta$$

$$X = \frac{V_{\beta} c_{\beta\alpha}}{V_0(\bar{c} - c_{\alpha\beta})}$$

where V_0 is the total volume of the system, V_{β} is the volume of β particles at time t , and the concentration terms have their usual meaning. Now the

Extended volume fraction is given by,

$$X_{\text{ext}} = \frac{4\pi r^3 N_v c_{\beta\alpha}}{3(\bar{c} - c_{\alpha\beta})} \quad \text{----- (a)}$$

$$r = \left[\frac{3X_{\text{ext}}(\bar{c} - c_{\alpha\beta}^{\infty})}{4\pi N_v c_{\beta\alpha}} \right]^{1/3}$$

$$(a) \Rightarrow \quad \text{----- (b)}$$

Differentiating equation (a) wrt t ,

$$\frac{dX_{\text{ext}}}{dt} = 4\pi r^2 \frac{dr}{dt} \frac{N_v c_{\beta\alpha}}{(\bar{c} - c_{\alpha\beta}^{\infty})} \quad \text{----- (c)}$$

Where, Growth rate U :

$$\frac{dr}{dt} = U = \frac{D(\bar{c} - c_{\alpha\beta}^{\infty})}{r(c_{\beta\alpha} - c_{\alpha\beta}^{\infty})} \quad \text{for } r \geq r^* \quad \text{----- (d)}$$

Substituting for r & dr/dt in eqn (c) we get,

$$\begin{aligned} \frac{dX_{\text{ext}}}{dt} &= \frac{4\pi D N_v c_{\beta\alpha}}{(c_{\beta\alpha} - c_{\alpha\beta}^{\infty})} \left[\frac{3X_{\text{ext}}(\bar{c} - c_{\alpha\beta}^{\infty})}{4\pi N_v c_{\beta\alpha}} \right]^{1/3} \\ &= D N_v^{2/3} X_{\text{ext}}^{1/3} \kappa \quad \text{----- (e)} \end{aligned}$$

Where,

$$\kappa = \left[\frac{48\pi^2 c_{\beta\alpha}^2 (\bar{c} - c_{\alpha\beta}^{\infty})}{(c_{\beta\alpha} - c_{\alpha\beta}^{\infty})^3} \right]^{1/3}$$

Integrating eqn (e) we get,

$$\int_0^X \frac{dX_{\text{ext}}}{X_{\text{ext}}^{1/3}} = DN_0^{2/3} \kappa \int_0^t dt$$

OR

$$X = \left(\frac{2}{3} D_{\alpha} N_0^{2/3} \kappa \right)^{3/2} t^{3/2}$$

Above equation is not valid for Impingement of β - particle.

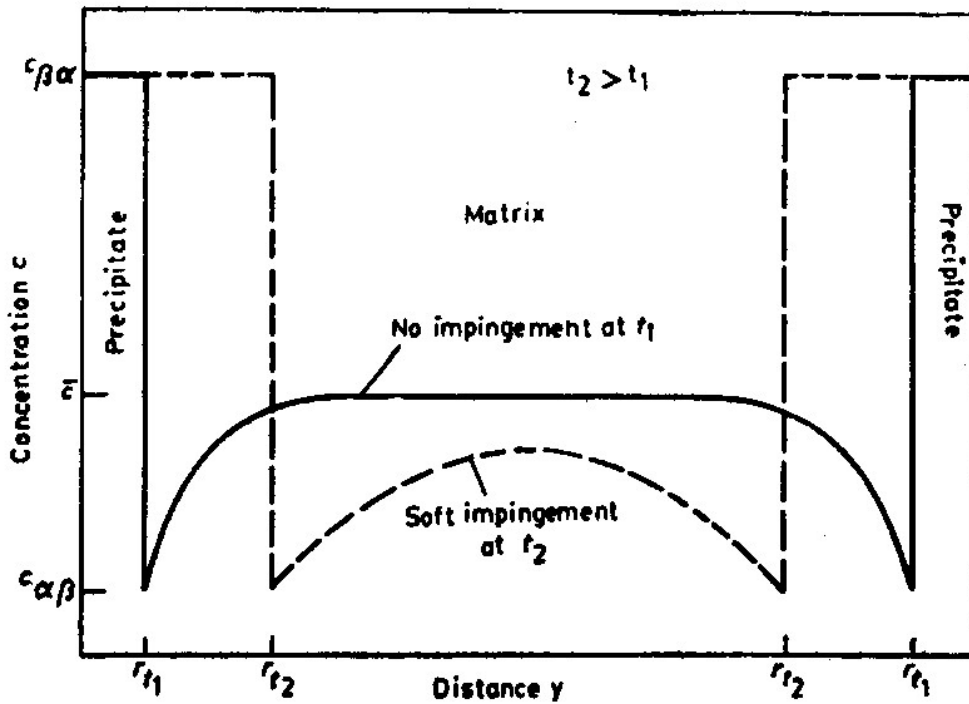


Fig. 6.6 During soft impingement, the diffusion fields of neighbouring precipitate particles overlap.

$$\frac{dX}{dt} = \frac{(1 - X) dX_{\text{ext}}}{dt}$$

Rearranging and Integrating we get,

$$X \approx 1 - \exp \left[- \left(\frac{2}{3} D_{\alpha} N_0^{2/3} \kappa \right)^{3/2} t^{3/2} \right]$$

So time exponent is 3/2 & reaction rate constant is $K = \frac{2}{3} D_{\alpha} N_0^{2/3} \kappa$.

Lecture 11

Phase Diagram

Equilibrium Diagram/ Constitutional Diagram / Phase Diagram:

It is a map which gives relationship between phases in equilibrium in a system as a function of temperature, pressure & composition.

They correspond to state of minimum free energy of system- stable states of a metal/alloy.

When graphical representation deals with phases which are in equilibrium with the surroundings, it is called an Equilibrium diagram otherwise it is called Phase diagram.

Example: In Iron-Carbon system, stable phases are solid solution of C in Iron & Graphite. But under normal conditions, solid solution & compound Fe₃C (cementite) are formed.

The graphical representation of Fe- Fe₃C system is a Phase diagram/metastable diagram but that of Iron-Graphite is an Equilibrium diagram.

Phase Rule:

It is the rule which relates the independent thermodynamic variables i.e. P & T to that of no. of components & phases present in the system.

Changes in no. of phases in an alloy under equilibrium conditions are expressed by Gibb's Phase rule.

Gibbs phase rule is stated as: $F = C - P + 2$

Where F- degree of freedom, C- no. of components, P- no. of phases in system.

N.B.-

For a system with P phases, total variables = $P(C-1) + 2$.

Degree of freedom F is equal to or less than the total no. of variables i.e.

$$F = C - P + 2 \leq P(C-1) + 2$$

For a single phase system (P=1), $F = C + 1 \leq C + 1$

Degree of freedom cannot be less than zero.

F decreases as no. of phases increase.

For binary phase diagrams, pressure variable & vapour phase is ignored. So

$$F = C - P + 1 \text{ -----} \rightarrow \text{Condensed phase rule.}$$

Classification of equilibrium diagram on basis of no. of components in system :

- Single component (Unary diagram)
- Two component (Binary system)
- 3- component (Ternary diagram)
- 4-component (Quaternary diagram)
- 5- component (Quinary diagram)

Important phase changes in unary and binary systems:

Let us start with the simplest system possible: the unary system wherein there is just one component. Though there are many possibilities even in unary phase diagrams (in terms of the axis and phases), we shall only consider a T-P unary phase diagram.

- Let us consider the Fe unary phase diagram as an illustrative example.
- Apart from the liquid and gaseous phases many solid phases are possible based on crystal structure. (Diagram on next page).
- Note that the units of x-axis are in GPa (i.e. high pressures are needed in the solid state and liquid state to see any changes to stability regions of the phases).
- The Gibbs phase rule here is: $F = C - P + 2$. (2 is for T & P).
- Note that how the phase fields of the open structure (BCC- one in the low T regime (α) and one in the high T regime (δ)) diminish at higher pressures. In fact δ phase field completely vanishes at high pressures.
- The variables in the phase diagram are: T & P (*no composition variables here!*).
- Along the 2 phase co-existence lines the DOF (F) is 1 →i.e. we can chose either T or P and the other will be automatically fixed.

The 3 phase co-existence points are *invariant points* with $F = 0$. (Invariant point implies they are fixed for a given system).

The degrees of freedom for regions, lines and points in the figure are marked in the diagram shown before

- The effect of P on the phase stability of various phases is discussed in the diagram below

- It also becomes clear that when we say iron is BCC at RT, we mean at atmospheric pressure

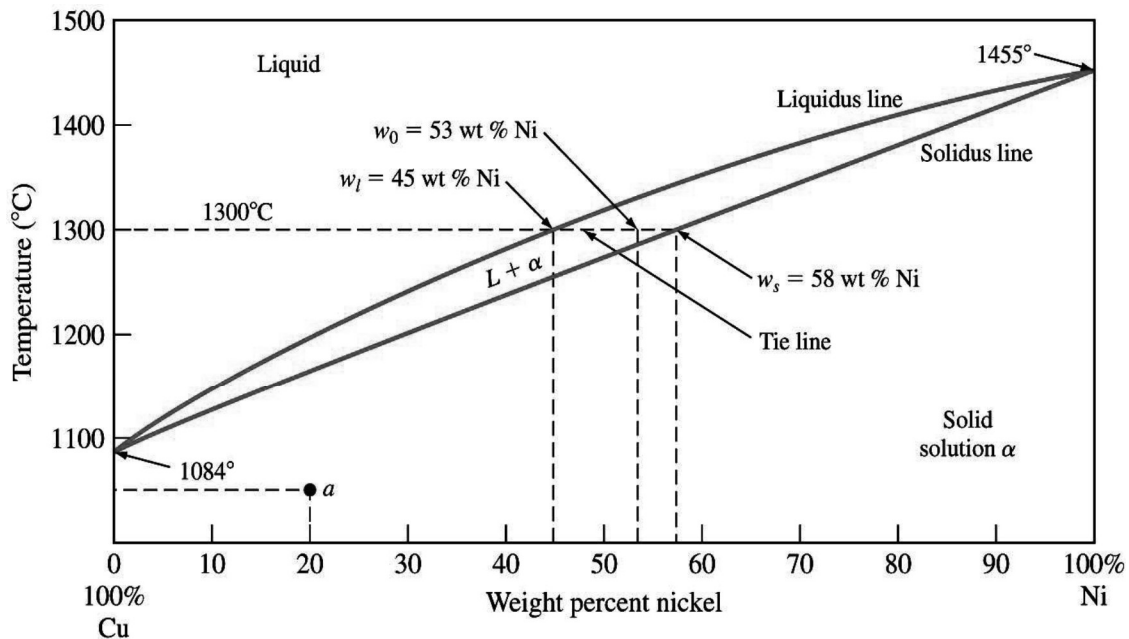
Binary Phase Diagrams

- Binary implies that there are two components.
- Pressure changes often have little effect on the equilibrium of solid phases (unless of course we apply 'huge' pressures).
- Hence, binary phase diagrams are usually drawn at 1 atmosphere pressure.
- The Gibbs phase rule is reduced to:
- Variables are reduced to: $F = C - P + 1$. (*1 is for T*).
- T & Composition (*these are the usual variables in Materials Phase Diagrams*)

ISOMORPHOUS SYSTEM:

When two metals (in metallic system) are completely soluble in each other in all proportions, both in the liquid and the solid states, this is called isomorphous system, because only a single type of crystal structure is obtained for all ratios of the components, that is, they form substitutional solid solution in all proportions.

Example: Cu- Ni system



Liquidus line: the line connecting T_s at which liquid starts to solidify under equilibrium conditions

Solidus: the temperature at which the last of the liquid phase solidifies.

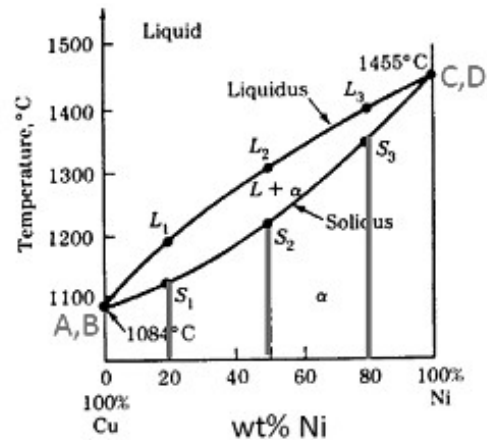
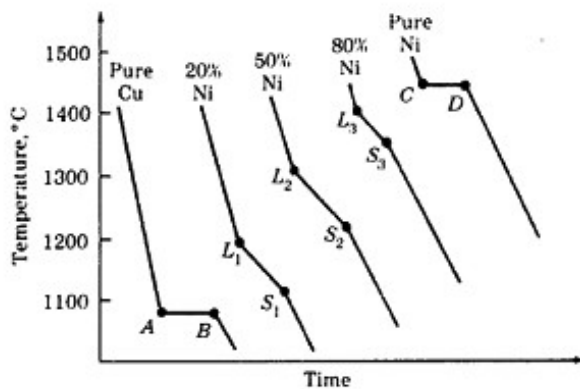
Between liquidus and solidus: $P=2$

M.P of Cu = 1084°C

M.P of Ni = 1455°C

Liquid phase (homogeneous)

α phase: substitutional solid solution



- Series of cooling at different metal composition are first constructed.
- Point of change of slope of cooling curves(thermal arrests) are noted and phase diagram is constructed.
- Pure metals solidifies at a constant temperature which is known as the melting temperature
- Binary alloys solidifies over a range of temperatures
- ❖ Phase rule can be applied at the freezing point of copper (or nickel), $C=1$, $P=2$ and $F=1-2+1=0$ (invariant point)
- ❖ For the single phase region , any point above the liquidus ($P=1$, liquid), or below the solidus ($P=1$, solid solution), $F=2-1+1=2$ (bivariant point)

- ❖ In the two phase region (between liquidus and solidus)
 $F = 2 - 2 + 1$
 $= 1$ (univariant point)

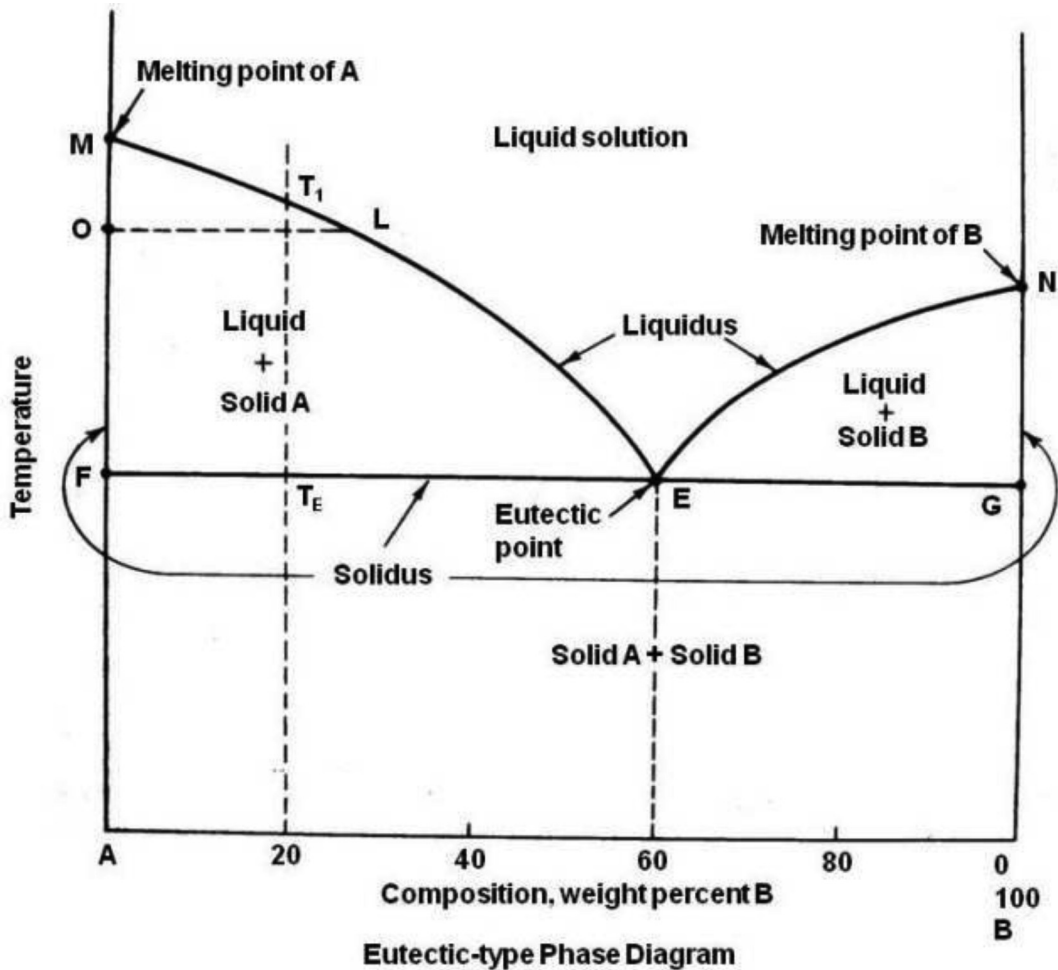
EUTECTIC SYSTEM:

In eutectic system two components are completely soluble in liquid state and are completely insoluble in solid state.

Example:

Pb(FCC) and Sn (tetragonal) -solder systems
 Fe (BCC) and C (graphite -hexagonal)-cast irons
 Al (FCC) and Si (diamond cubic)-cast aluminum alloys
 Cu(FCC) and Ag(FCC) –high temperature solder Cu

Liquid(L) \longleftrightarrow Solid solution -1(α) + Solid solution- 2(β)



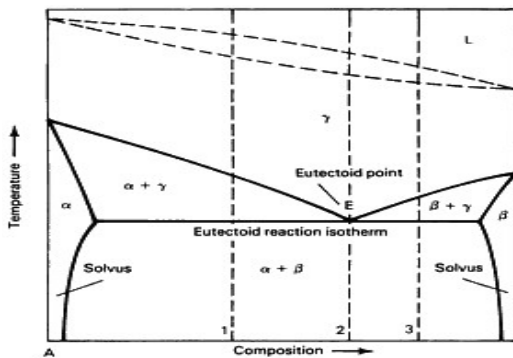
Lecture 12

Phase diagrams (continued...)

Phase diagrams showing Solid-state Phase Transformation:

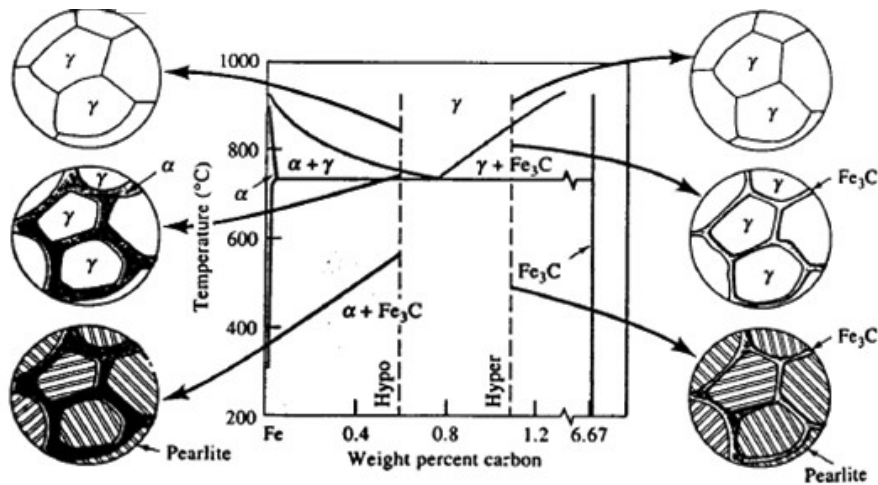
EUTECTOID SYSTEM:

Eutectoid reaction is similar to the eutectic reaction, but involves only solids. Here a solid solution upon cooling to some critical temperature, called eutectoid temperature, is seen to transform completely through alternate precipitation of two solid phases.



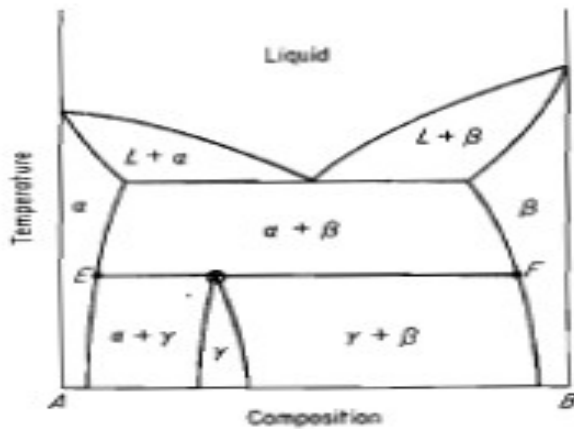
Hypoeutectoid

Hypereutectoid



PERITECTOID SYSTEM:

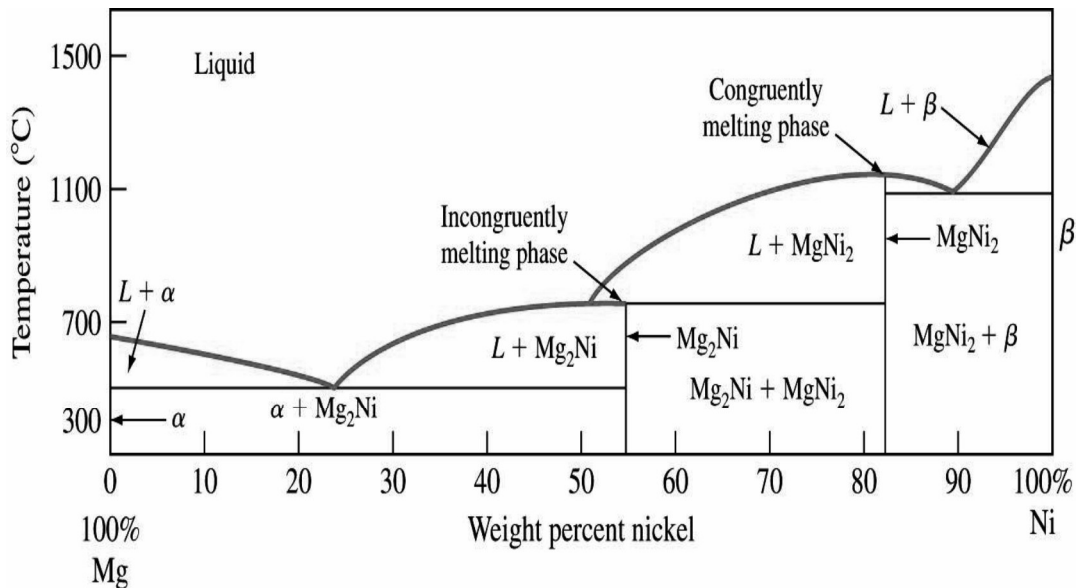
Peritectoid reaction is related to the peritectic reaction as does a eutectoid reaction to a eutectic. It occurs in the solid state (only solids are involved in it) due to thermal instability of a specific phase.



Phase Diagrams with Intermediate Phases and Compounds:

Terminal phase: a solid solution of one component in another for which one boundary of the phase field is a pure component

Intermediate phase: a phase whose composition range is between those of terminal phases.



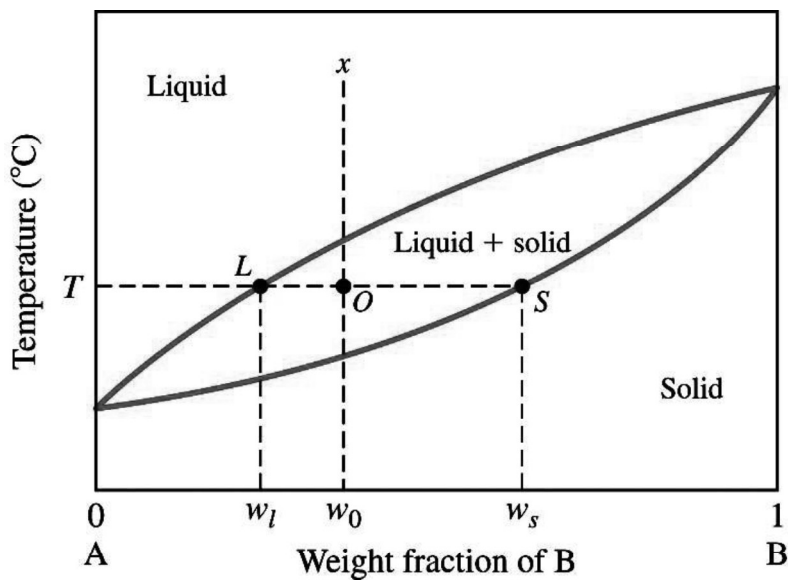
LEVER RULE:

The weight percentages of the phases in any 2 phase region can be calculated by using the **lever rule**.

Consider the binary equilibrium phase diagram of elements A and B that are completely soluble in each other

Let x be the alloy composition of interest, its mass fraction of B (in A) is C_0 .

Let T be the temperature of interest \Rightarrow at T alloy x consists of a mixture of liquid (with C_L - mass fraction of B in liquid) and solid (C_S - mass fraction of B in solid phase)



w_s & w_l be the fractional amounts by weight of solid and liquid respectively.

Since we have only 2 phases:

$$w_L + w_s = 1 \dots\dots\dots(1)$$

Conservation of mass requires i.e. the mass of metal B distributed between the two phases (liquid and the solid) must equal the mass of metal B in the overall alloy, and this can be expressed as:

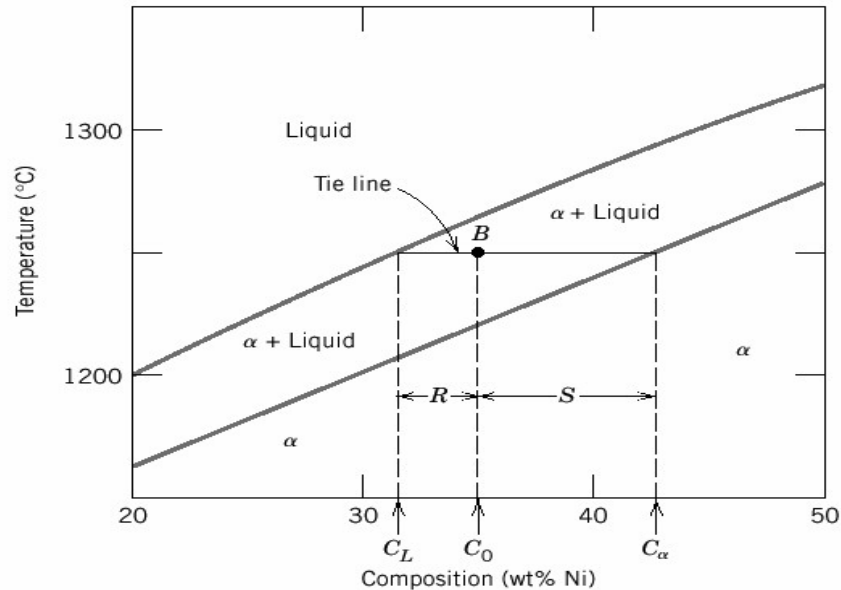
$$w_s C_s + w_L C_L = C_0 \dots\dots\dots(2)$$

From 1st condition, we have: $w_s = 1 - w_L$

Sub- in to (2): $(1 - w_L) C_s + w_L C_L = C_0$

Solving for W_L and W_α gives :

$$W_L = \frac{C_\alpha - C_o}{C_\alpha - C_L} \quad W_\alpha = \frac{C_o - C_L}{C_\alpha - C_L}$$



$$C_o = 35 \text{ wt. } \%, \quad C_L = 31.5 \text{ wt. } \%, \quad C_\alpha = 42.5 \text{ wt. } \%$$

Mass fractions:

$$W_L = S / (R+S) = (C_\alpha - C_o) / (C_\alpha - C_L) = 0.68$$

$$W_\alpha = R / (R+S) = (C_o - C_L) / (C_\alpha - C_L) = 0.32$$

Tie – Line rule:

The composition of the phases in the two-phase region is not equal. Ni or Cu redistributes/partitions itself in different concentrations in the 2-phases.

The compositions of the co-existing phases are determined from the tie-line rule. A horizontal line (called the tie-line) is drawn at temp of interest T say 1300° C. The intersection of this line with liquidus gives composition of liquid= c_l & intersection with solidus gives composition of solid = c_s .

Utility/uses of Phase Diagrams:

Phase diagrams are of immense importance to a metallurgist.

- To predict the temperature at which freezing/melting begins/ends for any specific alloy composition in an alloy system.
- To predict the safe temperature of working or heat treatment.
- To determine the number of phases, types of phases, composition of phases present in any given alloy at a specific temperature.
- To predict the microstructure of an alloy at any given temperature.
- To choose the composition to develop best properties.
- To calculate the relative amounts of phases present in a two-phase alloy.

Lecture 13

Free energy - Composition diagrams

What will be nature of Free energy – Composition diagram to alloys belonging to binary systems having 3-phase equilibrium?

(1) For a binary system exhibiting complete solid solubility: Isomorphous System:

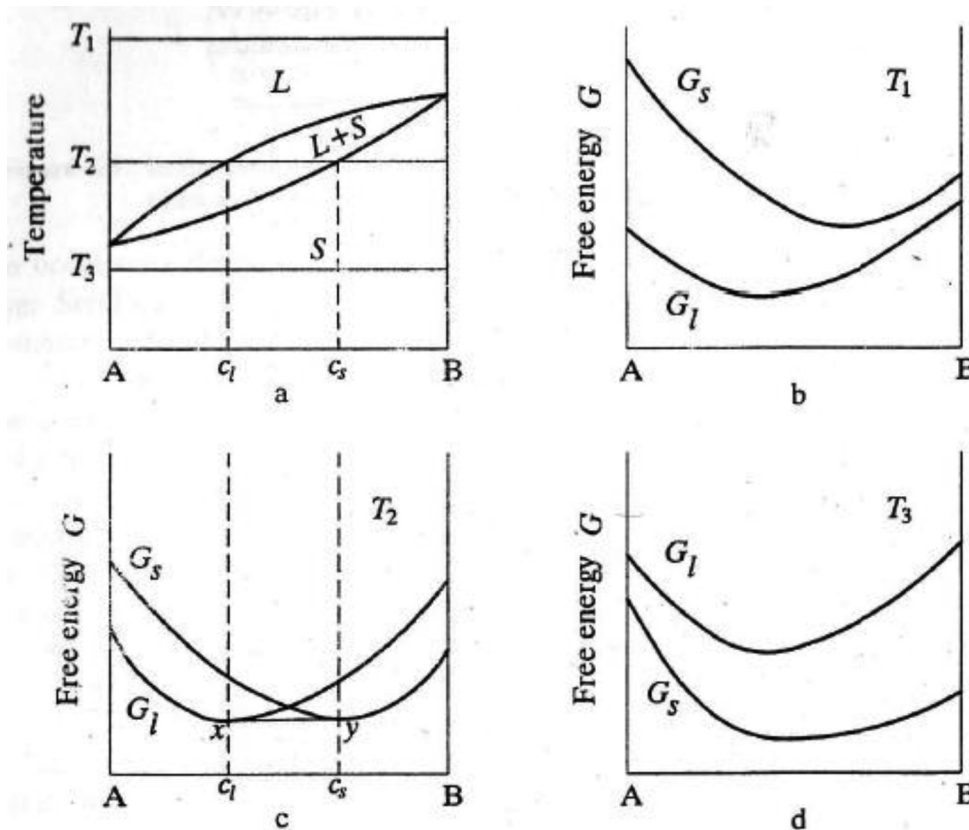


Fig. Free energy versus composition relationships for an isomorphous system at three different temperatures

Fig(a): **Phase** diagram for a binary system exhibiting complete solid solubility i.e. an Isomorphous system, showing 3 temperature T_1 , T_2 , T_3 .

Fig (b): Free energy curves for **temperature T_1** .

The liquid phase has a lower free energy than the solid at all compositions. So liquid is the stable phase.

Fig (c): Free energy curve for **temperature T_2** (which cuts across the 2 phase region). The corresponding free energy curves intersect each other.

There is a certain range of composition over which free energy of a mixture of liquid & solid phases are lower than either of the phases. This composition range is obtained by drawing a common tangent xy to the two curves. Compositions at point x & y are c_l & c_s respectively. Over the range of composition to the left of c_l , free energy of liquid is lower : so it is the stable phase.

For compositions to the right of c_s , solid phase is stable phase.

Fig (d): **At temperature T_3** , solid phase has lower free energy & is stable over the entire composition range.

(2) For a Eutectic system: For a binary system exhibiting complete liq solubility & partial solid solubility :

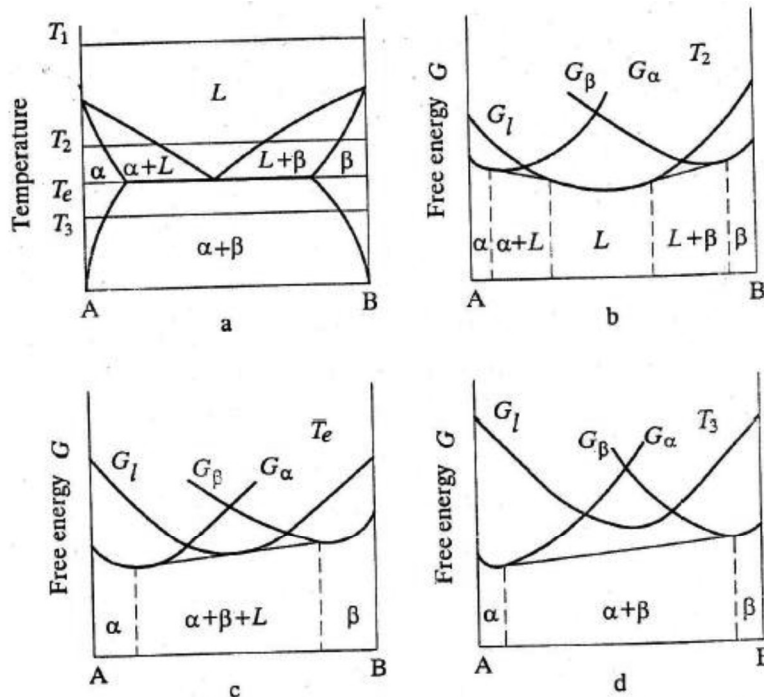


Fig. Free energy versus composition relationships for a simple eutectic system at three different temperatures

Here three phases α , β , L: so 3 free energy –composition curves i.e. G_α , G_β , G_L one for each phase.

Fig (a): Eutectic system.

Fig (b): At T_2 : liquid free energy curve intersects both α and β free energy curves.

Two common tangents are drawn to delineate the two-phase regions, on either side of the eutectic composition.

Fig (c): At eutectic temperature T_e , all 3 phases have same free energy curves.

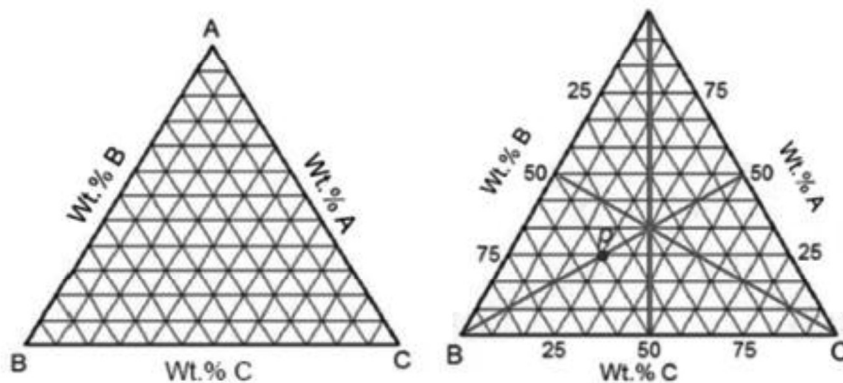
Fig (d): At T_3 , liquid phase has a higher free energy than either of the solid phases at all compositions & there is no liquid present at this temperature.

The α and β free energy curves intersect each other, the common tangent delineating the ($\alpha+\beta$) region of the phase diagram.

Lecture 14

TERNARY PHASE DIAGRAMS

Many useful metallic alloys (stainless steel, aluminium-based age-hardenable alloys) contain not just two important components, but three or more to obtain much greater improvements in the properties). To simplify the representation of three components, pressure is fixed at one atmosphere (i.e. pressure made constant), as three independent variables can only be specified i.e. two to define the composition and third to define the temperature (in ternary systems, % of the third component, say $C=100-\%A-\%B$). The most convenient figure is an equilateral triangle, Fig. also called Gibbs triangle.



-A ternary or three component phase diagram has the form of an triangular prism with an equilateral triangle as a base.

-Pure components are at each vertex, sides are binary compositions and ternary compositions are within the triangle.

-The composition lines on the triangle is constructed from projections of surfaces.

- The temperature varies along the height of the prism. The composition triangle is an isothermal section. Alternatively projections of different surfaces and lines can be shown as temperature contours.
- The composition of any point in the triangle is determined by drawing perpendiculars from corners to the opposite sided and measuring the distance of the point along the perpendicular.
- The point p lies for the isocomposition line 25% A along the perpendicular A-50. Hence, percentage of A in the alloy is 25%. Similarly B is 50% and C is 25%.

$$\% A = Bx = Cy$$

$$\% B = Cx' = Ay'$$

$$\% C = Ax'' = By''$$

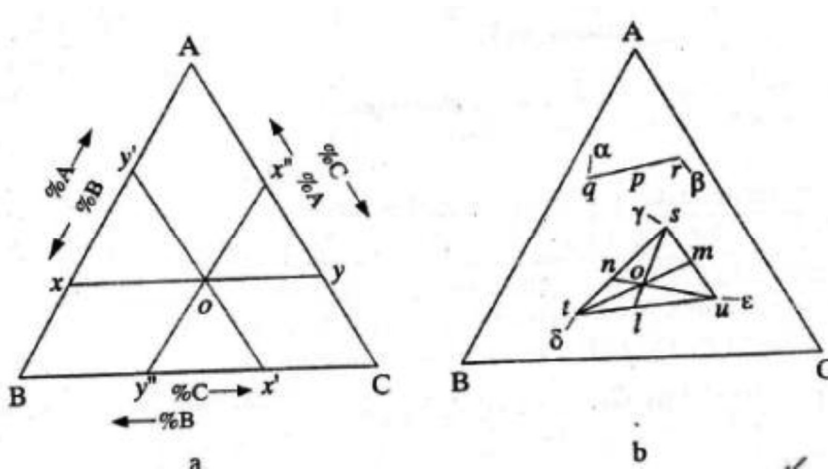


Fig. (a) the reading of composition on a ternary phase diagram, (b) use of the tie-line and the tie- triangle to calculate the relative amounts of coexisting phases.

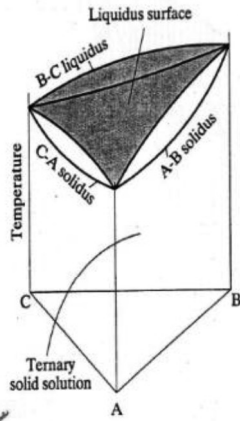


Fig. The three-dimensional view of the ternary phase diagram for the case of complex liquid and solid solubility.

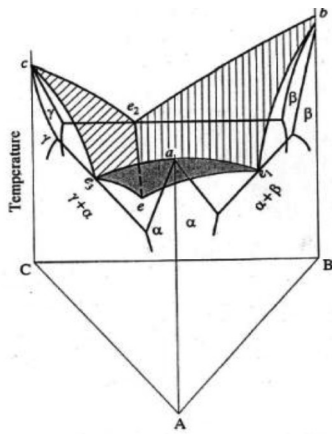


Fig. The three-dimensional view of the ternary phase diagram between three components, which pair up as simple binary eutectic systems.

Model questions:

1. In what type of transformation is a composition change is not possible.
2. In a Kirkendall diffusion experiment analysed by the Matano method, the following data are obtained:

Diffusion time $t=200\text{hrs}$, marker movement, $s= 1.44\text{mm}$, Interdiffusion coefficient $D= 10^{-11}\text{m}^2/\text{sec}$, compute D_A and D_B , slope of the penetration curve at the markers 0.2mm^{-1} , atom fraction of A 0.4.

- 3.

Module II

Lecture 15

Liquid-solid transformation: Solidification, nucleation and growth mechanisms and kinetics

Solidification is liquid to solid transformation in a material which is a first order phase transformation & occurs by nucleation and growth.

NUCLEATION: nucleation during solidification occurs heterogeneously at container walls in contact with the liquid and/or solid inclusion surfaces, if present in the liquid. Homogeneous nucleation may occur when negligible number of heterogeneous nucleation sites are available, e.g during solidification of small liquid droplets.

HOMOGENEOUS NUCLEATION:

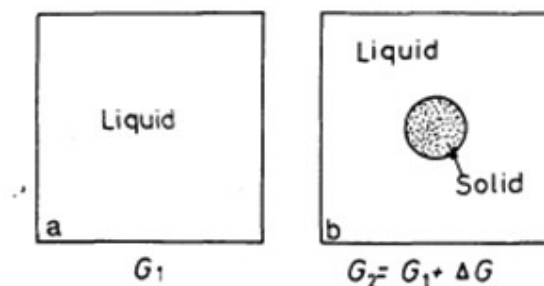


Fig. 1 homogeneous nucleation

A given volume of liquid at temperature ΔT below T_m with a free energy G_1 . Some of the atoms of liquid cluster together to form small sphere of solid, so free energy of system will change to G_2 .

$$G_2 = V_S G_V^S + V_L G_V^L + A_{SL} \gamma_{SL}$$

where V_S is the volume of the solid sphere, V_L the volume of the liquid, A_{SL} is the solid/liquid interfacial area, G_V^S and G_V^L are the free energies per unit volume of solid and liquid respectively and γ_{SL} the solid/ liquid interfacial free energy. The free energy of the system without any solid present is given by

$$G_1 = (V_S + V_L) G_V^L$$

The formation of solid results a change in free energy $\Delta G = G_2 - G_1$

$$\Delta G = -V_S \Delta G_V + A_{SL} \gamma_{SL} \dots \dots \dots (1)$$

and $\Delta G_V = G_V^L - G_V^S +$

for an undercooling ΔT , ΔG_V is given by

$$\Delta G_V = \frac{L v \Delta T}{T m}$$

Where $L v$ is the latent heat of fusion per unit volume.

N.B. - r^* and ΔG^* decrease with increasing Undercooling (ΔT). There is large increase in the rate of formation of critical nuclei, which gives more fine-grained solid metal.

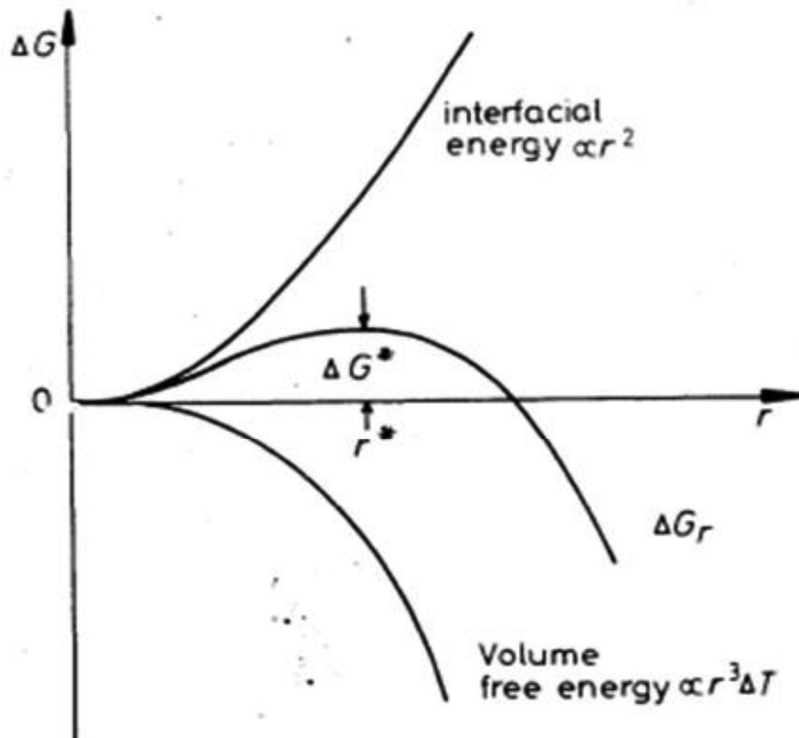


Fig.2 The free energy change associated with homogeneous nucleation of sphere of radius r

Since, Interfacial term increase as r^2 whereas volume free energy released only increases as r^3 , so creation of small particles of solid always leads to a free energy increase.

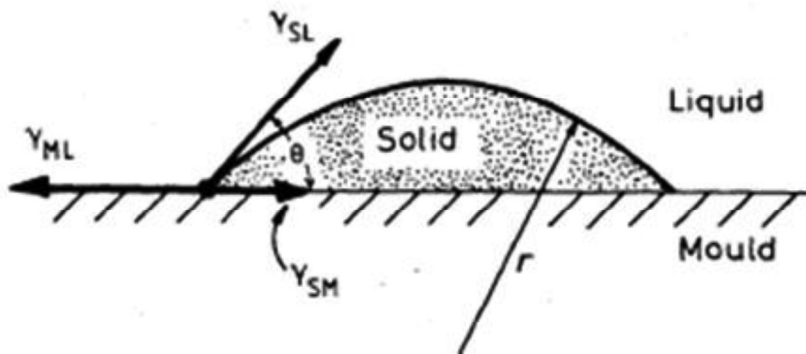
Total free energy ΔG passes through a maximum with increase in value of r. It is maximum at r^* .

If $r < r^*$, system can lower its free energy by dissolution of solid. Unstable solid particles with $r < r^*$ are known as Clusters/ Embryos.

When $r > r^*$, free energy of system decreases if solid grows. Stable particles with $r > r^*$, are called Nuclei.

Homogeneous nucleation rate as a function of undercooling ΔT

HETEROGENEOUS NUCLEATION:



Heterogeneous nucleation of spherical cap on flat mould wall

θ -> wetting angle/contact angle between embryo surface & mould wall.

If a solid embryo forms on mould wall as a spherical cap & under equilibrium condition following is the equation balancing the interfacial energies,

$$\gamma_{ML} = \gamma_{SM} + \gamma_{SL} \cos\theta$$

$$\cos\theta = (\gamma_{ML} - \gamma_{SM}) / \gamma_{SL}$$

The formation of such an embryo will be associated with an excess free energy given by

$$\Delta G_{\text{het}} = -Vs\Delta G_V + A_{\text{SL}}\gamma_{\text{SL}} + A_{\text{SM}}\gamma_{\text{SM}} - A_{\text{SM}}\gamma_{\text{ML}}$$

Where Vs is the volume of the spherical cap, A_{SL} and A_{SM} are the areas of the solid/liquid and solid/mould interfaces, and $\gamma_{\text{ML}}, \gamma_{\text{SM}}, \gamma_{\text{SL}}$ are the free energies.

$$\Delta G_{\text{het}} = \left\{ -\frac{4}{3}\pi r^3 \Delta G_V + 4\pi r^2 \gamma_{\text{SL}} \right\} S(\theta) \dots \dots \dots (2)$$

$$\text{Where } S(\theta) = (2 + \cos\theta)(1 - 4\cos\theta)^2/4$$

By differentiating equation 2, it can be shown that

$$r^* = \frac{2\gamma_{\text{SL}}}{\Delta G_V}$$

$$\text{and } \Delta G^* = \frac{16\pi\gamma_{\text{SL}}^3}{3\Delta G_V^2} S(\theta)$$

therefore the activation energy barrier against heterogeneous nucleation (ΔG^*_{het}) is smaller than (ΔG^*_{hom}) by the shape factor $s(\theta)$. In addition the critical nucleus radius (r^*) is unaffected by the mould wall and only depends on the undercooling. This result was to be expected since equilibrium across the curved interface is unaffected by the presence of the mould wall.

- ⇒ Activation energy barrier against heterogenous nucleation is smaller than the activation energy against homogenous nucleation by $S(\theta)$ (shape factor.)
- ⇒ So rate of heterogenous nucleation is much higher than rate of homogenous nucleation because $\Delta G^*_{\text{het}} < \Delta G^*_{\text{homo}}$.

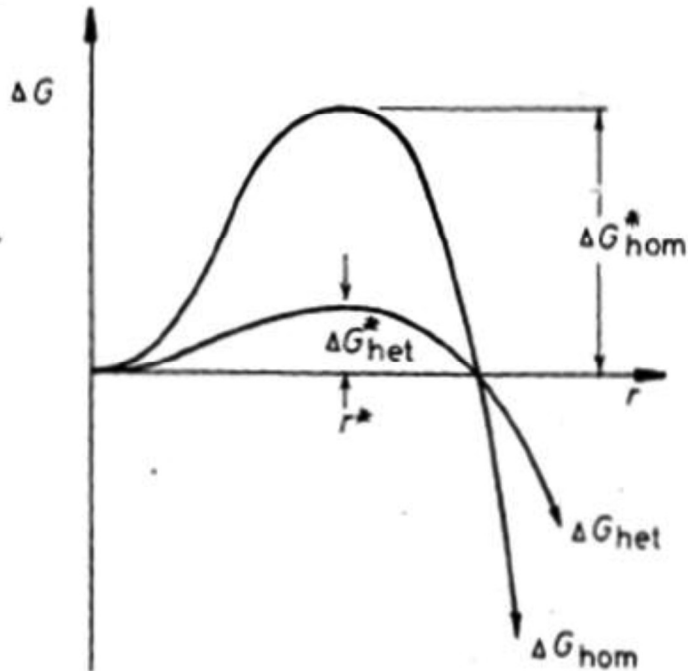


Fig. The excess free energy of solid clusters for homogeneous and heterogeneous nucleation. Note r^* is independent of the nucleation site

CONCLUSION:

Case I : If $\theta = 180^\circ$ i.e. point contact then : $\Delta G_{\text{het}}^* = \Delta G_{\text{homo}}^*$.

Case II : If $\theta = 0^\circ$ i.e. solid forms a thin film on mould wall , then : $\Delta G_{\text{het}}^* = 0$

i.e. there is no energy barrier to heterogenous nucleation & it can start just almost at freezing tempr i.e. nucleation occurs without supercooling.

Case III : If $\theta = 90^\circ$ then : $\Delta G_{\text{het}}^* = \frac{1}{2} \Delta G_{\text{homo}}^*$.

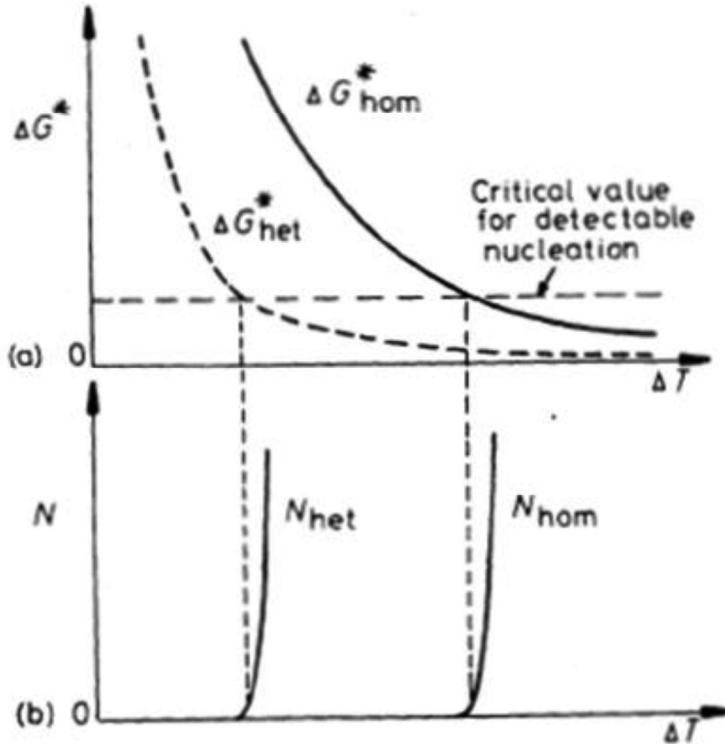


Fig.(a) Variation of ΔG^* with undercooling(ΔT) for homogeneous and heterogeneous nucleation. (b) the corresponding nucleation rates assuming the same critical value of ΔG^* .

GROWTH OF A PURE SOLID:

Growth mechanism and growth kinetics during solidification strongly depends on the nature of solid-liquid interfaces. When the interface is rough, rough interfaces migrate by a continuous growth process while flat interfaces migrate by a lateral growth process. An atom in liquid encounters an activation Gibbs energy (ΔG_D) during its transfer from liquid to solid and when it becomes part of the solid its Gibbs energy is reduced by Δg . Hence an atomic transfer from solid to liquid encounters an activation barrier of $(\Delta G_D + \Delta g)$.

$$\Delta g = \frac{L\Delta T}{T_m}$$

Where L is the latent heat of melting per atom, T_m is equilibrium melting point and $\Delta T = T_m - T$ is undercooling below T_m .

If N_L , N_S are number of atoms per unit area across the interface in liquid and solid, respectively, then number of atoms crossing the interface from liquid to solid, n_{L-S} and from solid to liquid n_{S-L} , per unit area per unit time can be written as:

$$n_{L-S} = N_L \nu \exp\left(-\frac{Q}{kT}\right)$$

$$n_{S-L} = N_S \nu \exp\left(-\frac{Q+(L\Delta T/Tm)}{kT}\right)$$

where ν is vibrational frequency of atoms normal to the interface and k is Boltzmann's constant. If average jump distance across the interface is a and assuming $N_S = N_L = N$, growth velocity of the interface v ,

$$v = \frac{a}{N} (n_{L \rightarrow S} - n_{S \rightarrow L}) = a \nu \exp\left(-\frac{Q}{kT}\right) \left[1 - \exp\left(\frac{L\Delta T}{kT_m T}\right)\right]$$

at small undercooling, when $\frac{L\Delta T}{kT_m T} \ll 1$

$$v = a \nu \left[\frac{L\Delta T}{kT_m T}\right] \exp\left(-\frac{Q}{kT}\right)$$

hence growth velocity of a rough solid-liquid interface at low undercooling is directly proportional undercooling ΔT .

Smooth surfaces:

Assuming that growth during solidification is dominated by transfer of atoms to a set of most favourable sites, growth equation can be modified by introducing a correction factor f

$$v = a \nu f \left[\frac{L\Delta T}{kT_m T}\right] \exp\left(-\frac{Q}{kT}\right)$$

Growth Kinetics

Many transformations occur as a result of continuous formation of critical nuclei in the parent phase and the subsequent growth of the particles. Growth is the increase in size of the particle after it has nucleated i.e. growth kinetics become important once an embryo has exceeded the critical size and become a stable nucleus. Growth may proceed in two radically different manners. In one type of growth, individual atoms move independently from the parent to the product phase, thus it is diffusion controlled and is thermally activated. In the other type of growth that occurs in solid-solid transformations many atoms move cooperatively without thermal assistance. Growth that is diffusion controlled is more common the other. Growth usually occurs by the thermally activated jump of atoms from the parent phase to the product phase. The unit step in the growth process thus consists of an atom leaving the parent phase and jumping across the interface to join the product phase. At the equilibrium temperature,

both phases have the same free energy, hence the frequency of jumps from parent phase to product phase will be equal to that from product phase to parent phase i.e. the net growth rate is zero. At lower temperatures, product phase is expected to have lower free energy, and thus a net flow of atoms from parent phase to product phase. This net flux of atoms results in interface motion i.e. growth rate is taken as the rate of increase of a linear dimension of a growing particle. As a function of temperature, the growth rate first increases with increasing degree of supercooling, but eventually slows-down as thermal energy decreases. This is same as for nucleation; however the maximum in the growth rate usually occurs at a higher temperature than the maximum in the nucleation rate. Figure-(a) depicts the temperature dependence of nucleation rate (U), growth rate (I) and overall transformation rate (dX/dt) that is a function of both nucleation rate and growth rate i.e. $dX/dt = f_n(U, I)$. On the other-hand, the time required for a transformation to completion has a reciprocal relationship to the overall transformation rate. Temperature dependence of this time is shown in figure-(b).

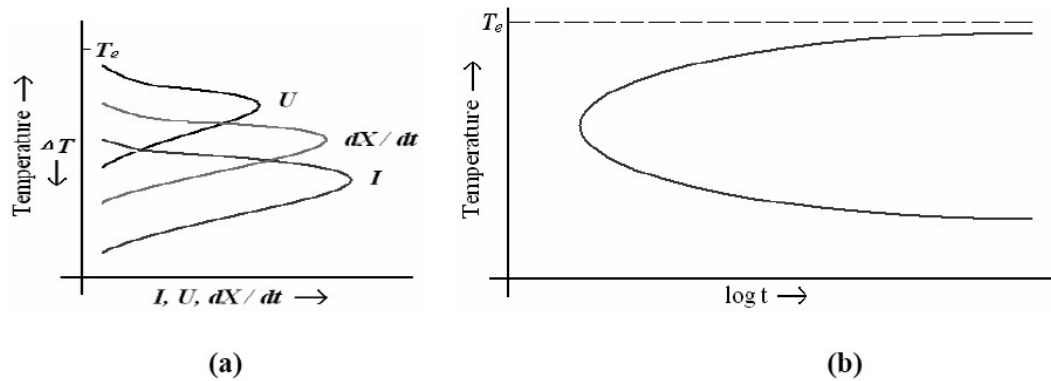


Fig. (a) Temperature dependence of rates, (b) Time dependence of transformation as a function of temperature.

LECTURE 16

Alloy solidification – cellular and dendritic morphology

When a solid freezes with a composition different from that of the liquid from which it forms such alloys have separate curves for solidus and liquidus such as in an isomorphous system.

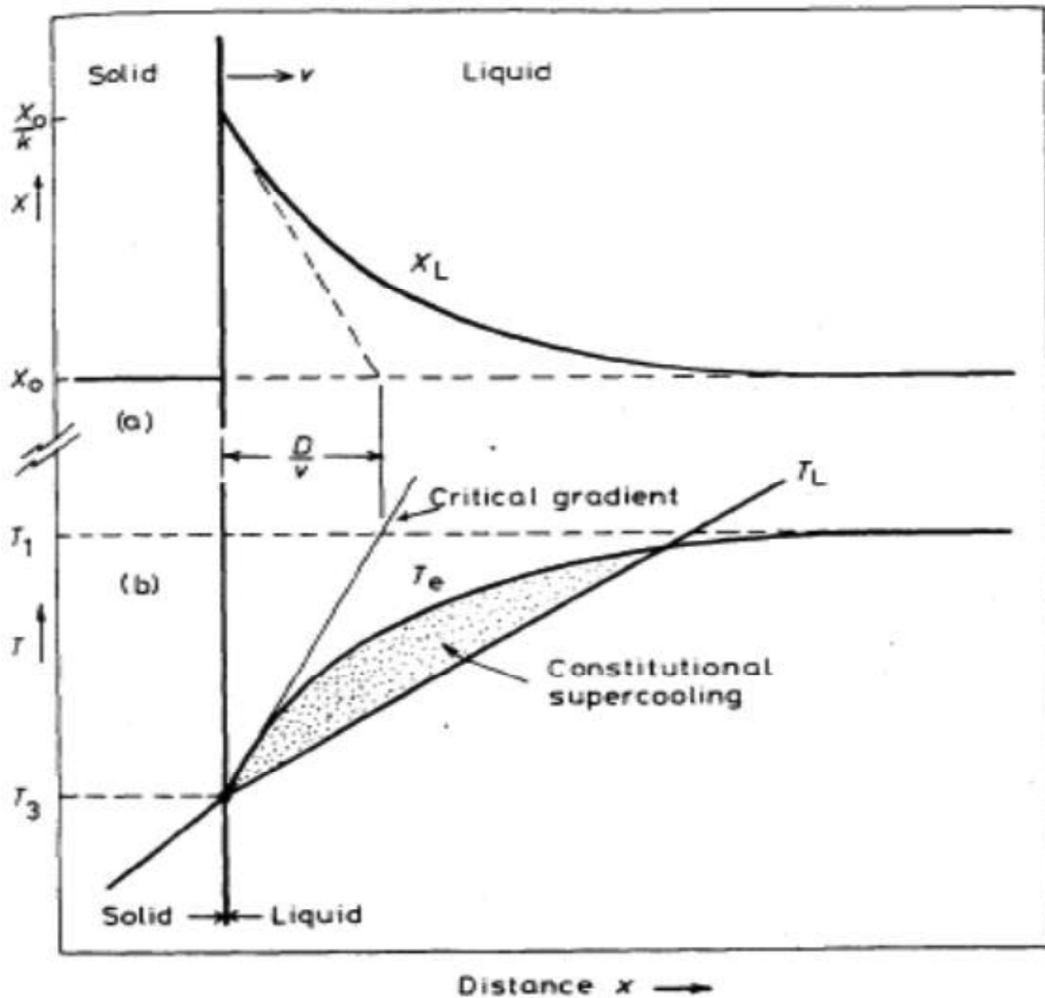


Fig.1 The origin of constitutional supercooling ahead of a planar solidification front. (a) Composition profile across the solid/liquid interface during steady-state solidification. The dashed line shows $\frac{dx_L}{dx}$ at the S/L interface. (b) The temperature of the liquid ahead of the solidification front follows line T_L . The equilibrium liquidus temperature for the liquid adjacent to the interface varies as T_e . Constitutional Supercooling arises when T_L lies under the critical gradient.

If the temperature gradient $<$ critical value (b), the liquid in front of solidification front exists below its equilibrium freezing temperature i.e. it is super cooled. Supercooling arises from compositional or constitutional effects, it is known as Constitutional supercooling.

When a liquid metal is poured in a metallic mould, the freezing starts from the mould wall. Thus temperature is lowest at the mould wall and rises towards the center of the mould. The increase of temperature of the liquid can be safely assumed to be linear with distance. But the freezing point of the liquid as a function of the distance from the interface is a curved graph as illustrated by second curve. In this liquid layer of x thickness the freezing point is higher than the actual temperature of the alloy. i.e. this layer of liquid is effectively supercooled. The amount of supercooling increases as one moves from the interface towards inside the liquid. This is called constitutional supercooling as it is due to the constitution of the alloy i.e. due to the concentration gradient in the liquid in front of the surface.

Under steady state growth the critical gradient can be seen from the fig. 1 to be given by $(T_1 - T_3)/(D/v)$ where T_1 and T_3 are the liquidus and solidus temperatures for the bulk composition X_0 .

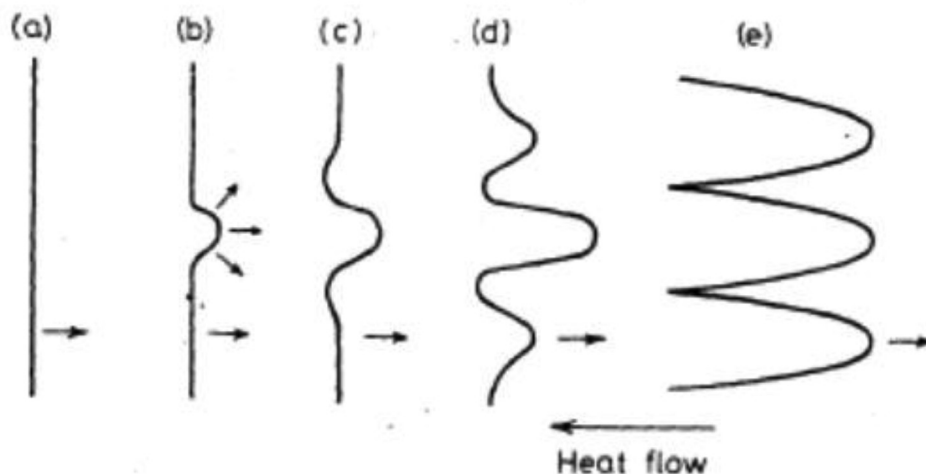


Fig.2 The breakdown of an initially planar solidification front into cells

(b) Formation of first protrusion causes solute to be rejected laterally & pile up at the root of protrusion. This lowers equilibrium solidification temperature causing recesses to form (c), which in turn trigger formation of other protrusion (d). Eventually protrusions develop into long arms or cells growing parallel to the direction of heat flow (e).

The solute rejected from the solidifying liquid concentrates into the cell walls which solidify at the lowest temperatures.

The tips of the cells grow into the hottest liq & therefore contain least solute. Cellular microstructures are only stable for a certain range of temperature gradients.

At sufficiently low temperature gradients the cell, or primary arms of solid are observed to develop secondary arms and at still lower tempr gradients tertiary arms develop i.e. Dendrites form.

Tendency to form dendrites increases as solidification range increases. Therefore, the effectiveness of different solutes can vary widely.

Reasons for change from cells to dendrites : It is probably associated with the creation of constitutional supercooling in the liquid between the cells causing interface instabilities in the transverse direction .

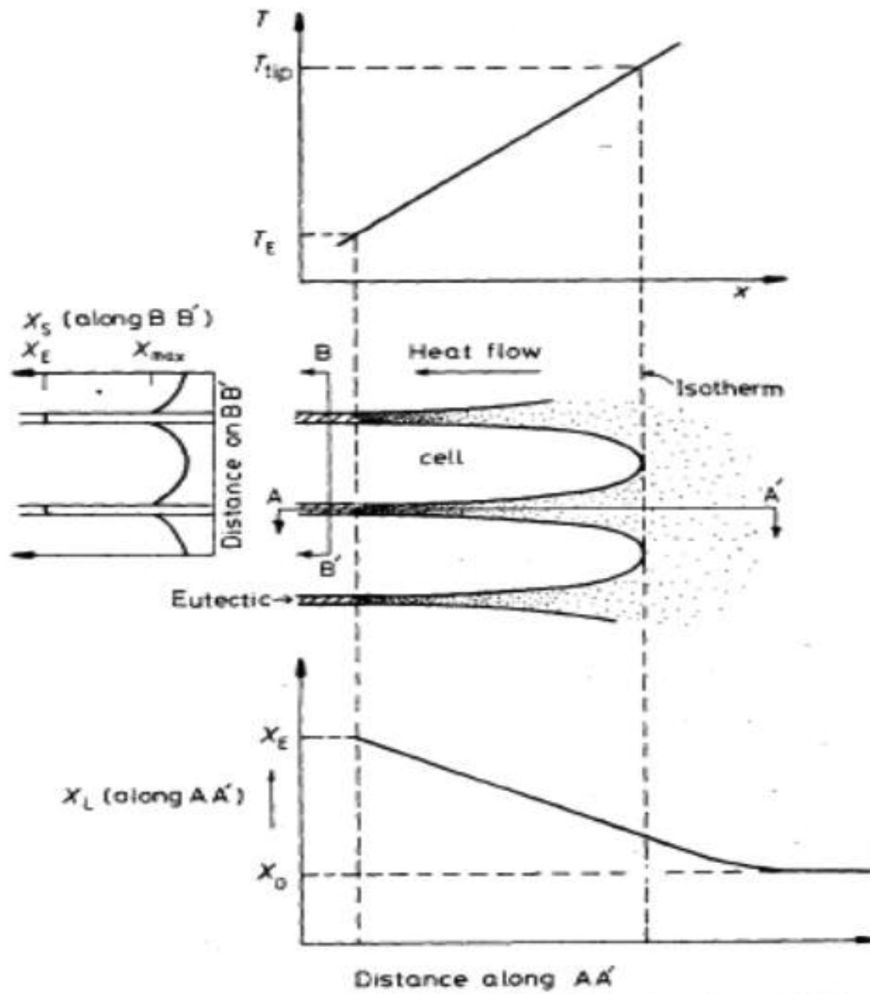


Fig. 3 Temperature and solute distribution associated with cellular solidification.

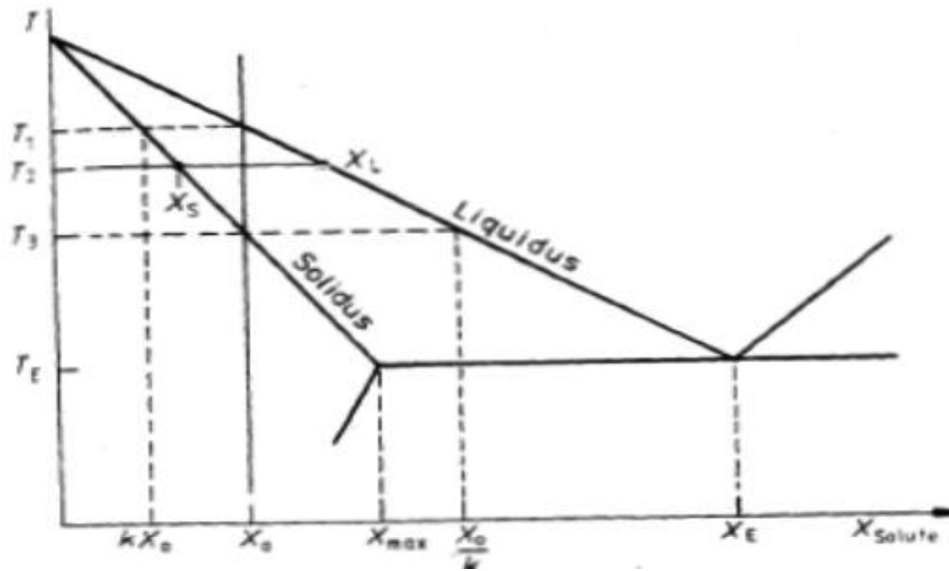


Fig. 4 Unidirectional solidification of alloy X_0

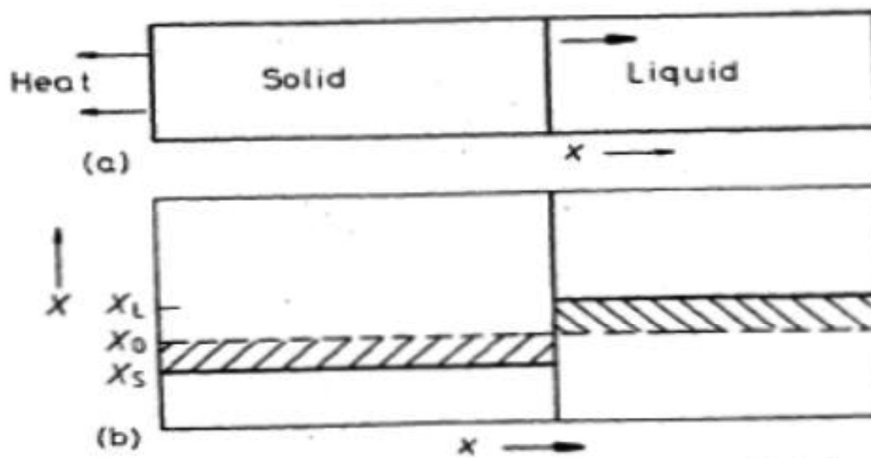


Fig.5.(a) A planar S/L interface and axial heat flow. (b) Corresponding composition profile at T_2 assuming complete equilibrium. Conservation of solute requires the two shaded areas to be equal.

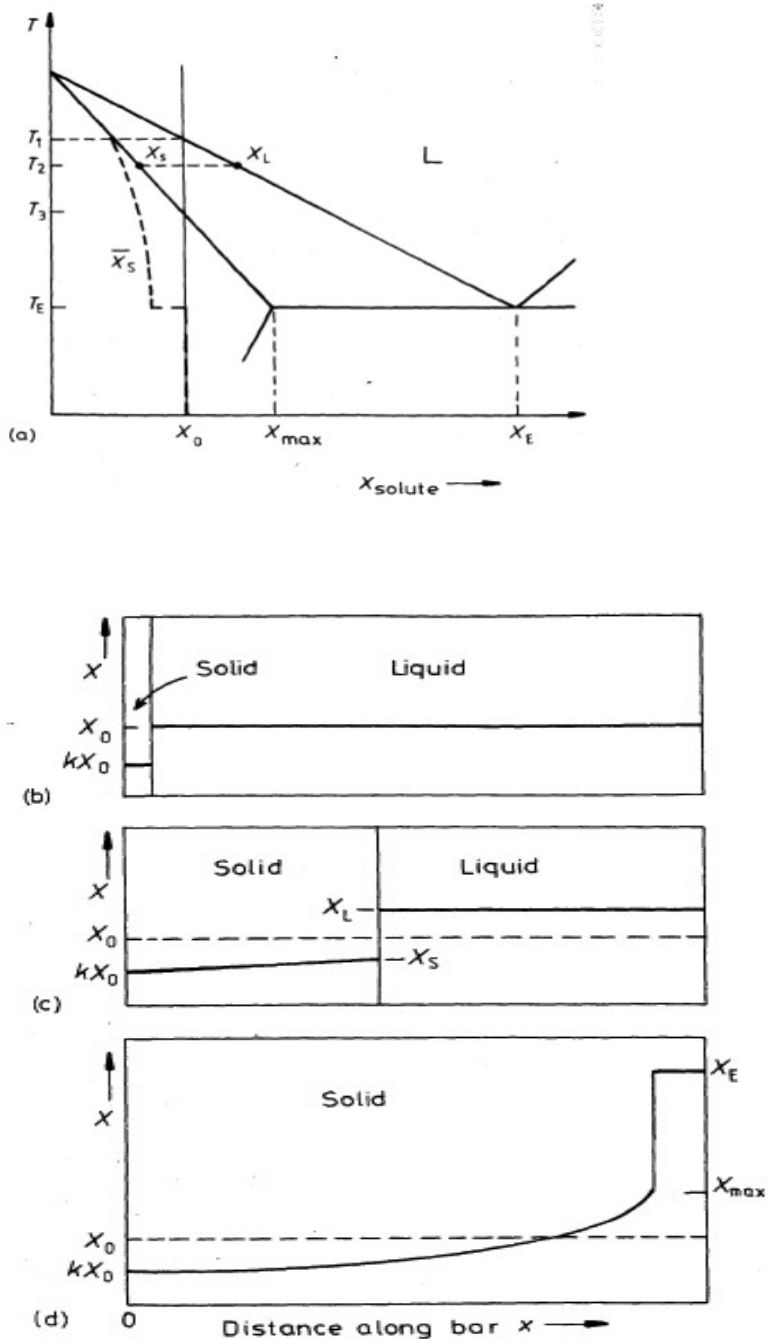


Fig. 4.21 (continued)

Fig. Planar front solidification of alloy X_0 in Fig.4, assuming no diffusion in solid, but complete mixing in the liquid. (a) As fig. 4, but including the mean composition of the solid. (b) composition profile just under T_1 . (c) Composition profile at T_2 , (d) compositional profile at the eutectic temperature and below.

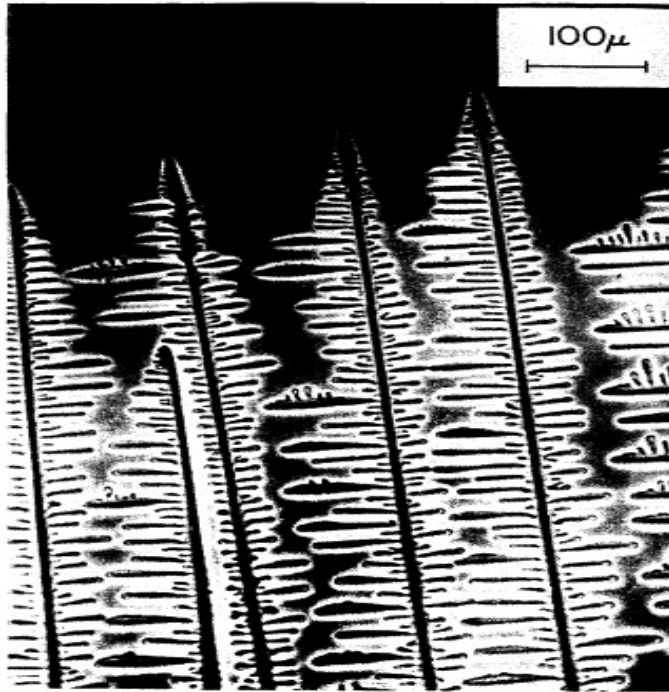


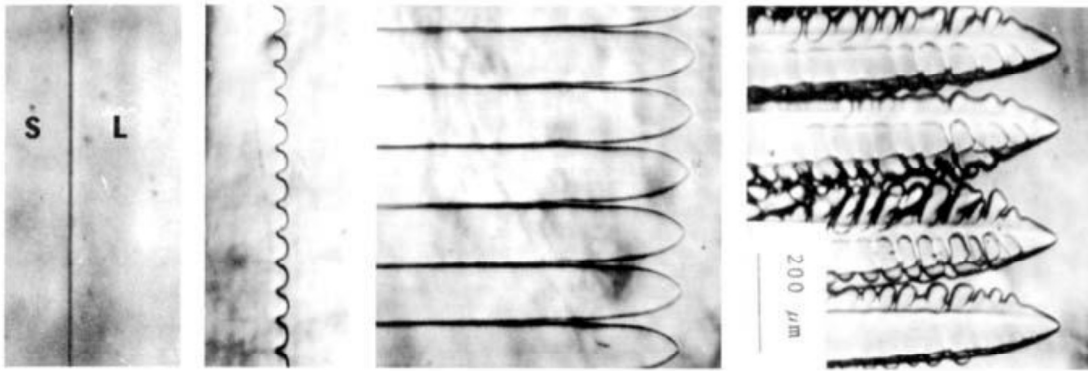
Fig. 4.28 Columnar dendrites in a transparent organic alloy. (After K.A. Jackson in: *Solidification*, American Society for Metals, 1971, p. 121.)

Morphological development of the s/l front

planar

cellular

dendritic



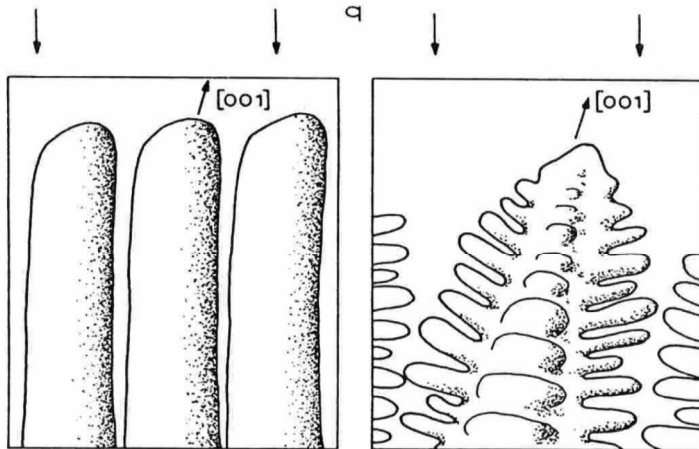
Increasing const. undercooling →

Cellular growth

- Cells grow at low constitutional undercooling
- No side branching

- Direction antiparallel to heat flow
- Accumulation of solute between cells
- Adjustment of cell spacing by stopping or division of cells

Transformation from cells to dendrites



- Dendrites form at higher const. undercooling
- Side branches
- Growth in preferred crystallographic directions

Summary/ Conclusions :

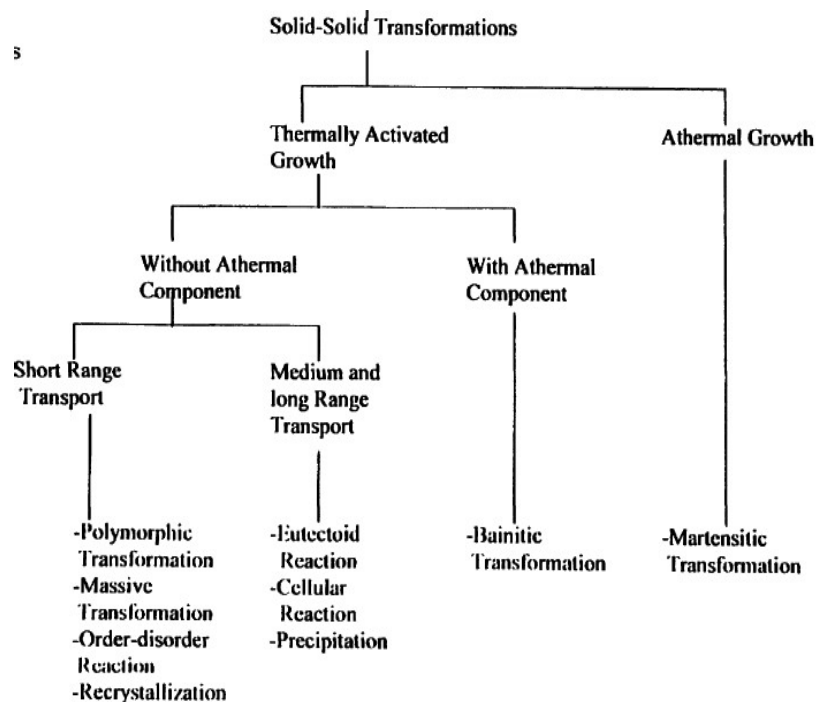
- Solute in an alloy will redistribute during solidification. In eutectic systems ($k < 1$), alloying elements will enrich in the liquid.
- With limited diffusion, solute will pile up at the s/l interface and form a boundary layer. Width of the boundary layer is inversely proportional to growth rate
- At steady state the boundary layer is fully developed. Growth of a solid with constant composition = C_0
- The liquid boundary layer causes local variations of liquidus temperature ahead of the s/l interface. If the liquidus temperature gradient, mG_c is larger than the actual temperature gradient, G , the liquid will be constitutionally undercooled.
- Constitutional undercooling occurs in most casting operations of alloys
- Constitutional undercooling leads to breakdown of a planar growth front

- Cells form at low constitutional undercooling, just after breakdown of planar front. Cells have no side branches and grow independent of crystallographic orientation, antiparallel to heat flow. Cells grow at temperatures far below liquidus.
- Dendrites grow at high constitutional undercooling. They grow just below liquidus in preferred crystallographic directions.
- Solute diffuses radially at the dendrite tip. Growth undercooling and growth morphology is determined by curvature and diffusion.
- Dendrites are characterized by a primary arms (trunk) with a spacing, λ_1 , and secondary arms (branches) with spacing λ_2 .
- Dendrites coarsen as they grow increasing λ_2 with local solidification time.

Lecture 18

Solid state diffusive transformation: Classification of solid-solid transformations; Nucleation in solids

Classification of solid- solid transformation:



Polymorphic transformation, massive transformation, order-disorder reactions and recrystallization categorized under phase changes occur by nucleation and thermally activated growth. Polymorphic transformation involves a change of structure but no change in composition. Polymorphic transformations in metals and ceramic materials are effected by the nucleation and growth of the lattice of the product phase. Massive transformation is characterized by no compositional change, the composition of the product phase remains the same as that of the parent phase. Martensitic transformation is a special type of solid-solid transformation in which single phase reactant transforms into a single phase product with a change of shape and without change in composition.

1.3.1. Buerger's classification of solid state phase transformations:

Based on changes in co-ordination and bond type, Buerger classified the solid state phase transformation into the following [7-9]:

- i. Transformations of first co-ordination
 - (a) Reconstructive (sluggish)
 - (b) Dilatational (rapid)
- ii. Transformations of second co-ordination
 - (a) Reconstructive (sluggish)
 - (b) Displacive (rapid)
- iii. Transformations of disorder
 - (a) Substitutional (sluggish)
 - (b) Rotational (Rapid)
- iv. Transformations of bond type (usually sluggish).

In transformation involving primary co-ordination by reconstructive transformation, the first co-ordination bonds are broken and reformed. Reconstructive transformation is sluggish in nature because the activation energy involved will be generally very high. This type of transformation gives rise to large discontinuities in cell dimensions. Another type of transformation involving primary co-ordination is dilatational. This is rapid compared to the reconstructive transformation.

The features of reconstructive transformations involving higher coordination may resemble those of the reconstructive first coordination transformations since changes in higher coordination may also have to proceed through the breaking of primary bonds. In some transformations, changes in higher coordination can be effected by a distortion of a primary bond. Such transformations may be called as distortional or displacive transformations. These distortional or displacive transformations will involve considerably smaller changes in energy and are usually fast.

Disorder transformations are thermodynamically of second or higher order, and many of them display first order characteristics. Buerger classifies order-disorder transformations in to two types; rotational and substitutional. Groups of tightly bound atoms in an ordered structure can rotate relative to the rest of the structure and so induce disorder. Rotational transformation has some characteristics of displacive transformation. Interchanging the position among atoms in random fashion can also cause disordering. Substitutional transformations are commonly found in metals and alloys. Buerger has defined transformation of bond type where two polymorphs differ greatly in nature of bonding. This transformation is normally sluggish in nature.

Typical classification:

Precipitation Transformations: Generally expressed as $\alpha' \longrightarrow \alpha + \beta$, where α' is a metastable supersaturated solid solution β is a stable or metastable precipitate, α is a more stable solid solution with the same crystal structure as α' but composition closer to equilibrium

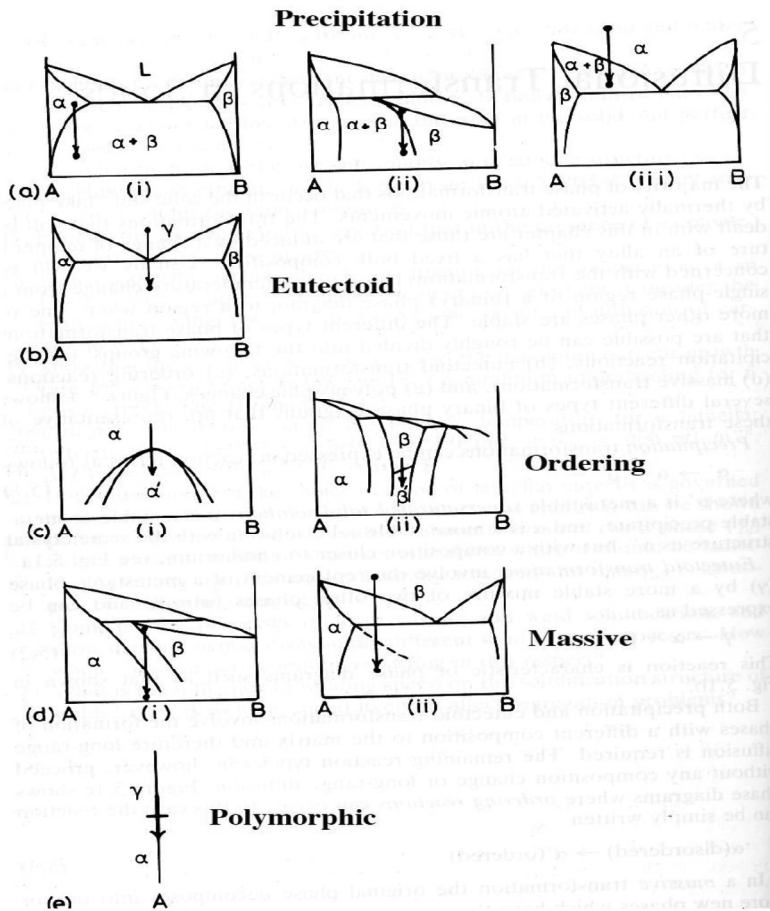
Eutectoid Transformation: Generally expressed as $\gamma \longrightarrow \alpha + \beta$ Metastable phase (γ) replaced by a more stable mixture of $\alpha + \beta$

Precipitation and eutectoid transformation require compositional changes in the formation of the product phase and consequently require long-range diffusion

Massive transformation: Generally expressed as $\beta \longrightarrow \alpha$

Original phase decomposes into one or more new phases which have the same composition as the parent phase but different crystal structures

Polymorphic transformations: Typically exhibited by single component systems where different temperature ranges. eg. bcc-fcc transformation in Fe



Nucleation in solids

Volume change during solid phase transformations is partly or totally accommodated by strains in the system which affects the energetics and kinetics of nucleation in solid state.

Let us consider formation of a β embryo with incoherent α/β interface formed homogeneously in α matrix during an $\alpha \rightarrow \beta$ solid state transformation.

Assume no plastic deformation occurs.

Energy associated with these strains increase Gibbs energy of formation of β embryo & is proportional to its volume. Due to presence of elastic strains the equilibrium embryo shape is not spherical but it is ellipsoidal.

Assume:

- All volume change is accommodated by elastic strains only in α matrix (i.e. β phase is rigid)
- No plastic flow occurs
- α is elastically isotropic
- the embryo is an ellipsoid of revolution of semi-axis r

Strain energy per unit volume of embryo is given by:

$$\Delta G_E = [2\mu_\alpha \cdot (\Delta V / V)^2 \phi (c/r)] / 3$$

Where $\Delta V / V \rightarrow$ total volume strain, $\mu_\alpha \rightarrow$ shear modulus of α matrix.

Hence volume strain energy is a function of volume & shape of embryo.

Gibbs energy of formation of an embryo is given by :

$$\Delta G' = V (\Delta G_v + \Delta G_E) + A \sigma_{\alpha\beta}$$

Where V – volume of embryo, ΔG_v & ΔG_E are Gibbs energy of transformation & strain energy respectively per unit area of embryo, A & $\sigma_{\alpha\beta}$ are area & interface energy per unit area of α/β interface respectively .

Gibbs energy of formation of a disc shaped β embryo of radius r & semi-thickness c is,

$$\Delta G' = (4\pi r^2 c/3) (\Delta G_v + A (c/r)) + 2 \pi r^2 \sigma_{\alpha\beta} \text{ -----(1)}$$

$$A = (\pi/2) \mu_\alpha (\Delta V/V)^2$$

For critical embryo ,

$$(\partial \Delta G' / \partial r) = 0 \quad \& \quad (\partial \Delta G' / \partial c) = 0$$

Which gives,

$$C^* = (-2 \sigma_{\alpha\beta}) / \Delta G_v \quad \& \quad r^* = 4 A \sigma_{\alpha\beta} / (\Delta G_v)^2$$

Where C^* & r^* are parameters of critical disc shaped embryo.

Putting these values in eqn (1), Gibbs free energy is obtained as :

$$\Delta G' = 32 \pi A^2 \sigma_{\alpha\beta}^2 / 3(\Delta G_v)^4$$

If transformation involves pure dilation, then strain energy per unit volume of embryo is independent of its shape & is given by,

$$\Delta G_E = A \delta^2$$

Where A is a function of elastic constants of α and β , δ is lattice mismatch across the coherent interface.

Lecture 19

Precipitate growth ; Age hardening

AGE HARDENING :

Age hardening is a type of heat treatment used in metallurgy to strengthen metal alloys. It is also called precipitation hardening, as it strengthens metal by creating solid impurities, or precipitates, in the alloy that prevents dislocations in the alloy's crystalline structure. Its name comes from the point in the hardening process in which the metal is aged, either by heating it for an extended period of time or keeping it stored at a lower temperature for an extended period before use so that these precipitates can form. This treatment is used on malleable alloys, such as those made from nickel, magnesium, and titanium as well as some types of steel.

Next the metal is aged. In some alloys, this is done by keeping the metal heated for several hours at a temperature lower than that of the initial phase but still much hotter than room temperature. Other alloys are stored for days or weeks at room temperature. At lower temperatures, it is no longer possible for all of the alloying materials to remain dissolved in the supersaturated metal, and so some of it undergoes precipitation and separates from the solid solution, becoming impurities spread throughout the metal. The temperature at which the aging process occurs affects how this precipitation occurs, and so influences the mechanical properties of the resulting alloy.

These impurities created by the hardening process strengthen the metal by interfering with the movement of crystallographic defects called dislocations, which result from

misalignments in the atoms that form the metal's crystalline structure. Dislocations make metal more vulnerable to being irreversibly bent by outside forces. Their resistance to dislocation gives age-hardened alloys high yield strength and the ability to resist permanent deformation when under heavy strain.

Steps in Age- hardening:

- 1) Solutionizing: Process of heating the alloy just above the solvus temp to obtain a single phase solid solution say α .
- 2) Quenching: The solutionised alloy is cooled fast to retain the high temp single phase solid solution at room temp as metastable supersaturated solid solution (SSSS).
- 2) Ageing: Process of controlled decomposition of SSSS to form finely-dispersed-precipitates usually at one end & sometimes at two intermediate temps for a suitable time period.

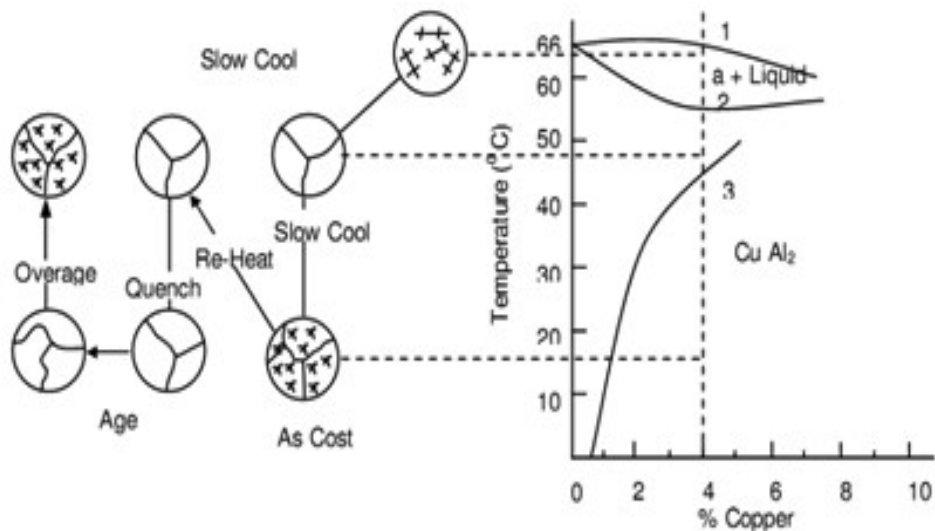
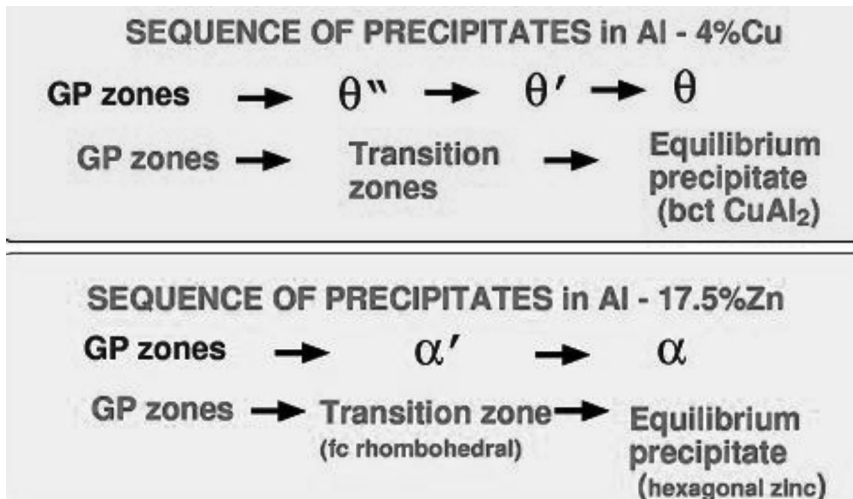


Fig. Age hardening case of Al-Cu diagram

Precipitation sequence during Ageing of alloy (Al – 4.5% Cu quenched from 550° C) :



- The sequence is:
 $\alpha_0 \rightarrow \alpha_1 + \text{GP-zones} \rightarrow \alpha_2 + \theta'' \rightarrow \alpha_3 + \theta' \rightarrow \alpha_4 + \theta$
- The phase are:
 α_n - fcc aluminum; n^{th} subscript denotes each equilibrium
 GP zones –coherent, mono-atomic layers of Cu on (001)_{Al}
 θ'' - thin discs, fully coherent with matrix
 θ' - disc-shaped, semi-coherent on (001) bct.
 θ - incoherent interface, ~spherical, complex body-centered tetragonal (bct).

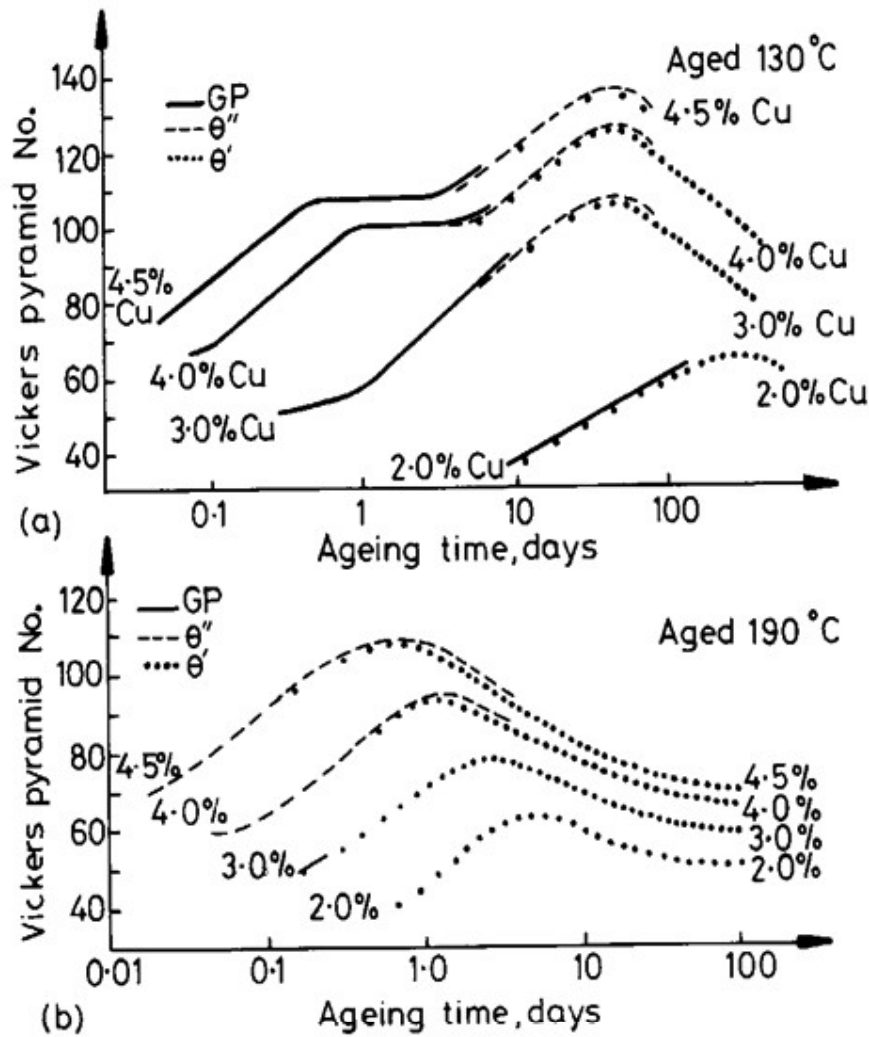
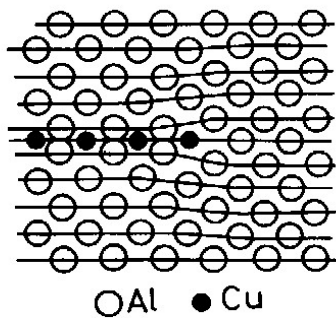


Fig. Hardness vs. time for various Al-Cu alloys at (a) 130°C , (B) 190°C

Al-Cu ppt structures :



GP zone structure

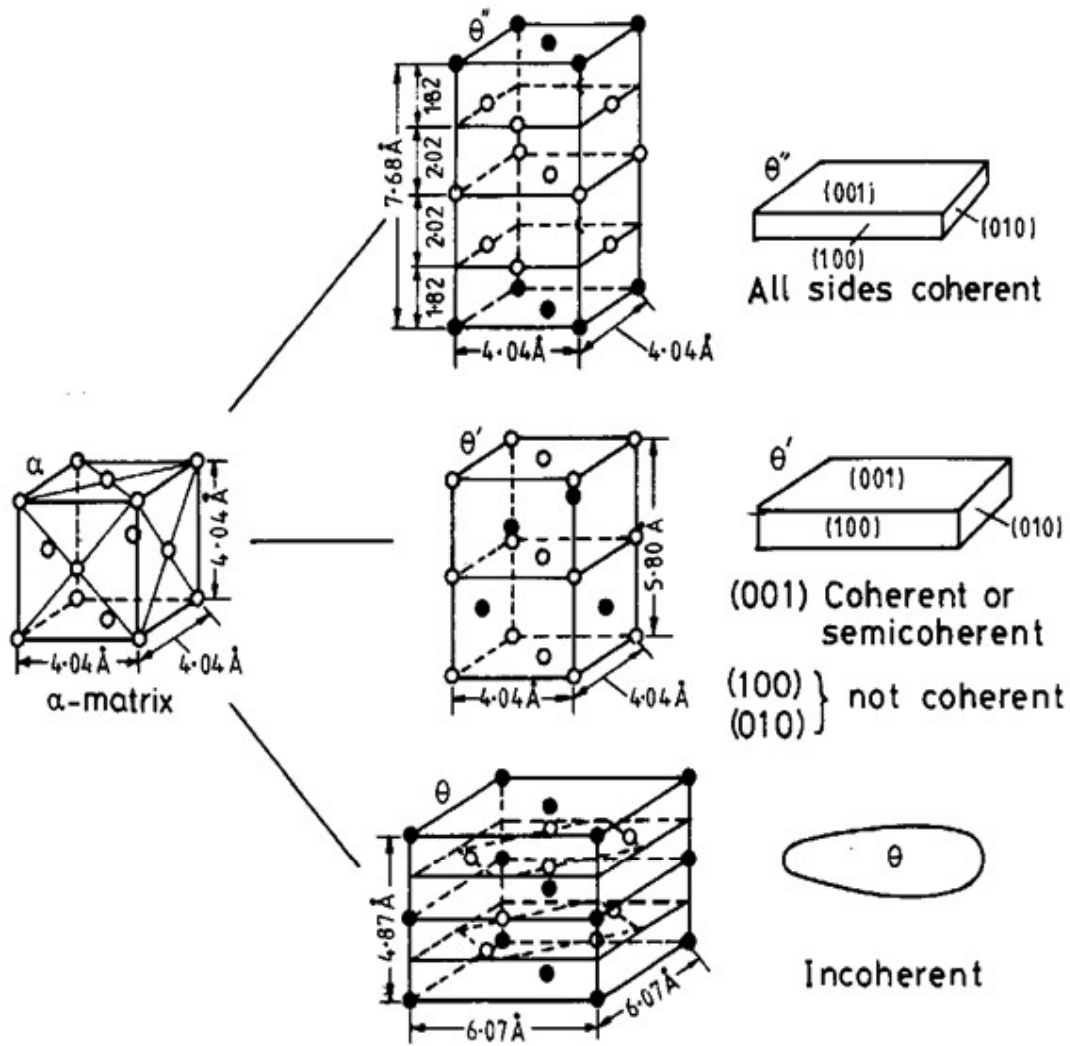
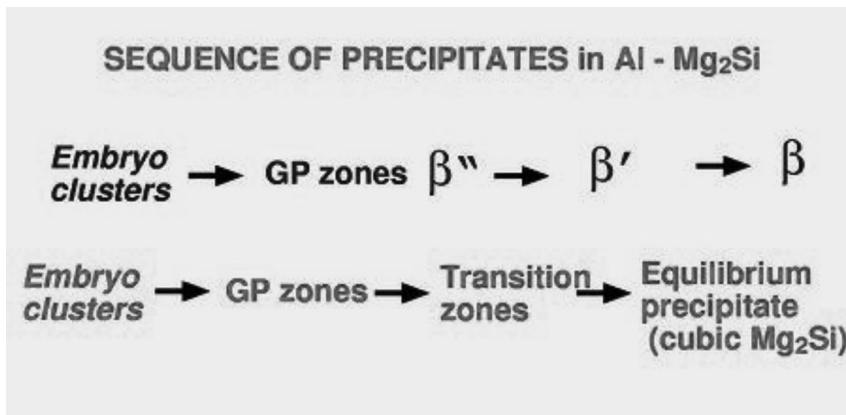


Fig. Structure and morphology of θ'' , θ' and θ in Al-Cu



Mechanisms of particle strengthening :

- 1) Coherency Hardening: differences in density between the particle and the matrix give rise to elastic stresses in the vicinity of the particle.
- 2) Chemical Hardening: creation of new surface when a particle is sheared increases the area of the interphase boundary, which increases the energy associated with the interface and hence an additional force must be exerted on the dislocation to force it through the particle.
- 3) Order Hardening: passage of a dislocation through an ordered particle, e.g. Ni₃Al in superalloys, results in a disordered lattice and the creation of antiphase boundaries.
- 4) Stacking-fault Hardening: a difference in stacking fault energy between particle and matrix, e.g. Ag in Al, increases flow stress because of the different separation of partial dislocations in the two phases.
- 5) Modulus Hardening: a large difference in elastic modulus results in image forces when a dislocation in the matrix approaches a particle. Consider, e.g., the difference between silver particles (nearly the same shear modulus) and iron particles (much higher shear modulus) in aluminum.

Lecture 20

Spinodal decomposition; Precipitate coarsening

Spinodal Decomposition:

The existence of concentration fluctuations in a multicomponent fluid system is an implicit assumption in the Gibbs theory of homogeneous nucleation. Two types of phase transition (nucleation) have been postulated, viz. composition fluctuations large in degree and infinitesimal in spatial extent (e.g. an infinitesimal droplet with properties approaching those of the bulk supercooled phase) or infinitesimal in degree and large in extent (e.g. continuous changes of phase). Classical nucleation theory, based on the former postulate, requires the further assumption that a sharp interface exists between the nucleating (stable) and supercooled (unstable) phases. The latter mode of transition, known as *spinodal decomposition*, does not require this assumption; a diffuse interface may be considered to exist between the phases.

The underlying theory for spinodal decomposition rests on Gibbs' derivation for the limit of stability of a fluid phase with respect to continuous changes of phase, represented by

$$\left. \frac{\partial^2 G}{\partial c^2} \right|_{T,P} = 0$$

where G is the Gibbs free energy per mole of solution and c is the solution concentration. On a phase diagram the locus of such points, representing the limit of stability, is referred to as the *spinodal* (see *Figure*). Thus, for spinodal decomposition to occur, a spontaneous phase transition is necessary and the condition

$$(\partial^2 G / \partial c^2) \leq 0$$

should apply. Within the spinodal region any phase separation can lower the free energy of the system and no nucleation step is required. Outside

this boundary, nucleation is essential to effect a phase change. The spinodal curve represents the limit of the metastable zone and is characterized by the condition of zero diffusivity (Myerson and Senol, 1984).

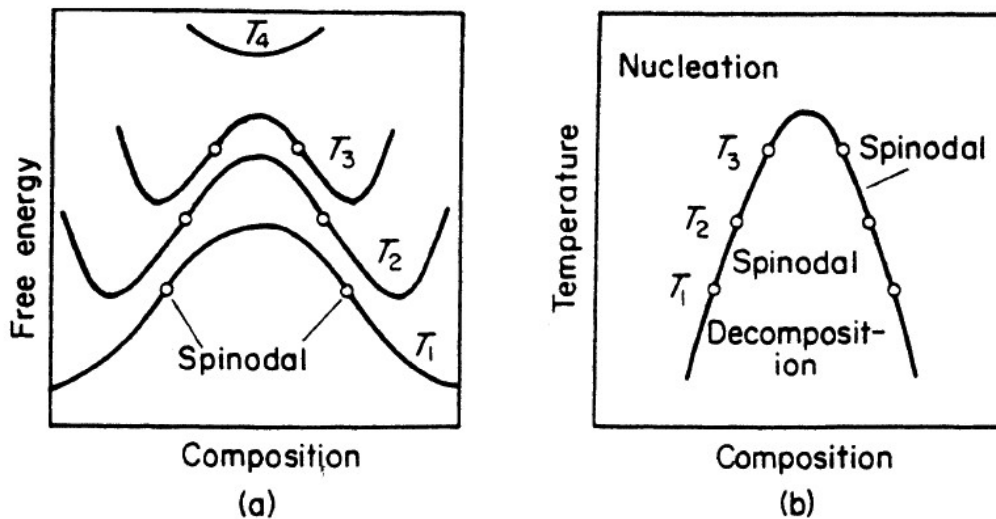


Figure (a) Free energy–composition–temperature surface, showing the location of the spinodal; (b) temperature–composition graph of the spinodal

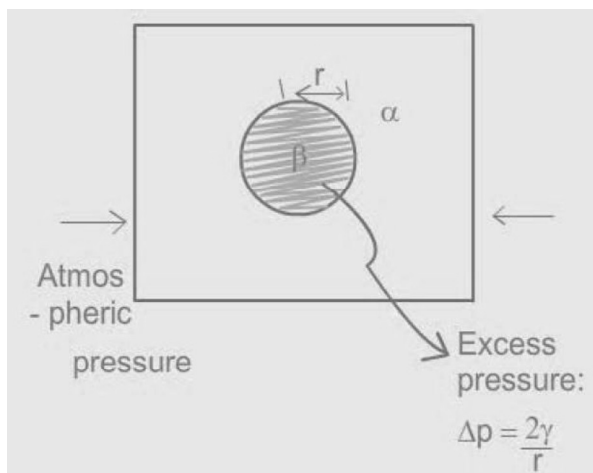
Precipitate Coarsening:

Coarsening is a process that is quite similar to grain growth in that the interphase interfacial energy provides the driving force for this process; coarsening is curvature driven; the small precipitates grow at the cost of larger precipitates during coarsening. During coarsening, the overall volume of the precipitate remain the same; however, since the precipitate sizes are larger, their separation is also larger which leads to degradation of material properties.

Gibbs- Thomson effect

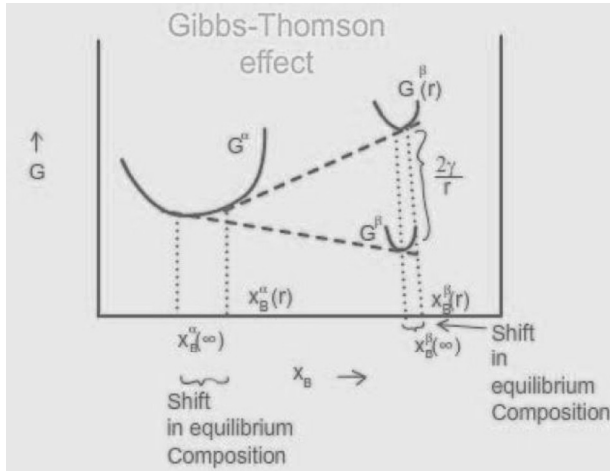
The curvature driven increase in the interfacial free energy and hence the overall free energy of the system is known as capillary or Gibbs-Thomson effect.

Consider the β phase particles in an α matrix as shown in fig. , let the interphase interfacial energy be α ; much like the excess pressure exerted inside a soap bubble, the excess pressure in such a β particle is given by α . The free energy increase associated with this pressure is $2\gamma/r$ where $2\gamma V_m/r$ is the molar volume of the β phase.



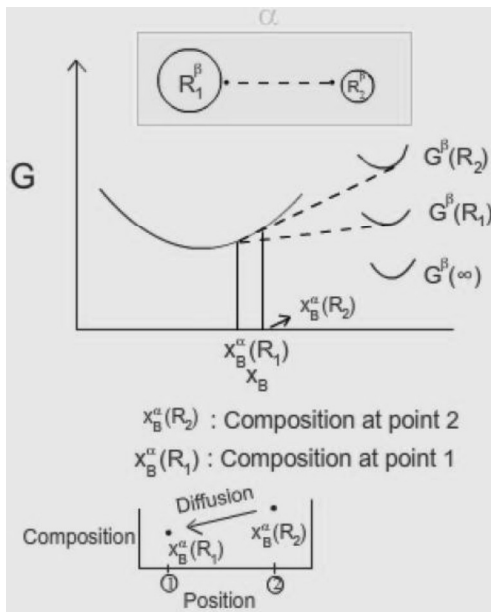
Excess pressure inside a β precipitate of radius r inside a matrix.

The increase in interfacial energy with the curvature of the particle in turn, affects the equilibrium properties. The composition of the phase in equilibrium composition is Gibbs-Thomson of capillary effect.



Gibbs-Thomson / Capillary effect: shift in equilibrium composition with curvature of β precipitate.

Let us consider two β particles of two different sizes, as the accompanying free energy versus composition diagram shows, the composition on the α phase across the α - β interface for the two particles are such that the β atoms in the α matrix next to the smaller particle migrate to the regions of α matrix next to the bigger particle; this, in turn makes the smaller β particle shrink; hence, once set in, the process continues till the smaller β particle completely disappears with a corresponding increase in the size of the bigger particle. This process is known as coarsening or Ostwald ripening.



Gibbs-Thomson/Capillary effect facilitates the mechanism of Ostwald ripening or Coarsening.

Lecture 21

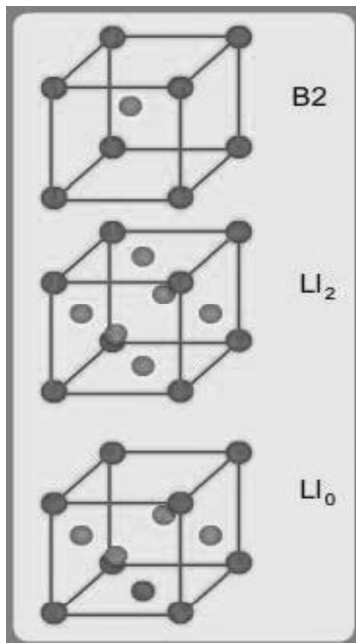
Order-disorder change, Polymorphic change

In the crystalline lattice, specific lattice positions are occupied by specific atoms, thus leading to more of the preferred unlike bonds.

Consider for example a bcc lattice occupied by A and B atoms. If it is disordered, then, the probability of the cube corners and cube centers are occupied by the A or B atoms is 50% (that is, the same as the alloy composition in at%). However, when this system orders, the cube corners preferentially occupy one of the positions, say, cube corners while the other preferentially occupies the cube centers.

That is, the bcc lattice now can be considered to be consisting of two interpenetrating cubic lattices. Such a structure is known as B2. Notice that in the (ideal) B2 structure, there are only AB bonds and no AA/BB bonds. NiAl is a system in which, for example, such B2 ordered structure is known. There are also fcc based ordered structures such as L12 (example: Ni₃Al) and L10 (example: CuAu).

In Fig. , we show these three ordered structures :



Ordered structures: three examples.

Long range and short range order parameters :

There are two different order parameters that one can define. The first is the short range order parameter s defined as follows:

$$s = \frac{P_{AB} - P_{AB}(\text{random})}{P_{AB}(\text{max}) - P_{AB}(\text{random})} \quad \text{----- (1)}$$

Here, $P(\text{max})$ and $P(\text{random})$ refer to the maximum number of bonds that can exist and the number of bonds in a random solution. As one can see, the short range order parameter is closely related to the , regular solution parameter; this type of ordering is possible in alloys of all compositions.

In case the alloy composition is in simple ratios of the constituent atoms, then, one can define the so called long range order parameter in terms of the alloy composition as follows:

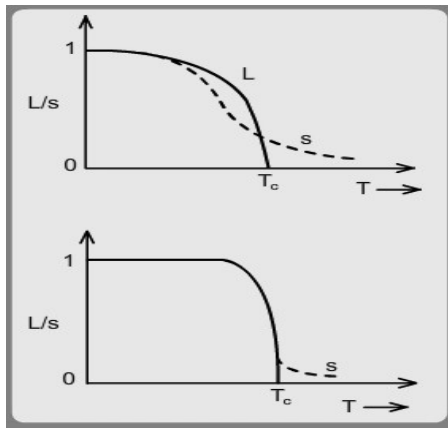
$$L = \frac{p - x}{1 - x} \quad \text{----- (2)}$$

Where p is the probability of occupancy of the given site by the right kind of atom.

At absolute zero, the system will choose a state with $L=1$; however, as temperature increases, the effects of configurational entropy come into play; so the value of L decreases from unity and eventually reaches zero. The temperature at which this change of LRO from unity to zero takes place is known as the critical temperature (T) for the order-disorder transformation.

In Fig. we show the variation of L and δ with temperature in two systems, namely, one that undergoes an order-disorder transformation from B2 to disordered bcc and another that undergoes an order-disorder transformation from L12 to disordered fcc. As is clear from the figures, the changes are of two different types; in the equiatomic case of B2 to bcc (NiAl type), the variation is continuous; however, in the case of L12 to fcc (Ni3Al type), the variation is abrupt. These differences in the behaviour is a consequence of the differences in atomic configurations in the two ordered lattices.

Figure : Order parameter variation with temperature: continuous (B2 type) and abrupt (L12).



Order parameter variation with temperature: continuous (B2 type) and abrupt (L12).

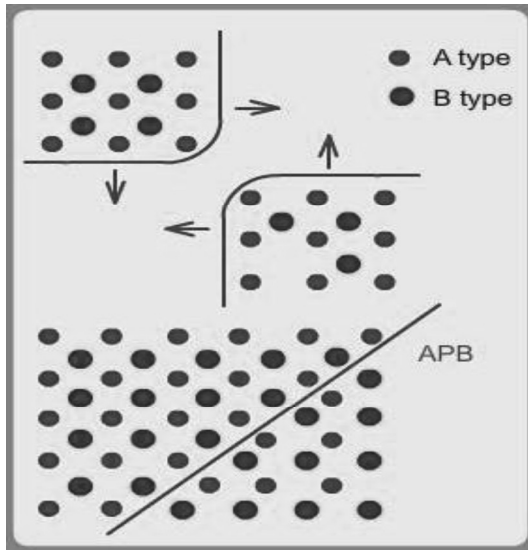
Microstructural features :

The order-disorder transformation can take place both through the nucleation and growth mechanism and spinodal mechanisms. In spinodal mechanism there is continuous increase in homogeneously all through the crystal leading to the transformation. In the nucleation and growth mechanism, small regions form overcoming an energy barrier and these regions grow. In ordered alloys, the two phases have near-identical lattice parameters and the interfacial energies between the ordered and disordered phases is very low. Hence, the barrier for nucleation is very small.

Hence, order-disorder transformation, when takes place through the nucleation and growth mechanism, takes place through homogeneous nucleation.

The surface defects that come about in ordered alloys is known as anti-phase boundaries (APB). These come into existence due to accidents of nucleation and growth. For example, in bcc-B2 transformation, since the two sites in B2 are completely equivalent, at some nuclei the cube corner is occupied by A while in some nuclei the cube corner is occupied by B. Hence, as these nuclei grow and the ordered regions impinge, there is predominant AA or BB bonds (unpreferred bonds). Such defects are known as APBs and in Fig. we show, schematically, the formation of APBs. In Fig. we show a schematic ordered microstructure in B2 and L12 alloys. As is clear from the figures, the nature of APBs and hence the microstructures are different in these two cases.

Figure :



Schematic domain structures in ordered systems.

POLYMORPHIC CHANGE:

- ➔ It involves a change of crystal structure but no change in composition. Polymorphic transformation in metals and ceramic materials are affected by nucleation and growth of the lattice of product phase.
- ➔ It is typically exhibited by single component systems where different crystal structures are stable over different temperature ranges.
- ➔ Example: BCC-FCC transformation in Fe.

Polymorphic changes in Iron:

Below 910° C , Iron has BCC crystal structure and is called α -iron. But above 910° C, iron is called γ -iron with FCC crystal structure. At 1394°C, γ - iron changes to δ -iron (BCC structure), the second allotropic change.

- ➔ Polymorphic change is a phase change in solid state which occurs with supercooling and evolution of heat of reaction.
- ➔ It helps in refining the grains if we had earlier coarse grains.
- ➔ Polymorphic transformations have also been induced by applying high pressure. Example- Pure iron at 1 atm pressure exists as alpha-iron (BCC) and gamma (FCC) iron but changes to a new crystalline phase HCP (ϵ) at pressures above 100 kbar.

Lecture 22

Recovery, Recrystallization

Cold working

There are many ways in which materials can be strengthened; work or strain hardening is one of the strengthening mechanisms. To work harden a material, it is cold worked: that is, it is deformed at low temperatures - typically at the ambient temperature, but any temperature which is below 0.3 to 0.5 of the melting temperature of the material will qualify as low temperature. Cold working introduces defects in the material (typically point defects and dislocations) which act as impediments to the movement of dislocations and hence the material is strengthened. The defects generated during cold working can store about 1 to 10 % of the energy of plastic deformation.

A cold worked material, however, cannot be used at high temperatures; typically, 0.3 to 0.5 of the melting temperature of the material is considered as high service temperature. In this temperature range, the microstructure of a cold worked material undergoes changes which reduce the strength of the material. In this module we study these microstructural changes, namely, recovery and recrystallisation.

Three stages of Annealing: Recovery, Re-crystallization, Grain Growth.

RECOVERY:

Definition: Annihilation and rearrangement of imperfections within the deformed material without the movement/migration of high angle boundaries.

Here,

- excess defects are annealed out,
- dislocations of opposite signs annihilate each other, and
- dislocations align to form low energy configurations, namely tilt and twist boundaries.

For example, we show how a wall of edge dislocations form a tilt boundary.

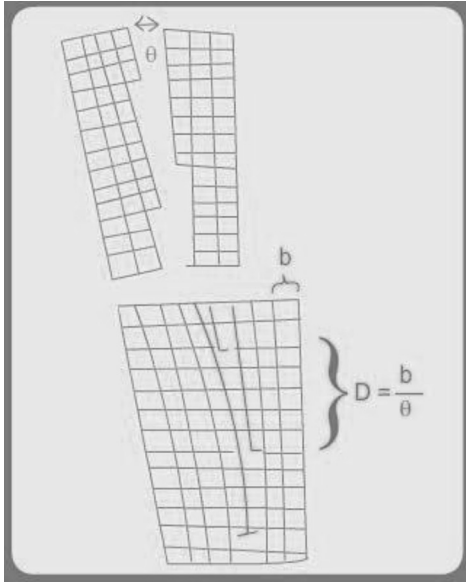


Fig.- A wall of edge dislocations form a tile grain boundary; it is a small angle grain boundary; the inter-dilocation separation in the grain boundary is decided by the misorientation between the two grains and the Burgers vector.

Driving force for Recovery: Energy stored during cold deformation.

N.B.—If process of movement of dislocations into subgrains/grain boundaries takes place during cold working, then the recovery process is called **Dynamic Recovery**.

Fraction of recovery process X,

$$X = \frac{\sigma_m - \sigma}{\sigma_m - \sigma_0}$$

Where σ_m is the flow stress of the deformed material, σ_0 is that of the undeformed material and σ is that of the partially recovered solid.

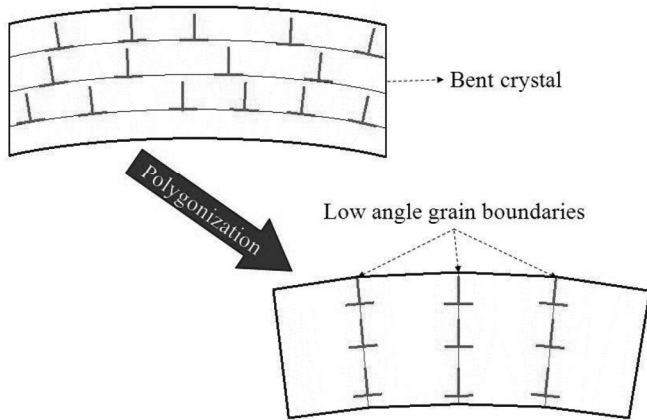
Polygonization :

After local annihilation of opposite signed dislocation in early stages of recovery, excess dislocations of the same sign are left over in the metal. The stored elastic strain energies of these dislocations get reduced further when they arrange themselves in sub-boundaries.

Definition : Polygonization is the recovery process of arranging excess edge dislocations in the form of tilt boundaries and the excess screw dislocations in the form of twist boundaries, with the resultant lowering of the stored cold work energy i.e. the elastic strain energy.

Driving force of Polygonization : The decrease in the total strain energy.

POLYGONIZATION



Excess edge dislocations on parallel slip plane on bending a single crystal.

Its polygonization on annealing.

AS

Polygonized structure is relatively stable & does not recrystallize on heating at higher temperature.

RECRYSTALLISATION:

Definition: The nucleation and growth of new strain-free grains by the migration of high-angle boundaries between the distorted matrix and the new crystals, until impingement occurs among the new crystals.

Recrystallisation is the process in which deformed grains are replaced by strain-free grains. It is generally observed that higher cold work and smaller initial grain size lead to finer recrystallized grains.

Driving force for recrystallisation is the stored strain energy in the material.

For recrystallisation to take place, a minimum of cold working is needed; if the deformation is very low, recrystallisation does not occur.

During recrystallisation, the stress-free grains nucleate and grow. In a recrystallised microstructure is textured; that is, most of the grains have similar orientation.

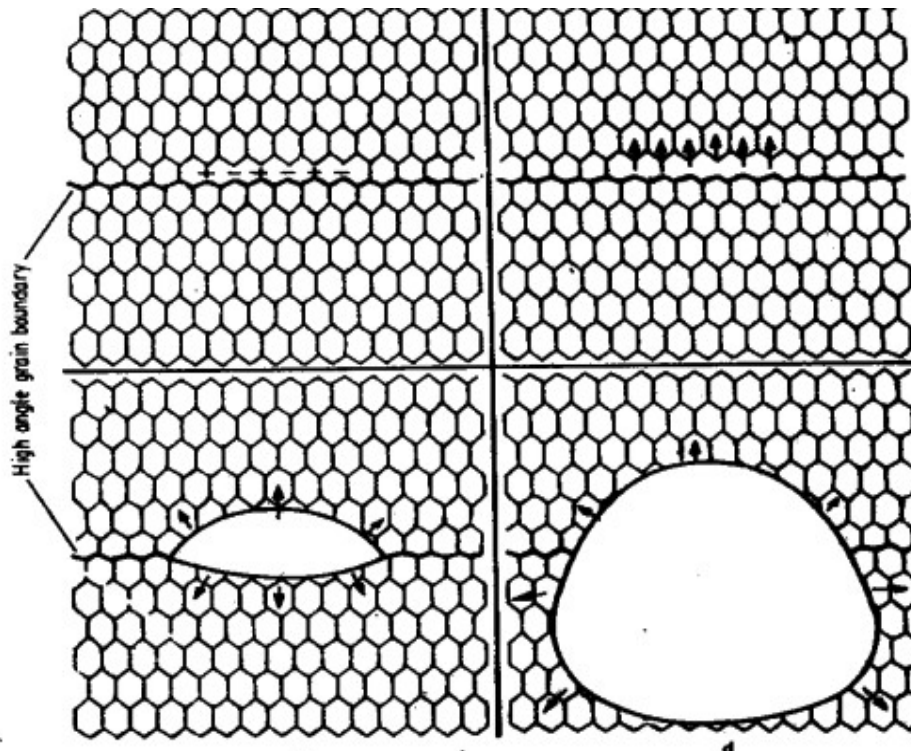


Figure. Schematic representation of the formation of a recrystallised nucleus by subgrain coalescence

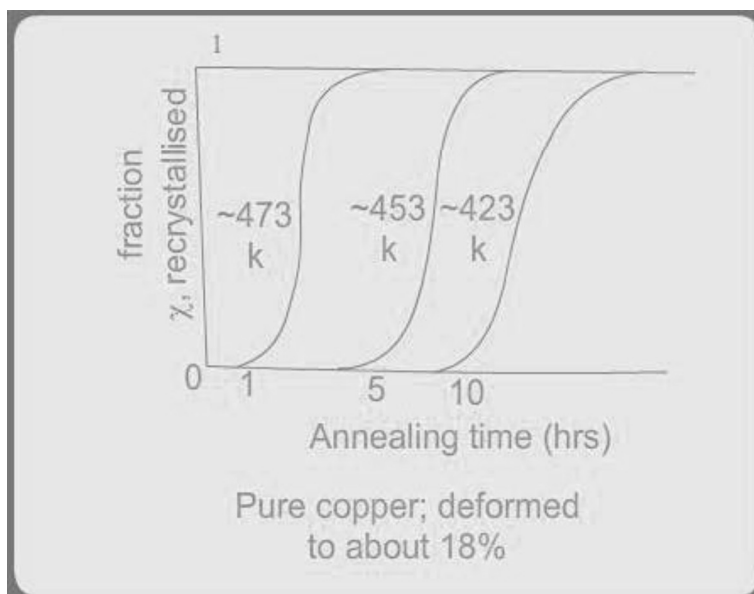


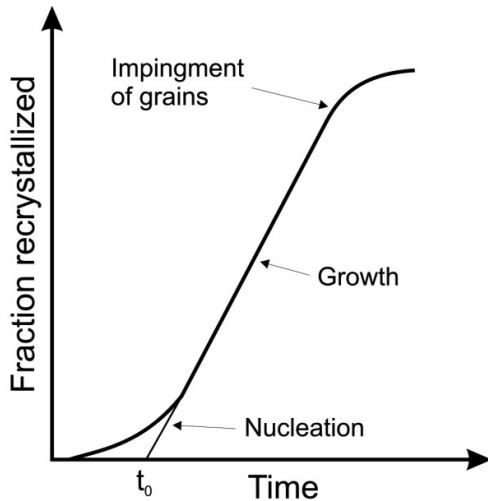
Fig. -Annealing time versus fraction of recrystallised copper as a function of temperature. Note that the time changes from 1 to 5 to 10 hours with a decrease of about 20 K in temperature indicating the strong influence of temperature on recrystallisation kinetics.

Recrystallization Kinetics :

Rate of recrystallization continuously increases with temperature.

Recrystallization kinetics depends on :

- Extent of deformation
- Initial grain size of material
- Annealing temperature
- Deformation temperature.



Typical Isothermal Recrystallisation curve resembling phase transformation.

The main feature of the curve are:

- There is an incubation period.
- The kinetics of recrystallisation is such that recrystallisation starts slowly and gradually reaches to a maximum rate and then rate of recrystallisation slows down again.

Kinetics of recrystallisation resembles a phase transformation i.e. Recrystallisation is a nucleation & growth process. The strain-free nuclei forms and begins to grow in the deformed metal, when the temperature is high enough, and gradually absorb the whole of the deformed matrix.

Cold work, recovery, recrystallisation and material properties :

The processes of cold work, recovery and recrystallisation, because of the changes they produce in the microstructure of the material, also affect the properties of the materials. In Fig., we show, schematically, variations in tensile strength, electrical conductivity and ductility with these processes.

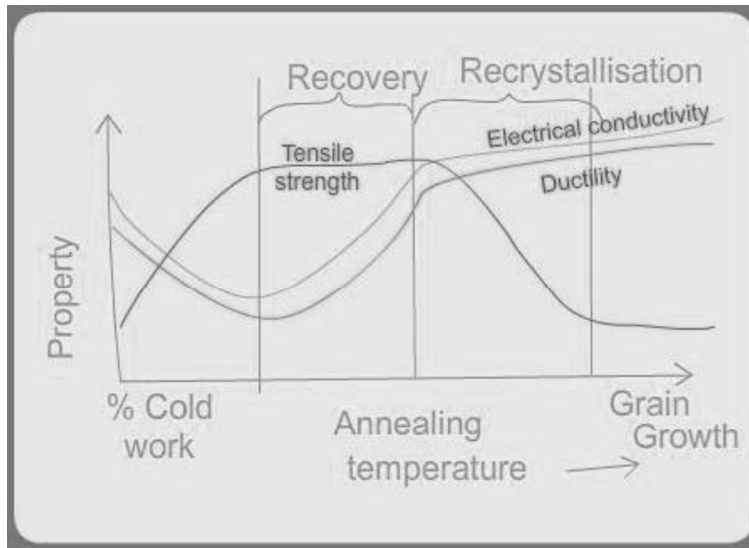


Fig. - Changes in properties with % cold work and annealing temperature; increasing annealing temperatures leads to recovery and recrystallisation. Note that still higher annealing temperatures leads to grain growth.

DYNAMIC RECRYSTALLIZATION: When a material is deformed above its recrystallisation temperature (hot worked), the recrystallisation kinetics is generally so rapid that it recrystallizes almost simultaneously with deformation. It is called Dynamic recrystallisation.

Lecture 23

Recrystallisation Cont., Grain growth

Solute Drag effect :

Recrystallisation rate is lower in impure metals. So their recrystallisation tempr increases in the presence of impurities.

Example: Very pure aluminium recrystallises at 75° C (348 K = 0.37 T_m) whereas commercially pure aluminium recrystallises at 275° C (548 K = 0.59 T_m).

The solute atoms drastically lower the boundary migration rates. A solute atom has a binding energy V that attracts it to the boundary.

Under an equilibrium distribution, concentration of solute at boundary C_b is larger than any average concentration C_o ,

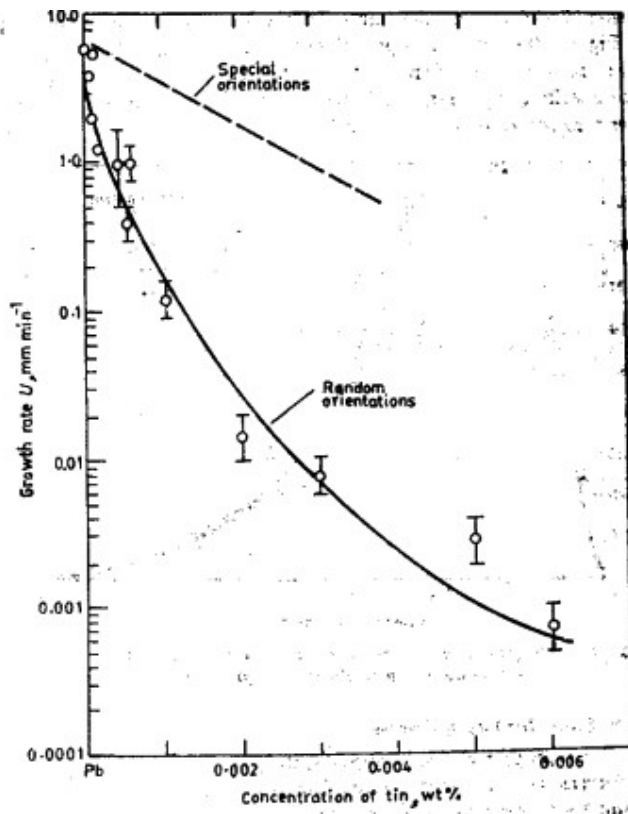


Fig. Growth rates during recrystallisation of zone refined lead dopewith tin

$$c_b = c_0 \exp\left(\frac{V}{kT}\right)$$

When boundary migrates, solute atoms are also dragged behind it due to attraction.

A steady state velocity of boundary is attained when force due to free energy difference between the strain-free and deformed crystals pulling forward is equal to the dragging force that is pulling back the boundary.

This velocity U of the boundary is given by,

$$U = \frac{\Delta g D}{kT\Gamma}$$

where

Δg is the driving force per unit volume,

D is the bulk diffusion coefficient of the solute, and

Γ is the number of solute atoms per unit area of the boundary.

Γ is given by

$$\Gamma = \alpha c_0 \exp\left(\frac{V}{kT}\right)$$

Where α is a geometrical factor.

So,

$$U = \frac{\Delta g D}{kT \alpha c_0} \exp\left(-\frac{V}{kT}\right)$$

Force F arising from interaction between solute atoms and boundary has a maximum value of,

$$f \sim \frac{V}{2r} \quad \text{where } r \text{ is atomic radius.}$$

GRAIN GROWTH:

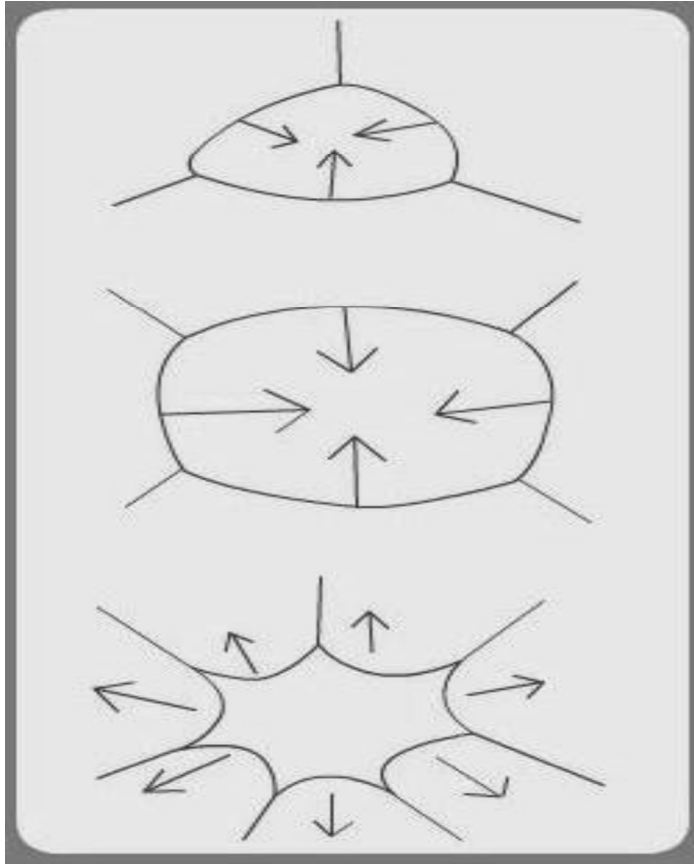
Definition: The increase in average grain size on further annealing after the recrystallisation process is complete.

The interfaces in a material cost the system energy: the excess free energy associated with the interfaces is the interfacial free energy.

Grain boundaries are the interfaces between two crystallites which are differently oriented in space; the excess free energy associated with the grain boundary is the grain boundary energy.

The grain boundary energy acts as the driving force for the movement of grain boundaries. Hence, if a recrystallised material is further annealed, then grains growth takes place; bigger grains grow at the cost of smaller ones. This process is known as grain growth.

Since the driving force for grain growth is the interfacial energy, and since the excess energy associated with a system due to interfaces is related to the curvature of the interface, the grain growth is curvature driven.



Curvature driven growth of grains (in 2D).

The above figure shows the direction of movement of grain boundaries and their relationship to curvature (in 2D systems).

Grain size depends on :

- Degree of prior deformation.
- Time at any temperature
- Annealing temp
- Heating time
- Insoluble impurities.

Parabolic Grain Growth Law:

Grain growth kinetics is given by,

$$\bar{D} = C_1 t^n$$

where \bar{D} is the average grain diameter and C_1 is a constant.

$$n = \frac{1}{2}$$

Assume rate of change of D is proportional to Δg , then :

$$\frac{dD}{dt} = C_2 |\Delta g|$$

We know

$$|\Delta g| = \frac{2C\sigma}{R}$$

Combining above equations we get,

$$\frac{dD}{dt} = \frac{C_3\sigma}{D}$$

Integrating above equation we get,

$$\int_{D_0}^{D_t} D \, dD = C_3\sigma \int_0^t dt$$

or

$$(D_t^2 - D_0^2) = 2C_3\sigma t \quad \text{----} \rightarrow \text{Parabolic grain growth law.}$$

Where the subscript t & 0 refer to time.

At small initial grain sizes,

$$D_t \propto t^{1/2}. \quad \text{-----} \rightarrow \text{Parabolic grain growth law.}$$

Driving force for grain growth:

When the average grain size increases, the grain boundary area per unit volume decreases.

$$\Delta g = \frac{2C\sigma}{R}$$

Pinning by second phase particles:

Grain growth can be hampered in the presence of inclusions, voids and second phase particles.

When N_V precipitate particles of average radius r_p per unit volume, the driving force is reduced to

$$\Delta g = 2C\sigma \left(\frac{1}{R} - N_V \pi r^2 p \right)$$

Lecture 24

Eutectoid transformation

The mechanism of eutectoid transformation must transform a single solid phase into two others, both with compositions which differ from the original.

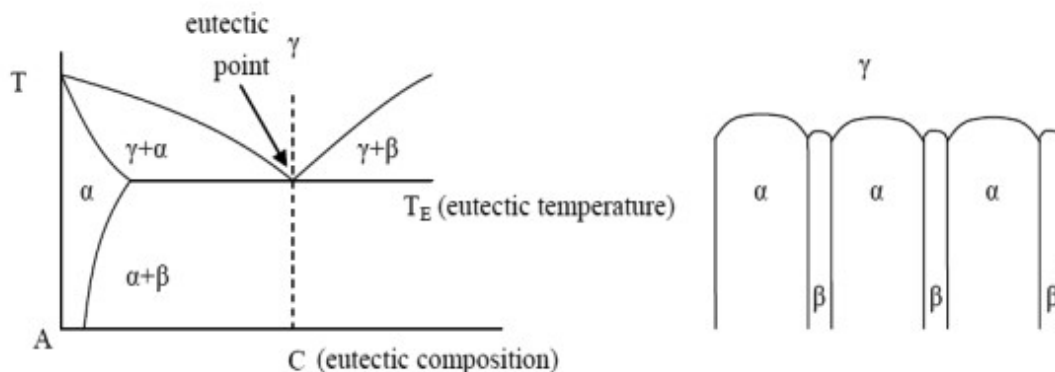
Eutectoid reaction is similar to the eutectic reaction, but involves only solids. Here a solid solution upon cooling to some critical temperature, called eutectoid temperature, is seen to transform completely through alternate precipitation of two solid phases.



Taking the eutectoid decomposition of iron as an example, austenite containing 0.8% C changes into ferrite (iron containing almost no carbon) and cementite (Fe_3C , containing 25 at% carbon) at 727°C . Hence carbon atoms must diffuse together to form Fe_3C , leaving ferrite. Nuclei of small plates of ferrite and cementite form at the grain boundaries of the austenite, and carbon diffusion takes place on a very local scale just ahead of the interface. Thus the plates grow, consuming the austenite as they go, to form pearlite.

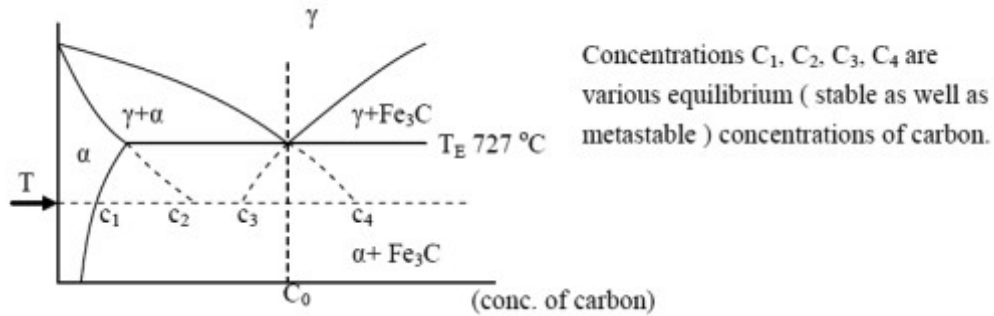
The eutectoid structure in iron has a special name: it is called *pearlite* (because it has a pearly look). It is important to note that pearlite is **not** a phase, but a mixture of two phases: ferrite and cementite.

We will consider another type of phase transformation: $\gamma \rightarrow \alpha + \beta$, namely cellular precipitation, where two phases α and β , are in equilibrium and form simultaneously at the expense of the original supersaturated solid solution (γ). The two phase form in the shape of colonies or cells, hence it is called cellular precipitation. The following discussion will be based on a eutectoid phase diagram.



Let us consider a special case of the formation of pearlite (a mixture of α iron and Fe_3C) from γ austenite in the iron carbon alloy system. A sample of the eutectoid composition is cooled

from a single-phase region(γ) for a temperature(T) below the eutectoid temperature(T_E). The following diagram shows a part of the iron-carbon phase diagram.



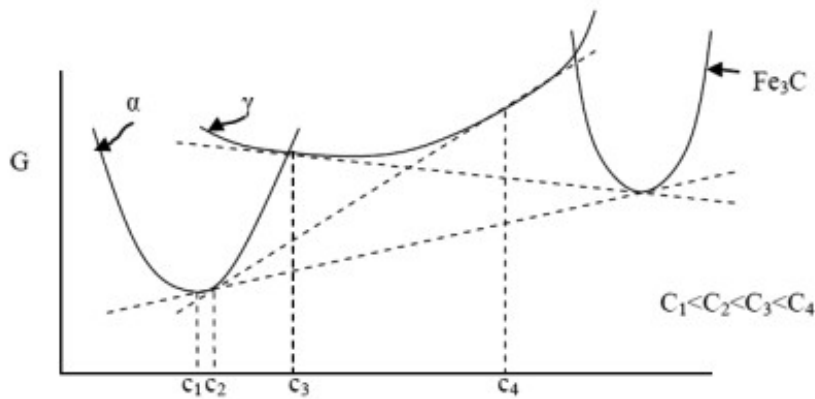
C_1 : carbon concentration in α for α - Fe_3C equilibrium.

C_2 : carbon concentration in α for α - γ equilibrium.

C_3 : carbon concentration in γ for γ - Fe_3C equilibrium.

C_4 : carbon concentration in γ for γ - α equilibrium.

In terms of the free energy vs. Composition diagrams at T , the composition C_1, C_2, C_3 and C_4 are identified as follows.



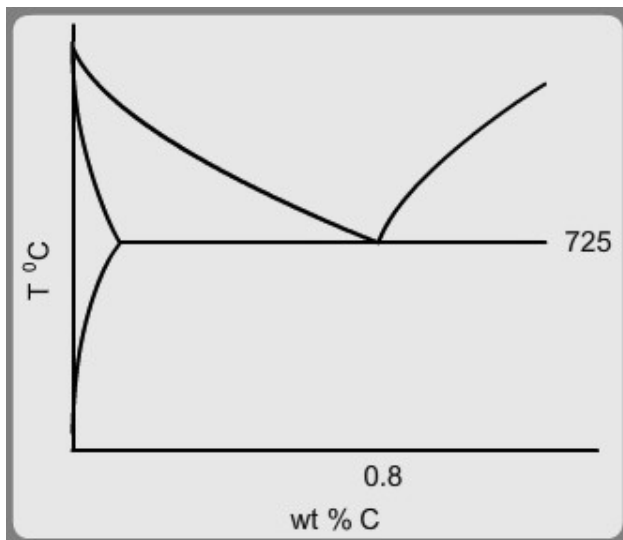
Thus, at a γ - α interface, concentration of carbon in α and γ phases near the interfaces are C_2 and C_4 respectively: at a γ - Fe_3C interface, concentration of carbon in γ phase near the interfaces is C_3 (while the concentration in the Fe_3C phase is constant): at a α - Fe_3C interface, concentration of carbon in α phase near the interface is C_1 . The following figure shows the various compositions:

Lecture 25

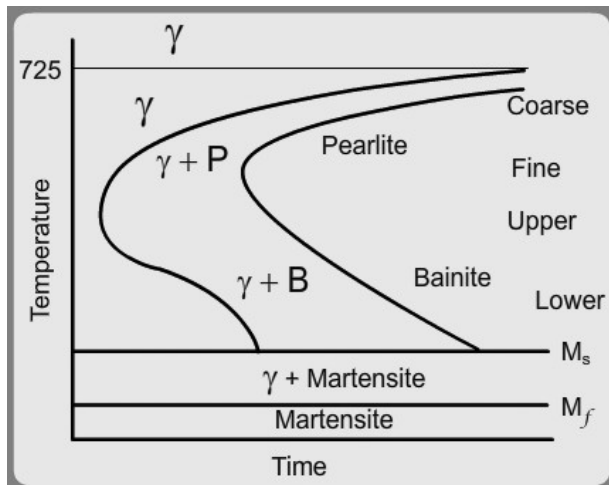
Pearlitic and bainitic transformations in steel

Pearlite is a common micro-constituent of a large variety of steels, where it substantially increases the strength. On cooling a steel below eutectoid temperature, Austenite transforms to pearlite, consisting of a mixture of alternate parallel plates of ferrite and cementite.

γ	=	α	+	Fe_3C
Austenite		Ferrite		Cementite
FCC		BCC		Orthorhombic
0.77		0.02		6.67% C



Phase diagram of the Fe-C system: eutectoid transformation



TTT diagram for Fe-0.8 wt% C system

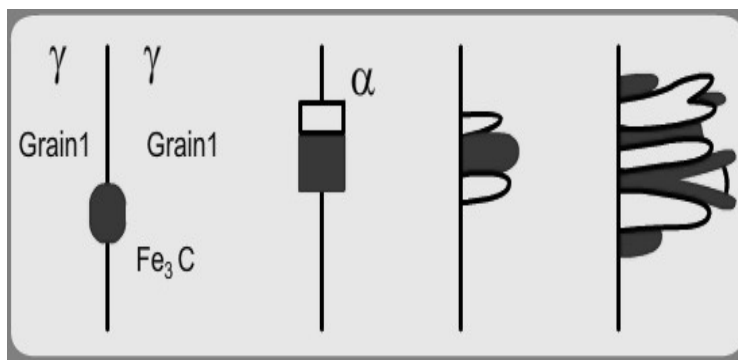
Nucleation and growth of pearlite:

Pearlite nucleates at austenite grain boundaries. The finer is the austenite grain size, the more is the grain boundary area per unit volume and more is the number of potential nucleation sites. Nucleation rate increases with decreasing austenite grain size. This increases the transformation rate.

Nucleation of pearlite occurs in two stages. First, a cementite plate nucleates at grain boundary and grows inwards into one of the austenite grains. As the cementite plate thickens, the carbon content of austenite on either side of cementite plate decreases. When it falls to a critical value, two ferrite plates, one on either side of cementite plate, nucleate. They grow by rejecting carbon in excess of $\approx 0.02\%$ into the adjacent austenite, thereby enriching it. As the carbon content of Austenite increases to a critical value, two cementite plates nucleate on either side and grow.

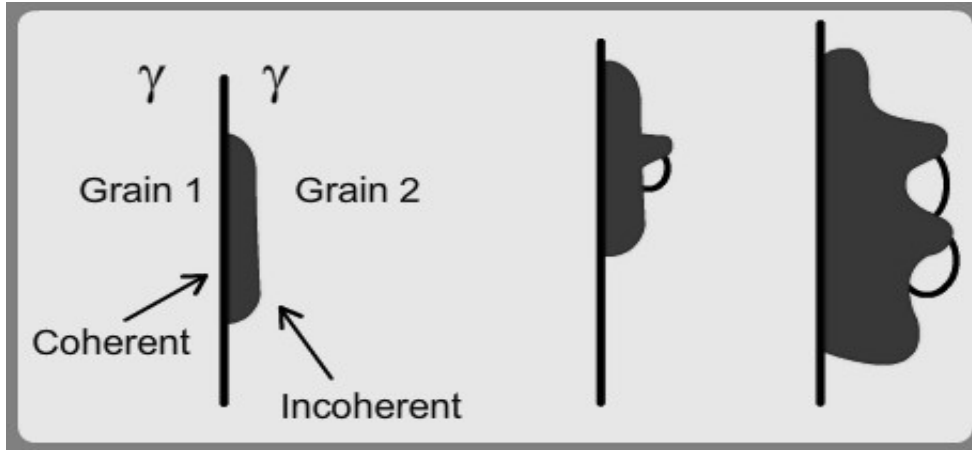
Thus the side-wise nucleation and growth of pairs of lamellae continue in a pearlitic colony.

Edge-wise growth of pearlite: In the austenite ahead of the growing plates, the carbon content opposite to a ferrite plate is higher than at a point opposite to the next cementite plate. Carbon diffuses down this concentration gradient.

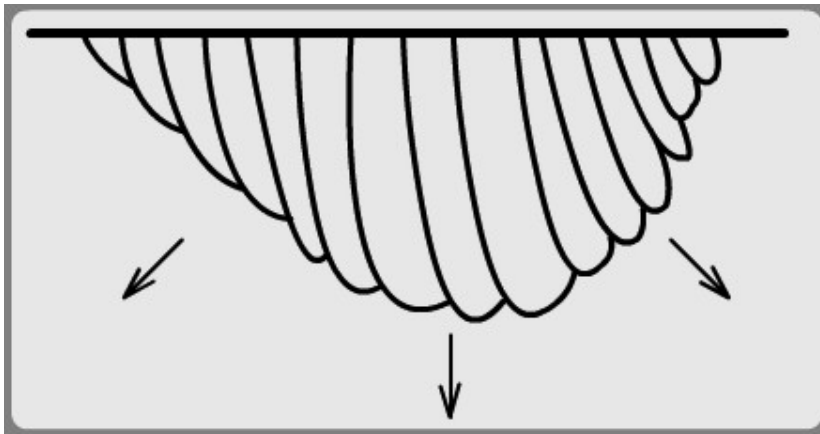


Nucleation of the eutectoid phases in a system with eutectoid composition.

If the composition of the steel is not the eutectoid composition, then, it is possible that proeutectoid ferrite or cementite is nucleated at the grain boundary. The other phase, be it cementite or ferrite, then forms on the incoherent boundary of this proeutectoid phase.



Nucleation of the eutectoid phases in a system with o-eutectoid composition



Pearlite colony during late stage growth.

Several colonies form together in an approximately spherical volume called a **Pearlitic nodule**.

N.B.- Nucleation of pearlite requires establishment of cooperative growth of two phases. It takes time for this cooperation to be established and the rate of colony nucleation therefore increases with time.

In some cases cooperation is not established and the ferrite and cementite grow in a non-lamellar manner producing **Degenerate pearlite**.

The growth of pearlite is analogous to growth of a lamellar eutectic with austenite replacing the liquid. Carbon can diffuse interstitially through the austenite to the tips of advancing cementite lamellae.

The minimum possible Interlamellar spacing (S^*) should vary inversely with undercooling below the eutectoid temperature A_1 (ΔT) and observed spacing S_o is proportional to S^* .

$$S_o \propto S^* \propto 1/\Delta T$$

Growth rate of Pearlite colonies,

$$v = k D_c^r (\Delta T)^2 \quad [k = \text{constant}]$$

Interlamellar spacing of a pearlite colony is defined as the distance from the centre of a ferrite (or cementite) plate to the centre of the next ferrite (or cementite) plate.

Transformation very near to the eutectoid temperature yields coarse pearlite, with interlamellar spacing of about 1-2 μm . Coarse pearlite is soft with hardness of about 5 R_c .

Pearlite formed near nose of C-curve (550° C) is very fine, spacing being less than 0.1 μm , hardness 40 R_c .

The extremely fine pearlite formed near the nose of C-curve is called Troosite and the air-cooled fine pearlite is called Sorbite.

Effect of alloying elements : Ni, Cr, Mn, Si, Mo (except Co) shift nose of C-curve to right & slow down the growth rate of pearlite. Austenite stabilizing elements like Ni & Mn lower eutectoid temp & for the same cooling rate, the effective transformation is lowered & a finer pearlite results.

Lecture 26

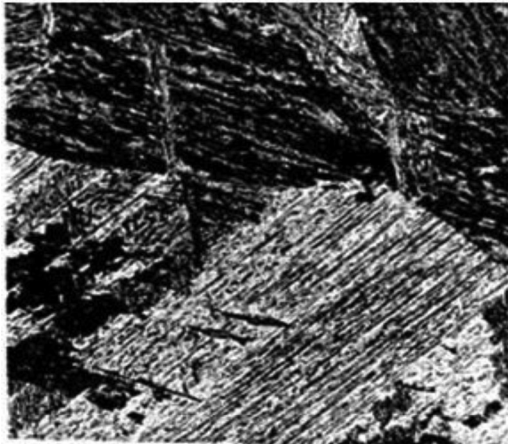
Martensite and martensitic changes in ferrous materials

Martensitic transformation is the name for any transformation that takes place in a diffusionless and military manner - that is, these transformations take place through atomic movements which are less than one atomic spacing; and in these transformations atoms change their positions in a coordinated manner (unlike thermally activated diffusional, or, so-called, civilian processes). In shape memory alloys such as Ni-Ti (nitinol), it is the martensitic transformation that is responsible for the shape memory effect. In this module, we describe some characteristic features of the martensitic transformations (with specific reference to steels in which, this transformation is responsible for hardening by quenching).

Since martensitic transformations are diffusionless, necessarily, the composition does not change during the transformation. It is only the crystal structure that changes. For example, in Fe-C alloys, the austenite (fcc) transforms into martensite (bcc); in Ni-Ti, an ordered bcc (called austenite) transforms to another ordered CsCl type structure (called martensite). Note

that since martensitic transformation is diffusionless, if the austenitic phase is ordered, the martensitic phase is also ordered.

Martensites are typically found in lath and plate morphologies:



Lathe martensite

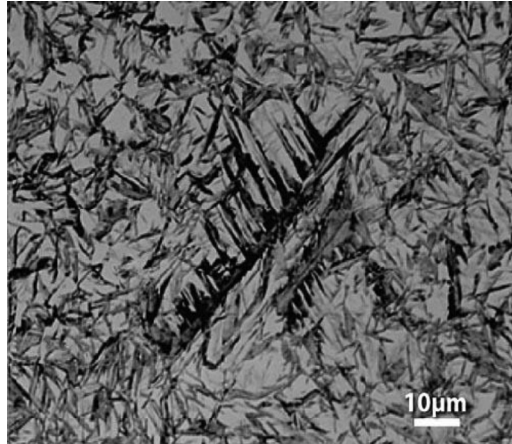
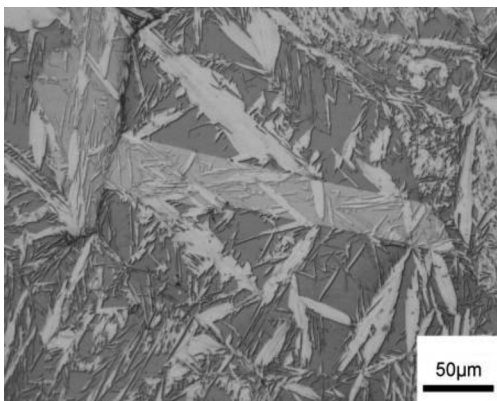
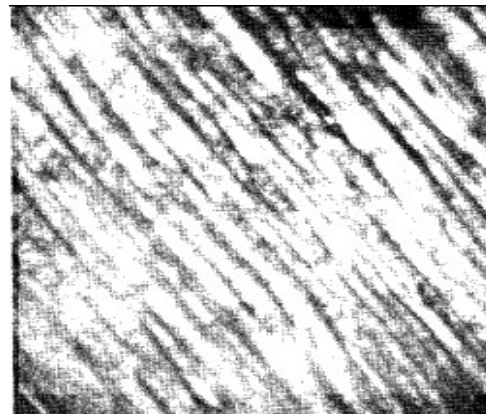


Plate martensite

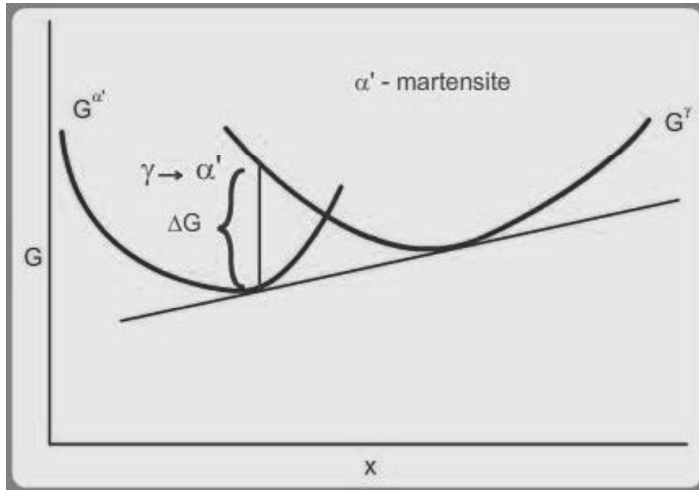


Plate

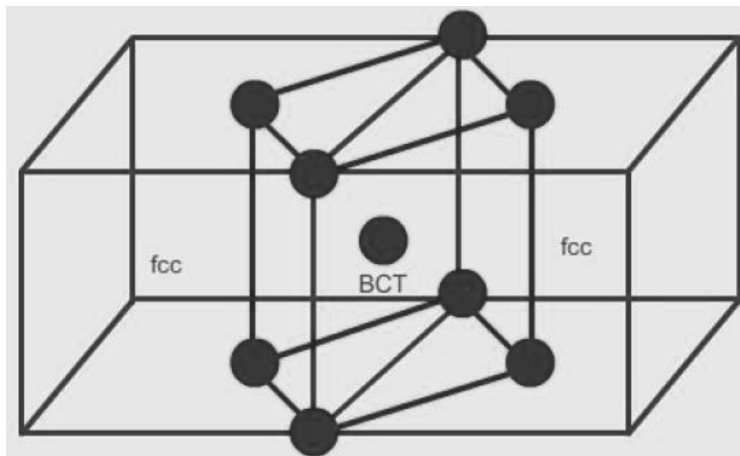


Lathe

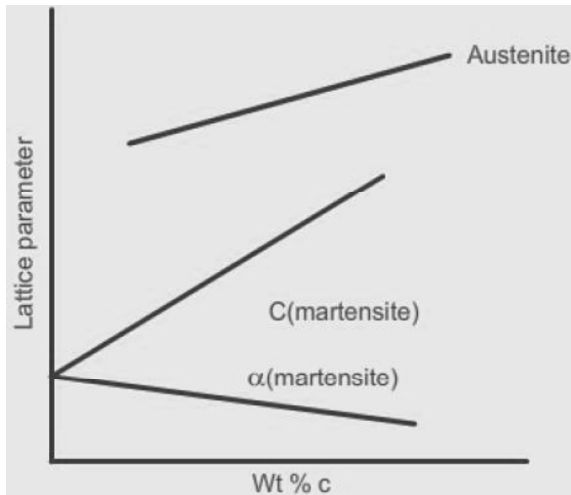
The martensites grow (almost) at the speed of sound in the material and hence need no thermal activation. They start forming on reaching the so-called martensite start (M_s) temperature and do not increase in volume after reaching the martensite finish temperature (M_f). The driving force for martensites to form is shown in Fig.



The most important aspect of martensitic transformation is the crystallography of the martensite; it is closely related to two things, namely, the presence of invariant plane in the austenitic phase (which is indicated by the tilt of lines drawn on a prepolished surface before the transformation) and the presence of a habit plane with specific (Kurdjumov-Sachs) orientation relationship. It is possible to obtain a bct crystal from the fcc one; however, such a bct unit cell has to be contracted by 20% in the c direction and expanded by about 12% in the a and b directions to account for the measured lattice parameters of the fcc and martensitic phases. This strain (-20% along c and +12% along a and b) is known as Bain strain. Further, the observed orientation relationships between the austenite and martensitic phases can be explained using such a (so called Bain) transformation of the fcc to bct phase. However, Bain strain alone is not sufficient to explain the presence of an invariant plane. Hence, theories of martensite crystallography typically involve Bain strain coupled with certain shears and lattice rotations to explain the observed invariant planes.



FCC versus BCT crystal structures.



Variation of lattice parameters in the austenite and martensite phases as a function of carbon composition.

Bain Strain :

The strains that transform one Bravais lattice into a different one in steels with minimum atomic movements is known as Bain strain.

Also called Homogeneous lattice-distortive strains.

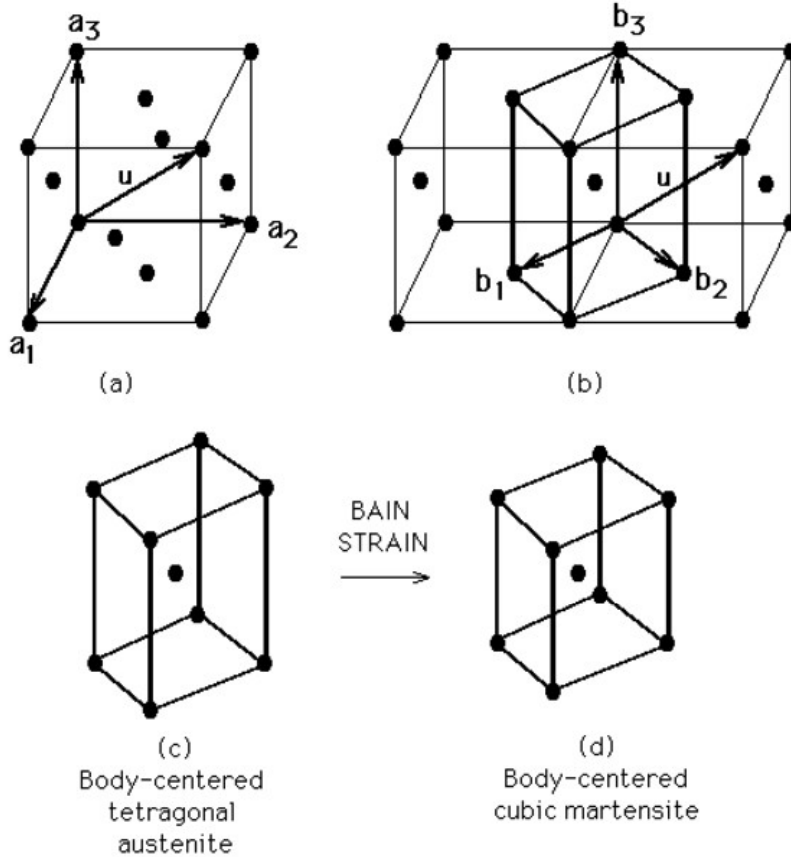
This can be represented by a strain matrix S which transforms one vector y into a new vector x .

$$y = Sx$$

This is homogeneous as straight lines are transformed to new straight lines.

Example : Cubic lattice increasing in size on all 3 axes (dilation) or shearing into a monoclinic structure .

Austenite lattice transforms to martensite lattice by bain strain.



∴ The Bain strain (not all lattice points illustrated)

MODEL QUESTIONS

1. FCC is a more close packed structure yet solubility of carbon in austenite which is FCC is higher than that in ferrite which is BCC. Why it is so?
2. Sketch the microstructure of 0.2% C steel. Calculate %Pearlite % cementite, % proeutectoid ferrite and % total ferrite.
3. Estimate the ratio of the widths of ferrite and cementite plates in lamellar pearlite.

MODULE III

Lecture 27

Review of Iron-carbon alloy system: Iron-cementite and iron-graphite phase diagrams

The Iron-Iron Carbide (Fe-Fe₃C) Phase Diagram

Steels are alloys of Iron (Fe) and Carbon (C). The Fe-C phase diagram is a complex one, but we will only consider the steel part of the diagram, up to around 7% Carbon.

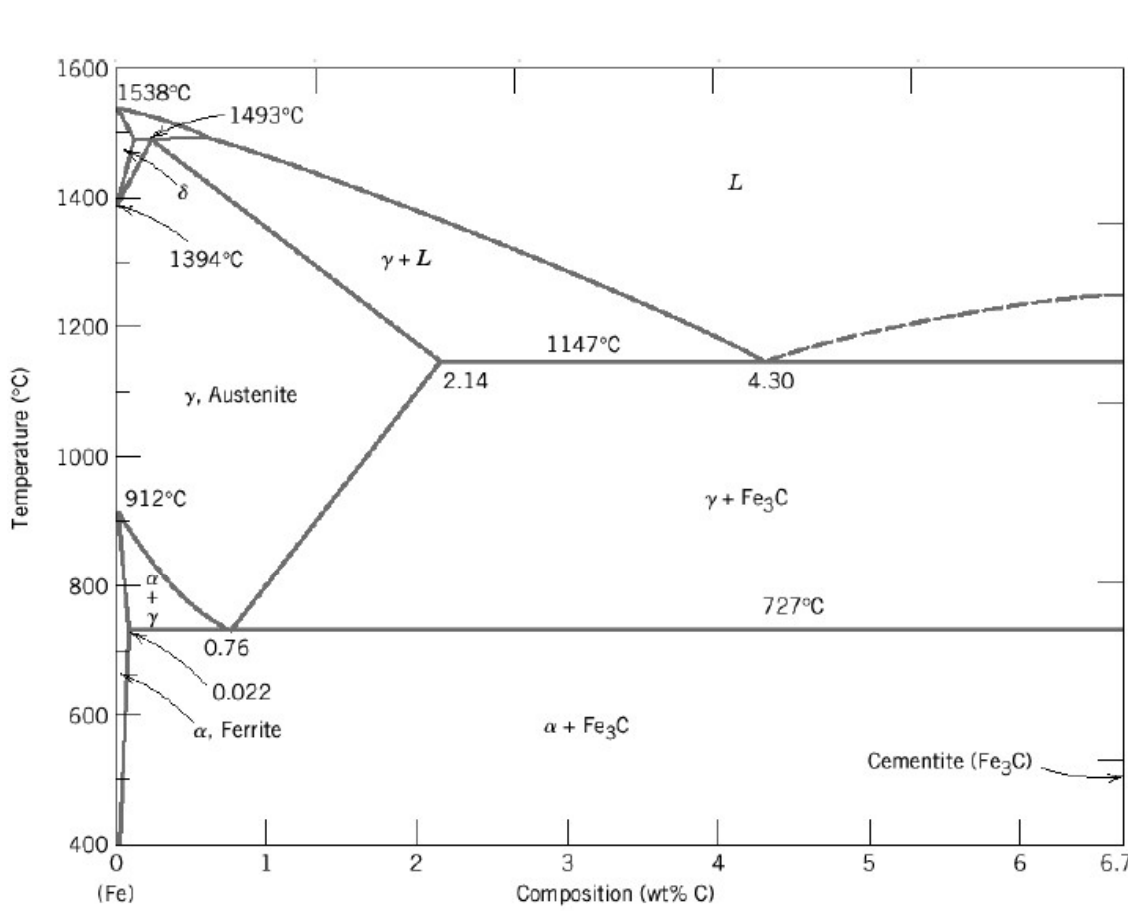


Fig.- Fe-Fe₃C Phase Diagram

Phases in Fe-Fe₃C Phase Diagram

α-ferrite - solid solution of C in BCC Fe

- Stable form of iron at room temperature.
- The maximum solubility of C is 0.022 wt%
- Transforms to FCC γ-austenite at 912 °C

γ-austenite - solid solution of C in FCC Fe

- The maximum solubility of C is 2.14 wt %.
- Transforms to BCC δ -ferrite at 1395 °C
- Is not stable below the eutectic temperature (727 °C) unless cooled rapidly

δ -ferrite - solid solution of C in BCC Fe

- The same structure as α -ferrite
- Stable only at high T, above 1394 °C
- Melts at 1538 °C

Fe₃C (iron carbide or cementite)

- This intermetallic compound is metastable, it remains as a compound indefinitely at room Temperature, but decomposes (very slowly, within several years) into α -Fe and C (graphite) at 650 – 700 °C

Fe-C liquid solution

A few comments on Fe–Fe₃C system

C is an interstitial impurity in Fe. It forms a solid solution with α , γ , δ phases of iron

Maximum solubility in BCC α -ferrite is limited (max.0.022 wt% at 727 °C) - BCC has relatively small interstitial positions Maximum solubility in FCC austenite is 2.14 wt% at 1147°C - FCC has larger interstitial positions Mechanical properties: Cementite is very hard and brittle - can strengthen steels. Mechanical properties also depend on the microstructure, that is, how ferrite and cementite are mixed.

Magnetic properties: α -ferrite is magnetic below 768 °C, austenite is non-magnetic

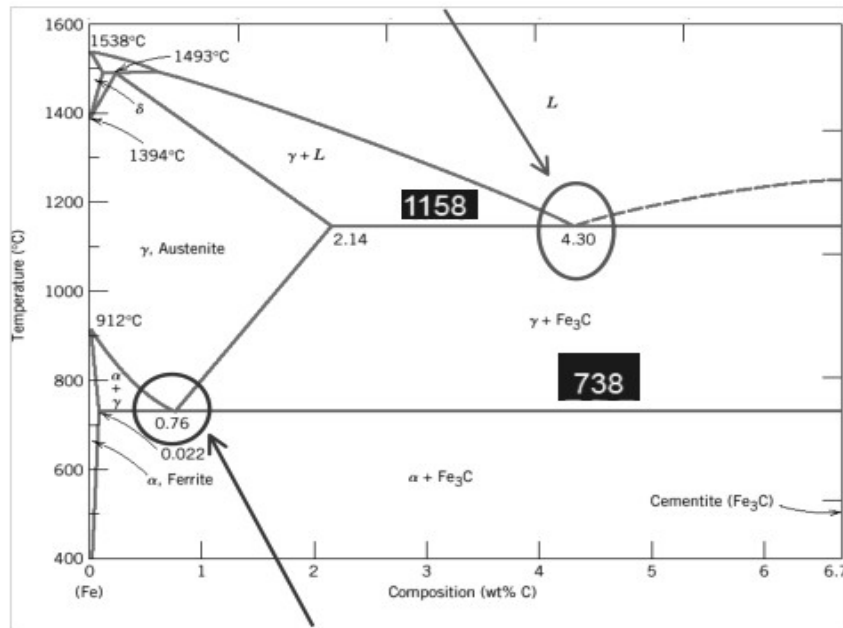


Fig.- Fe–Graphite Phase Diagram

Classification. Three types of ferrous alloys:

- Iron: less than 0.008 wt % C in α -ferrite at room T
- Steels: 0.008 - 2.14 wt % C (usually < 1 wt %) α -ferrite + Fe₃C at room T
- Cast iron: 2.14 - 6.7 wt % (usually < 4.5 wt %)

Peritectic. Eutectic and Eutectoid reactions in Fe–Fe₃C

Peritectic

Eutectoid: 0.76 wt% C, 727 °C

γ (0.76 wt% C) \leftrightarrow α (0.022 wt% C) + Fe₃C

Eutectic: 4.30 wt% C, 1147 °C

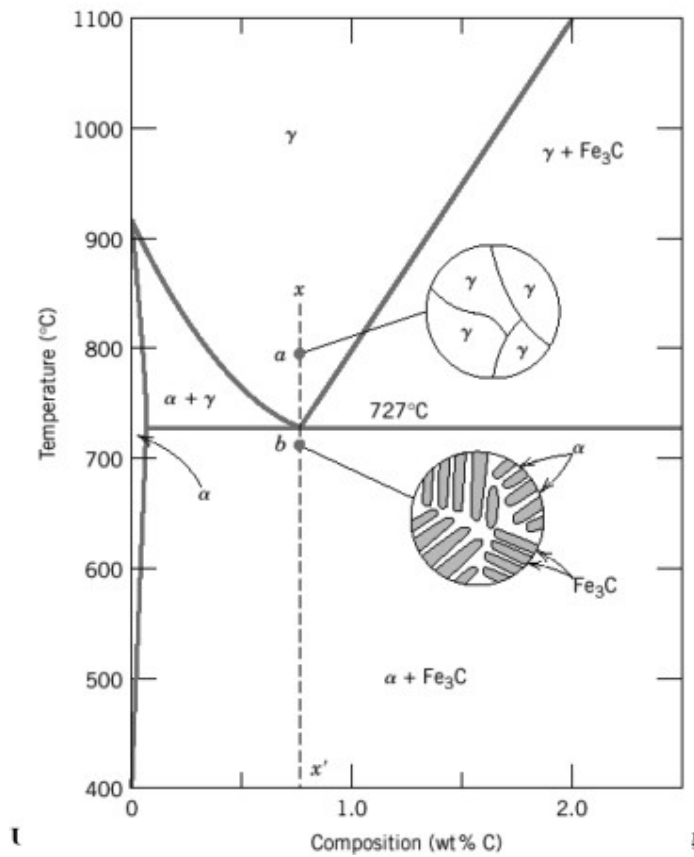
$L \leftrightarrow \gamma + Fe_3C$

Eutectic and eutectoid reactions are very important in heat treatment of steels

Lecture 28

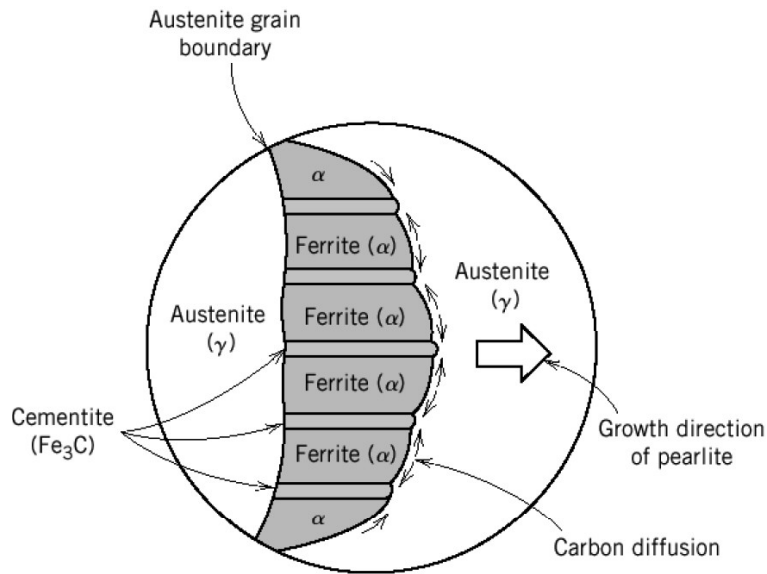
Development of Microstructure in Iron - Carbon alloys Microstructure depends on **composition (carbon content) and heat treatment**. In the discussion below we consider slow cooling in which equilibrium is maintained.

Microstructure of eutectoid steel (I)



When alloy of eutectoid composition (0.76 wt % C) is cooled slowly it forms **pearlite**, a lamellar or layered structure of two phases: α -ferrite and cementite (Fe_3C).

The layers of alternating phases in pearlite are formed for the same reason as layered structure of eutectic structures: redistribution C atoms between ferrite (0.022 wt%) and cementite (6.7 wt%) by atomic diffusion. Mechanically, pearlite has properties intermediate to soft, ductile ferrite and hard, brittle cementite.

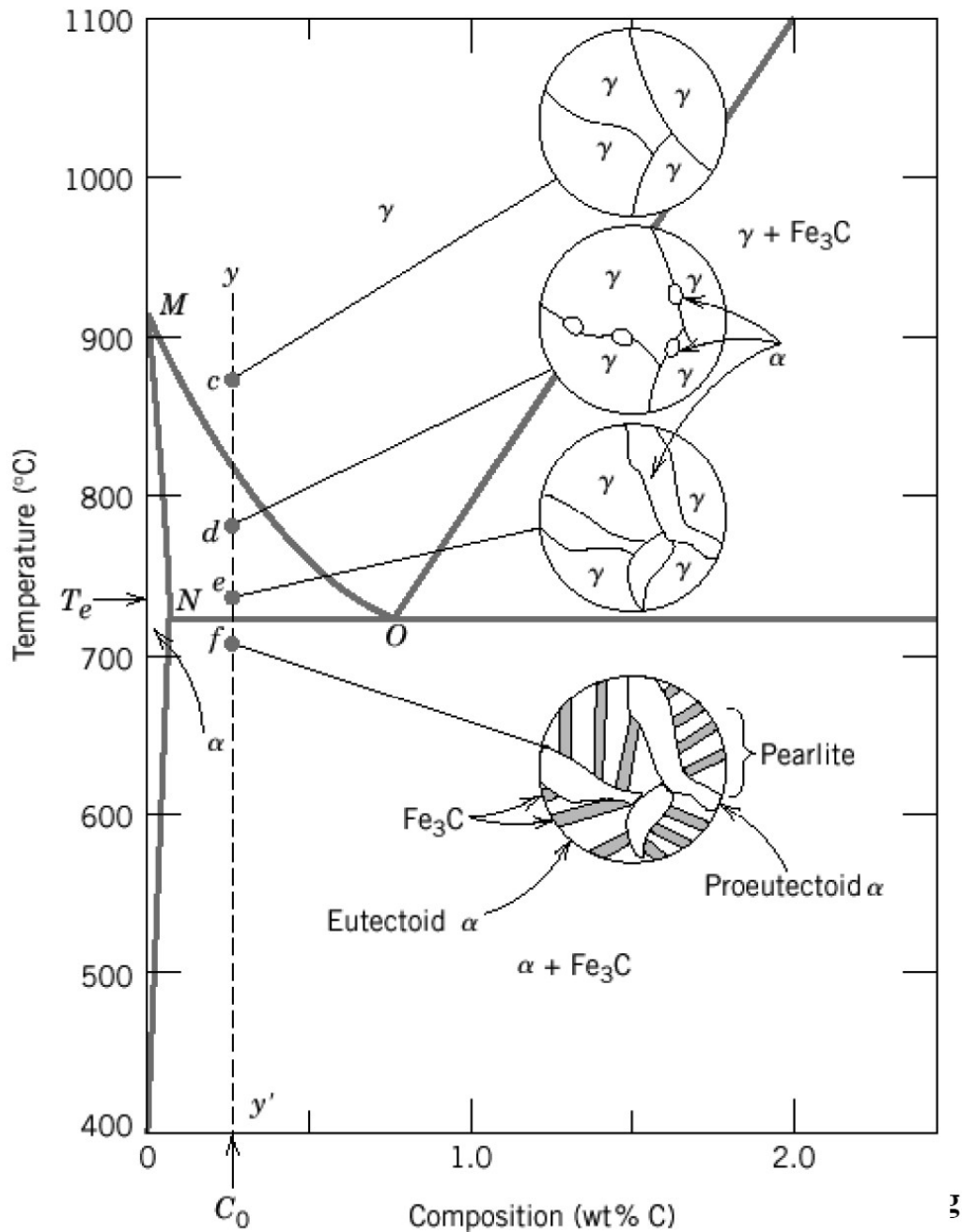


In the micrograph, the dark areas are Fe_3C layers, the light phase is α -ferrite.

Microstructure of eutectoid steel (II)

Compositions to the left of eutectoid (0.022 - 0.76 wt % C) **hypoeutectoid alloys**

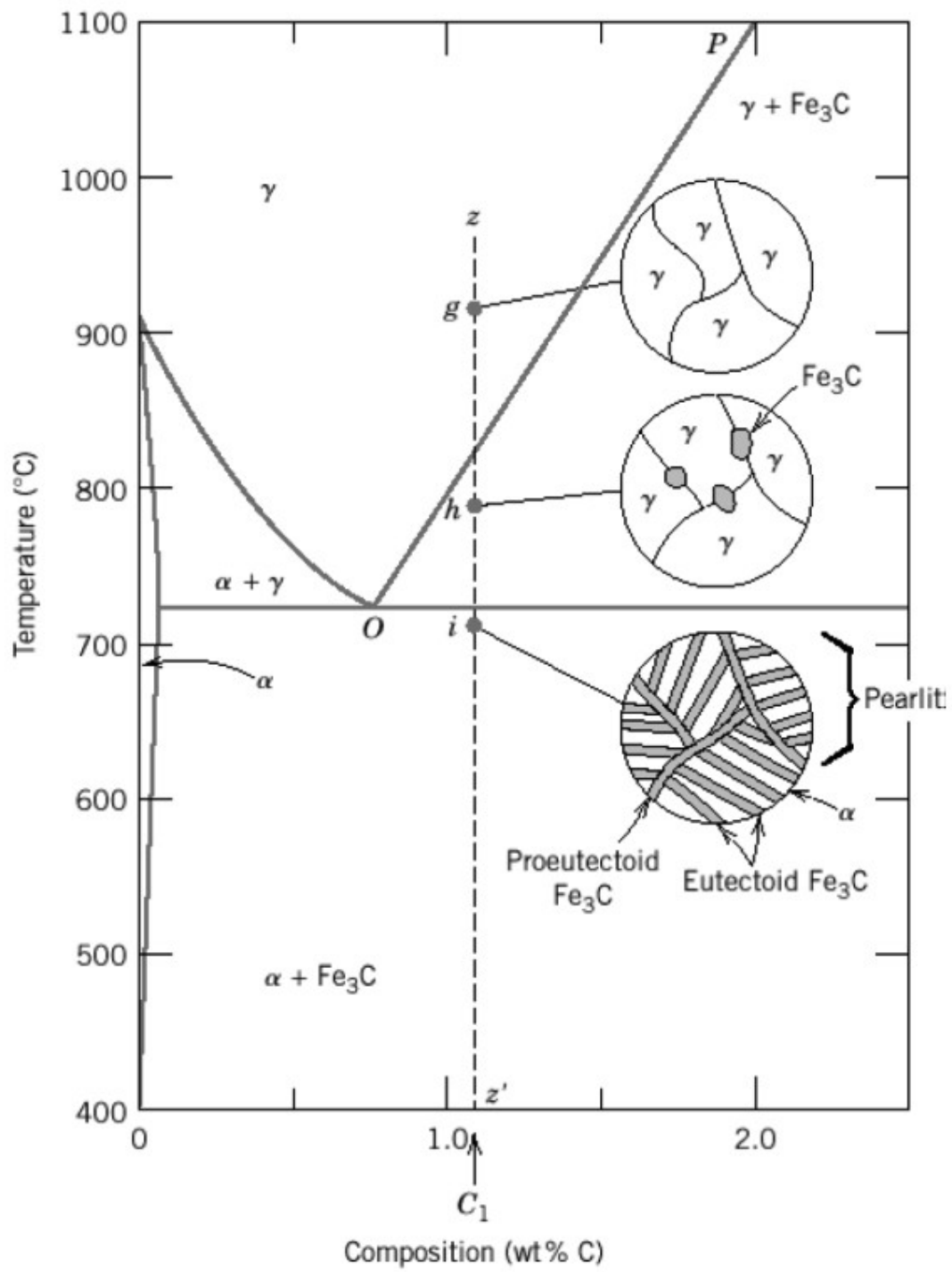
Hypoeutectoid alloys contain proeutectoid ferrite (formed above the eutectoid temperature) plus the eutectoid pearlite that contain eutectoid ferrite and cementite.



Compositions to the right of eutectoid (0.76 - 2.14 wt % C) **hypereutectoid alloys.**



Hypereutectoid alloys contain proeutectoid cementite (formed above the eutectoid temperature) plus pearlite that contain eutectoid ferrite and cementite.



Lecture 30

Heat treatment of steels: TTT and CCT diagrams

After completing the first step of heat treatment cycle, i.e. heating the steel to a predetermined temperature to obtain homogeneous and fine-grained austenite, the steel is cooled to room temperature at a rate depending on the heat treatment to be given (slow cooling or fast cooling). These cooling rates are much faster than equilibrium cooling rates for which Fe-Fe₃C diagram was constructed.

Time –Temperature Transformation (TTT) Diagrams

Temperature of transformation controls the nature of decomposed product of austenite which decides the resultant properties of steel. Therefore the study of transformation temperature effect on the nature of decomposed product is important. The kinetics of austenite transformation can be studied at a constant temperature rather than by a continuous cooling. The constant temperature transformation is also referred to as isothermal transformation which is studied by an experiment.

EXPERIMENT:

A number of small steel samples are heated to predetermined austenitizing temperature and are held at this temperature for a sufficiently long period so as to obtain a homogeneous austenite. These austenitised samples are transferred quickly to another bath maintained at a constant temperature below eutectoid temperature, selected for the study of kinetics of transformation. These samples are taken out one by one from the subcritical temperature bath after different time intervals and quenched immediately. The quenching of samples results in the formation of martensite from the untransformed austenite. By this technique, the amount of transformed austenite can be determined as a function of time at constant temperature. The amount of transformed austenite will increase by allowing samples to remain in constant temperature bath for a longer time. After a particular time all the austenite will transform to an aggregate of ferrite and cementite at a given temperature. Fig.1 shows the effect of time on the amount of transformed austenite for a given transformation temperature T . Transformation of austenite to ferrite-cementite mixture occurs after a definite time (t_1). The time period where transformation does not proceed is known as incubation period. This fig.1

has a limitation that it only correlates the amount of transformed austenite with transformed time for a constant temperature. Both time and temperature has significant effect on the decomposition of austenite therefore it is necessary to construct a time temperature and transformation diagram.

For the construction of TTT diagram the above mentioned procedure is repeated a for number of times at varying transformation temperature. Fig.2 shows the amount of transformed austenite at various time periods for different transformation temperatures. It can be analysed that higher the transformation temperature, the more is the incubation period and the time required for completion of the transformation. Both the incubation period and transformation time decrease with lowering of transformation temperature. However after a particular temperature the decreasing trend is reversed and both incubation period and transformation time increase again with further lowering of transformation temperature. With decrease in the isothermal transformation temperature, the austenite becomes more unstable and rate of nucleation increases.

From the result of Fig.2 another diagram can be constructed with time and temperature as abscissa and ordinate respectively. Fig. 3 shows the TTT diagram for a eutectoid steel.

Fig. 4 and 5 represents the TTT diagrams for hypoeutectoid and hyper eutectoid steels, respectively. A common feature of these TTT diagrams is that proeutectoid phase (ferrite for hypoeutectoid and cementite for hypereutectoid steels) separates out in upper temperature region. For hypoeutectoid steels, ferrite starts separating out from the austenite as soon as austenite is cooled below the upper critical temperature (A_3).

CONTINUOUS COOLING TRANSFORMATION(CCT)

The TTT diagrams have gained great importance because they are extremely useful to give information about the hardening response of steels and the nature of transformed products of austenite at varying degrees of supercooling. These diagrams have been of great practical importance to some special heat treatment processes such as austempering and iso thermal annealing. But in practically transformation occurs by continuous cooling not in isothermally. Therefore a diagram which correlates transformation, temperature and time during continuous cooling has to be studied.

Continuous cooling transformation (CCT) diagrams can be obtained by the same procedure which is used for the TTT diagram except that in case of CCT diagram points of start and end of austenite are recorded on continuous cooling. For the construction of CCT curve for eutectoid steel a large number of samples are heated above the lower critical temperature (A_1) to get a completely austenite structure. From this temperature, specimens are cooled at a constant cooling rate and repeating the same process at various cooling rates, different sets of start and end points for pearlitic transformation are obtained. On joining start and end points, two curves similar to those in TTT curves corresponding to start and end of transformation are obtained. Fig.6 shows the CCT diagram for eutectoid steel.

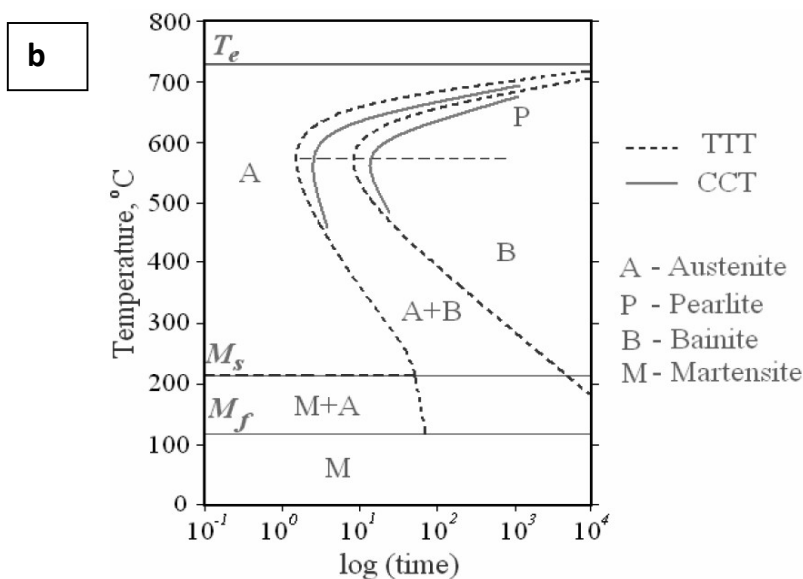
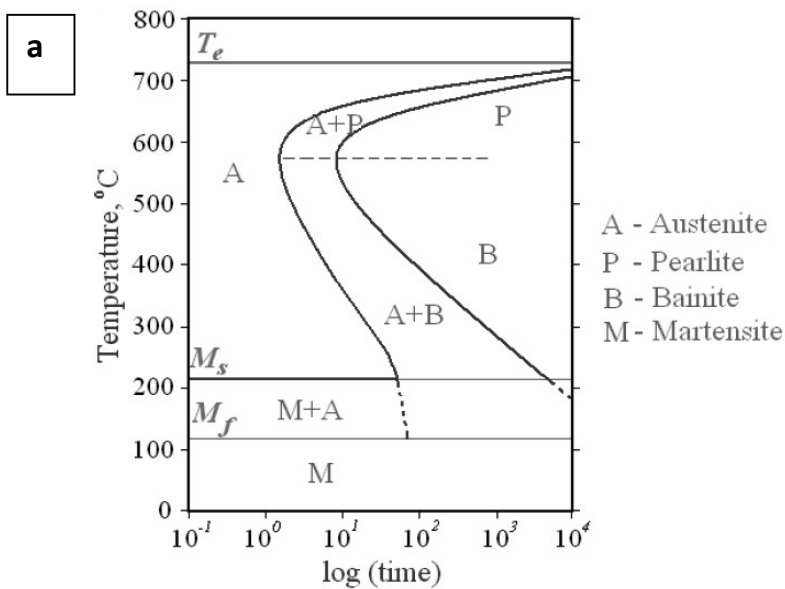


Fig. (a) Complete TTT diagram and (b) Superimposition of TTT and CCT diagram of a eutectoid steel.

Lecture 31

Conventional heat treatment processes – annealing, normalizing

Properties of steels can be controlled and varied over a very wide range by heat treatment. Thus a thorough understanding of heat treatment of steel is very important.

Annealing

Annealing involves heating to a predetermined temperature, holding at this temperature and finally cooling at a very slow rate. The temperature to which steel is heated and the holding time are determined by various factors such as chemical composition of steel, size and shape of steel component and final properties desired.

Purpose of annealing:

- (1) Relieve internal stress
- (2) Improve or restore ductility
- (3) Enhance machinability
- (4) Eliminate chemical non-uniformity
- (5) Refine grain size
- (6) Reduce the gaseous contents in steel

Depending on the heat treatment temperature annealing treatment can be subdivided into three classes:

- (1) Full annealing
- (2) Partial annealing
- (3) Subcritical annealing

Full annealing steel is heated above the upper critical temperature (A_3) and then cooled slowly.

Partial annealing involves heating steel to temperature lying between lower critical temperature (A_1) and upper critical temperature (A_3 or A_{cm}).

Subcritical annealing is a process in which the maximum temperature to which steel is heated is always less than the lower critical temperature (A_1).

Depending on the specific purpose, annealing is classified into various types:

- (1) Diffusion annealing

- (2) Spheroiding annealing
- (3) Full annealing
- (4) Recrystallization annealing

Full annealing

Steel is heated to about 30-50°C above the upper critical temperature for hypo-eutectoid steels. The steel is held at this temperature for predetermined time, followed by cooling at a very slow rate as cooling in the furnace.

Isothermal annealing

In hypo-eutectoid steel is heated above the upper critical temperature and held for some time at this temperature. The steel is then cooled rapidly to a temperature less than the lower critical temperature (A_1). This temperature is usually chosen between 600-700°C. Fast cooling can be achieved by rapidly transferring steel to another furnace maintained at the desired temperature.

Diffusion annealing

This process is also known as homogenizing annealing, is employed to remove any structural non-uniformity. Dendrites, columnar grains and chemical inhomogenities are observed in the case of ingots, heavy plain carbon steel castings and high alloy steel castings. Steel is heated sufficiently above the upper critical temperature (1000-1200°C) and held at this temperature for prolonged periods, 10-20 hours, followed by slow cooling.

Partial annealing

Partial annealing is also referred to as intercritical annealing or incomplete annealing. Steel is heated between the lower critical temperature and the upper critical annealing. It is followed by slow cooling. Hypoeutectoid steels undergo this process. The resultant microstructure consists of fine pearlite and cementite instead of coarse pearlite and a network of cementite at the austenite grain boundaries as observed in the case of full annealing.

Recrystallization annealing

Heavily cold worked are subjected to this treatment. The process consists of heating steel above the recrystallization temperature, holding at this temperature and cooling thereafter. The temperature for recrystallizing annealing is not fixed. Recrystallization temperature and also recrystallization annealing temperature depends on chemical composition, amount of prior deformation, holding time and initial grain size.

Process annealing

In this process steel is heated to a temperature below the lower critical temperature and is held at this temperature for sufficient time and then cooled. As it is subcritical annealing, cooling rate is of little importance. Purpose of this process is to reduce the hardness and increase ductility of cold worked steel so that further working can be carried out easily. It differs from recrystallization annealing in the sense that complete recrystallization of cold worked steel may or may not take place in this treatment.

Normalizing

Normalizing is a process of heating steel to about 40-50°C above the upper critical temperature, holding for proper time and then cooling in still air or slightly agitated air to room temperature. In special cases, cooling rate can be controlled either by changing air temperature or air volume. After normalizing the resultant microstructure should be pearlitic. This is particularly important for some alloy steels which are air hardening by nature.

Since the temperature involved in this process is more than that for annealing, the homogeneity of austenite increases and it results in better dispersion of ferrite and cementite in the final microstructure. This dispersion results in enhanced mechanical properties.

Application:

Refinement of grain size is one of the most important objectives of normalizing. Rolled and forged steel, possessing coarse grains due to high temperatures involved in these operations are subjected to normalizing treatment for grain refinement.

Another important application is adoption as post treatment after achieving a homogeneous structure. Generally heavy castings, including ingots, suffer from chemical inhomogeneity.

Normalizing Versus Annealing

1. Normalized steels are harder than annealed ones.
2. Relatively rapidly cooling results higher degree of supercooling, therefore
3. Austenite decomposes lower temperature. Better dispersion of ferrite carbide aggregate. Both of these factors result in higher strength and hardness.
4. Normalized steel has lower impact transition temperature than annealed steel.
5. Annealing improves the machinability of medium carbon steel, where as normalizing improves machinability of low carbon steels.

Lecture32

Hardening and Tempering

For heavy duty purposes high hardness is required. The process by which high hardness can be obtained is known as hardening. Hardening treatment consists of heating to hardening temperature, holding at that temperature followed by rapid cooling such as quenching in

water, oil or salt baths. The high hardness developed by this process is due to the phase transformation accompanying rapid cooling.

Hardening temperature depends on chemical composition, for plain carbon steel it depends on carbon content alone. Hypoeutectoid steels are heated to about 30-50°C above the upper critical temperature, whereas eutectoid and hypereutectoid steels are heated to about 30-50°C above the lower critical temperature. Ferrite and pearlite transform to austenite at hardening temperature for hypoeutectoid steels. This austenite transforms to martensite on rapid quenching from hardening temperature. The presence of martensite accounts for high hardness of quenched steel. If hypoeutectoid steel is heated to a hardening temperature equivalent to that of hypereutectoid steel, the structure will consist of ferrite and austenite. This will transform to ferrite and martensite on quenching. The preferred hardening temperature for hypereutectoid steel lies between the lower critical and upper critical temperature.

Advantages

1. The first is related to the presence of cementite in hardened steel which improves the wear resistance of the steel.
2. Hardening temperature is the attainment of fine martensite in the final microstructure.

Because of rapid cooling internal stresses are developed, so hardened parts are followed by another treatment known as tempering which reduces internal stresses and improves the ductility of the material.

FACTORS AFFECTING HARDENING PROCESS

Properties improved by hardening are depends on various factors:

1. Chemical composition of steel
2. Size and shape of the steel part
3. Hardening cycle i.e heating rate, hardening temperature, holding time and cooling rate
4. Homogeneity and grain size of austenite
5. Quenching media
6. Surface condition of steel parts

Hardening Methods

Rapid cooling is carried out in order to obtain martensite in hardened steel. Austenite to pearlite transformation is suppressed in this process.

(i) conventional or direct quenching

(ii) quenching in stages

(iii) spray quenching

Spray quenching is a specific hardening method in which the steel part is cooled from the hardening temperature by spraying quenchant continuously. The rate of heat extraction from the steel part is much higher as compared to direct quenching.

(iv) quenching in self tempering

(v) austempering or iso thermal quenching

This is a special heat treatment process in which austenite is transformed to bainite. Austempering consists of heating steel to above the austenitizing temperature. It is then quenched in a bath maintained at a constant temperature in the bath itself till all the austenite is transferred into bainite.

(vi) martempering

Heating the steel to the austenitizing temperature followed by quenching in a constant temperature bath maintained above M_s point. The usual temperature of the bath lies between 180 and 250°C. Steel is held in the bath till a uniform temperature is achieved through out the section and then cooled in air. The cooling rate should be sufficiently high and holding time is short to prevent transformation of austenite to pearlite or to bainite. Martensite is formed in the second stage. The resultant microstructure of martempered steel is martensite. In order to improve properties, martempered steels are generally tempered.

Tempering

Heating hardened steel below the lower critical temperature, followed by cooling in air or at any other desired rate, is known as tempering. It is already mentioned that hardening process is followed by tempering to improve the ductility of the steel. Tempering treatments lower

hardness, strength and wear resistance. However this is compensated by the advantages gained by relieving internal stresses, restoration of ductility and transformation of retained austenite.

STRUCTURAL CHANGES DURING TEMPERING

A number of structural changes take place during tempering treatment. These changes include isothermal transformation of retained austenite, ejection of carbon from body centred tetragonal lattice of martensite, growth and spheroidization of carbide particles and formation of ferrite-carbide mixture.

1. First stage of tempering is also referred to as low temperature tempering. The maximum temperature at this stage is 250°C and this results a low carbon martensite and a carbide by transformation of high carbon martensite. The carbide precipitation from the high carbon martensite during the first stage of tempering is not cementite. This carbide is known as epsilon carbide which has a hexagonal closed packed structure. The carbon content of epsilon carbide is more than that of cementite and the chemical formula $Fe_{2.4}C$. This carbide is forms at low temperature range in which martensite is metastable.

2. The second stage of tempering consists of heating steels in the temperature range (350-500°C) In this stage retained austenite is transformed to bainite. It consists of ferrite and epsilon carbide.

3. The third stage of tempering is known as high temperature tempering (500-680°C). At this high temperature a mixture of ferrite and cementite forms. Martensite changes to ferrite by losing its carbon. The release carbon combines with epsilon carbide which forms cementite.

Effect of alloying elements on tempering

Almost all alloying elements enhance the ability of steel to softening during tempering. Alloying elements is divided by carbide (Cr, Mo, W, V, Ti) and non carbide (Ni, Al, Mn) forming elements. Non carbide forming elements enters into ferrite and/or martensite hence they have less impact on tempered hardness of steel. In case of carbide forming elements they form their respective alloy carbides and the martensite formed in the alloy steel are more stable.

Lecture33

Hardenability, role of alloying elements in steels

When a piece of steel is heated to austenitizing temperature and then quenched, the cooling rate varies across the cross section. Since different grades of steel has its own depth of penetration of hardness across the cross section. Hardenability of steel is a measure of this property. It may be defined as the susceptibility of the steel to hardening when quenched and is related to the depth and distribution of hardness across a cross-section.

The maximum hardness depends on the carbon content in the steel. It can be achieved by fulfilling the following conditions:

- (i) All the carbon is in solution in austenite
- (ii) Critical cooling rate is achieved
- (iii) No retained austenite is present after quenching
- (iv) No auto tempering of martensite takes place

Significance of Hardenability

For heat treatment, hardenability is a very useful and important property of steel. It determines the rate at which the given steel should be quenched. This also tells about the maximum hardness that can be achieved on the surface of steel of larger cross section bars, subjected to drastic quenching.

Relationship of Hardenability with transformation rate

In general hardness of steel increases as the transformation temperature decreases. Low temperature transformation products and lower bainite and martensite, when tempered, shown improved ductility and toughness. Cooling rate should be very rapid to avoid high temperature transformation even at the nose of the TTT diagram. This rate which just allows the transformation of austenite to martensite is known as upper critical cooling rate and is one of the methods of expressing hardenability.

While the microstructure changes with distance along the diameter, there is a corresponding change in the hardness of the steel bar. This observation can be made by taking a circular cross-section of the quenched steel bar and noting the hardness at different points along a diameter. By plotting the results we get a curve which shown in Fig.1.

The hardness at the surface is Rc 65 and a corresponding martensitic structure. The pearlitic structure near the centre has hardness around Rc 40. On this fig. Hardness of Rc54 corresponding to hardness of eutectoid steel containing 50% martensite and 50% pearlite, is drawn as a horizontal line. This horizontal line intersects the hardness curve at the region where the specimen gets cooled at a rate which produces 50% martensite. The position corresponding to 50% martensite and 50% pearlite can be easily measured and can be used as

a criterion for measuring the depth to which a steel has hardened with a given quenching medium.

DETERMINATION OF HARDENABILITY

Hardenability of steel is determined by the following methods

- (i) Grossman's critical diameter method**
- (ii) Jominy-end quench test**
- (iii) Estimation of hardenability from chemical composition**
- (iv) Fracture test**

(i) Grossman's critical diameter method

If a large number of cylindrical samples of different diameters of the same steel, after austenitizing are quenched in a coolant and after cutting at half lengths, the centre hardness is measured and plotted against the diameter of that bar, then the most rapid fall in hardness occurs where it has 50% martensite structure. The position of the steepest fall in hardness or point of inflection is the critical diameter.

Severity of quench

The effectiveness of given cooling medium is specified by the value of a parameter called its severity of quench i.e. its quenching power and represented by a symbol H, H is defined as the rate of heat treatment by the quenching medium from an object.

$$H=S/K$$

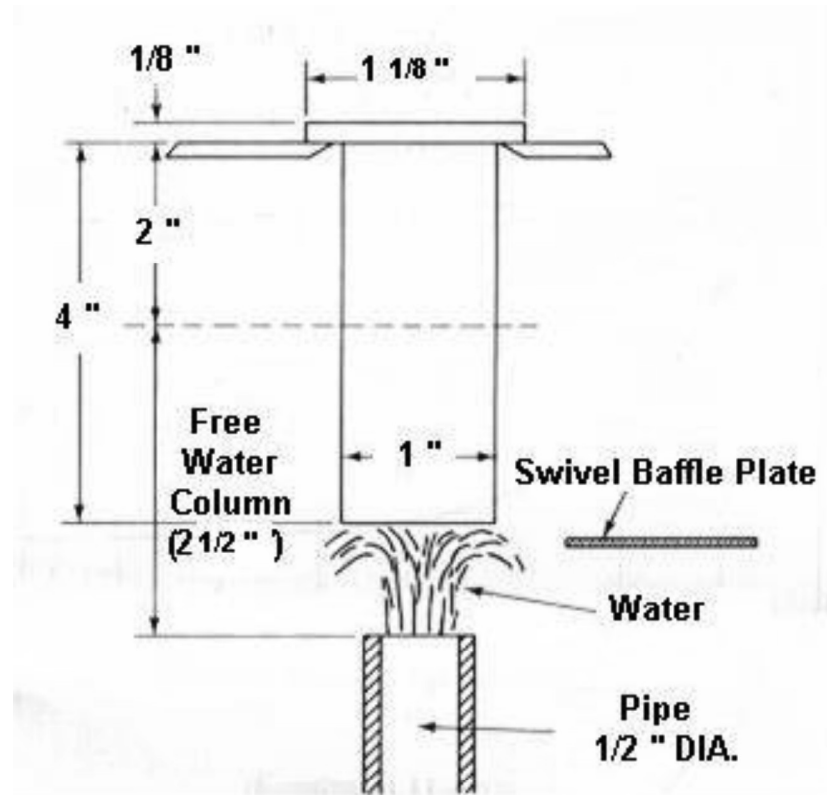
Ideal critical diameter

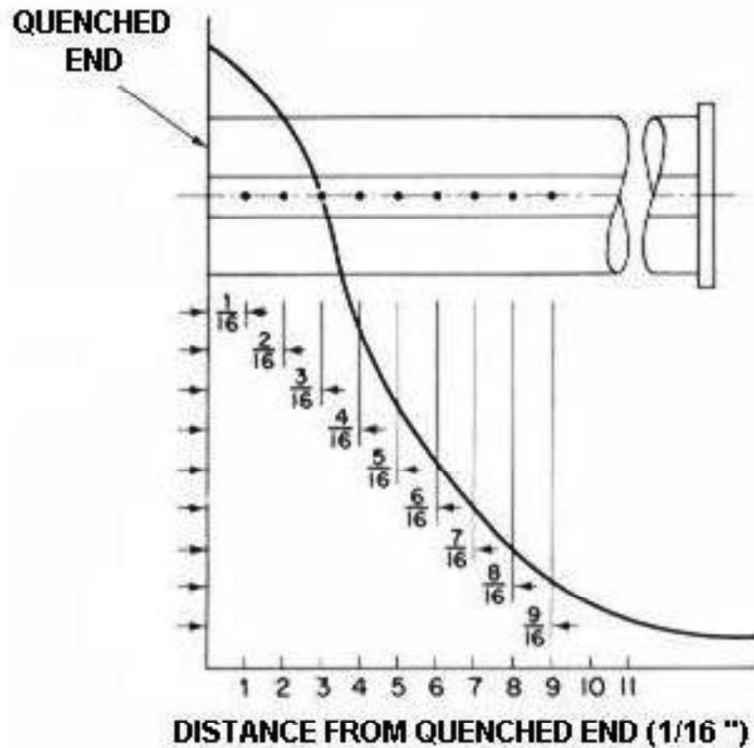
The critical diameter of a given steel changes depending on the quenchant i.e H value. Ideal critical diameter is defined as the diameter for which the unhardened core just disappears, if the bar is subjected to an ideal quench i.e. quench cools the surface of the bar instantly to the temperature of the quenching medium.

(ii) JOMINY END QUENCH TEST

Grossman method is laborious, difficult and time consuming. A relatively convenient and most common method of determining hardenability of a steel is the jominy end quench test. In this test a steel bar of 1 inch diameter and 4 inches long is heated to proper austenitizing temperature. After being soaked for sufficient time the specimen is quickly placed in a fixture as shown in fig. A water jet is opened quickly. Water comes out at a constant pressure through an orifice of ½ inch diameter. The distance between orifice and

the bottom end of the steel bar is kept at $\frac{1}{2}$ inch. The cooling rate is very rapid at the lower end and decreases gradually with increase in distance from the lower end where complete martensitic formation occurs. With 50% martensite hardness value of Rc 54 is





obtained. This distance is measured from the quenched end in units of 1/16 inch. The hardness is then plotted against the distance from the quenched-end of Jominy piece. As cooling rate decreases with the increasing distance, increased amount of non-martensitic products are formed and gradual decrease in hardness is observed. The resulting curve is called Jominy hardenability curve.

(iii) Estimation of hardenability from chemical composition

This method is based on the fact that the hardening of steel is controlled by the carbon content. Every steel has a base hardenability which depends only on carbon content and grain size. Alloying additions change the rate of reaction.

(iv) Fracture test

There is a contrast in the nature undergone by martensitic and pearlitic regions. Whereas martensitic formed on the case exhibits brittle fracture, the pearlite in the core undergoes ductile fracture. Where there is changeover from martensitic to pearlitic structure, there is corresponding sharp change from brittle to ductile fracture.

Factors affecting hardenability:

1. **Grain size:** Grain boundaries are preferential nucleation sites for ferrite and pearlite. If the austenite grain size is large, the grain boundary area is less, the probability of

nucleation to ferrite and pearlite decreases. Thus the hardenability of the steel increases as the grain size increases.

2. **Carbon content:** Carbon fixes the maximum attainable surface hardness on quenching. It also increases hardenability as it stabilises austenite and thus shifts the CCT curve to the right as its content increases upto 0.77% but beyond that hardenability decreases, because the undissolved proeutectoid cementite acts as nuclei for the pearlitic transformation and the CCT curve shifts towards left.
3. **Alloying element:** Most alloying elements (except Co) shifts the CCT curve towards right to increase the hardenability of steel, if the alloying elements are dissolved in austenite. The presence of undissolved alloy carbides, not only depletes the austenite of the alloying elements as well as carbon, which would have increased the hardenability, but helps to nucleate pearlite to decrease the hardenability.

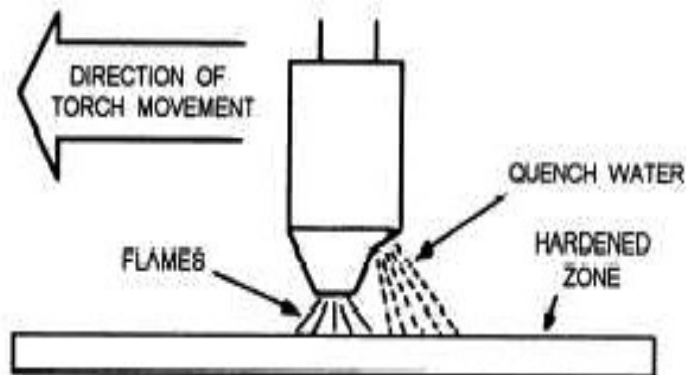
Lecture34

SURFACE HARDENING IN STEELS

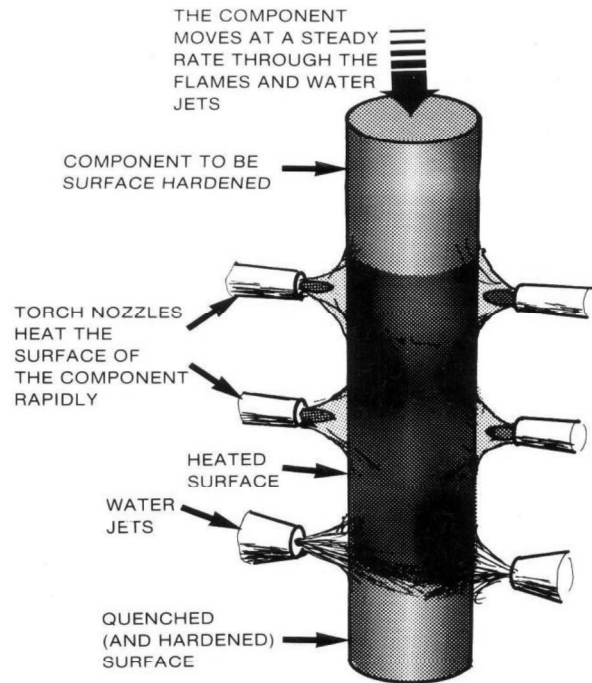
A large number of machine components require a combination of diverse properties such as high surface hardness and wear resistance along with good toughness and impact resistance.

These processes are flame hardening, induction hardening, laser hardening and induction beam hardening,

FLAME HARDENING:



This process consists of heating the large work piece, such as crank shaft, axel, cam, large gear by an oxy-acetylene or oxy-fuel blow pipe, followed by spraying of jet of water as coolant. After hardening, reheating of the parts is carried out in furnace or oil bath at about 180-200°C for stress relieving. Over heating of the work piece avoided. The carbon content required for flame hardening steels varies from 0.3% to 0.6%.



There are four different methods which are used in general for flame hardening:

- (i) stationary
- (ii) progressive
- (iii) spinning
- (iv) progressive spinning

INDUCTION HARDENING:

It is used to surface hardened crank shafts, cam shafts, gears, crank pins and axels. In this process heating of the component is achieved by electro magnetic induction. A conductor coil carries alternating current of high frequency which is then induced in the enclosed steel part placed within the magnetic field of the coil. As a result induction heating takes place.

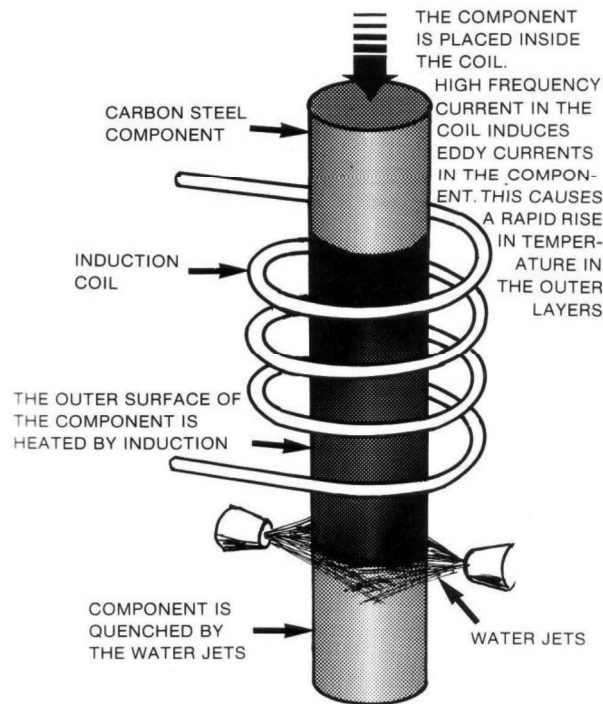
The degree of flow of current on the outer surface of a component depends on the frequency, resistivity and permeability of the component. For a given material resistivity and permeability depends on the temperature.

In cold state (20°C), $d_{20} = 20/\sqrt{f}$

In hot state (800°C), $d_{800} = 500/\sqrt{f}$

d =depth to which current flows and f frequency of current

From this it is observed that with increasing the frequency the depth of hardening decreases.



ELECTRON BEAM HARDENING

This process is used for hardening those components which cannot be induction hardened because of associated distortion. Automatic transmission clutch cams are hardened by this process. The work piece is kept in vacuum at 0.06m bar pressure. Electron beam is focused on the work piece to heat the surface.

LASER HARDENING

Laser beams are used for surface hardening treatment. Since these have very high intensity, they may melt the work piece when they are used at such high intensity. Therefore a lens is used to reduce the intensity by producing a defocused spot or scans from 1-25mm wide. A laser beam of 1KW produces a circular spot whose diameter vary from 0.5 mm to 0.25mm. In laser hardening process less time is required than in induction and flame hardening processes and the effect of heat on the surrounding surface is less, leading to less distortion.

The relationship between depth of hardening and power is

$$Y = -0.11 + \frac{3.02P}{(D_b V)^{1/2}}$$

Y=Case depth

P= laser power

D_b = incident beam diameter

V = traverse speed

ADVANTAGES:

1. It is possible to achieve high production rates since light has no inertia and consequently it is possible to obtain high processing speeds with rapid stopping and starting.
2. Input distortion is quite low because specific energy is very low.
3. It is possible to give localized treatment with this process.
4. No external quenching is needed.
5. There is hardly any contamination during surface hardening treatment.
6. It is possible to control the process with the help of a computer.
7. Those areas which are difficult to be treated by conventional methods can be easily treated with technique.
8. It is not necessary to carry out final machining operation subsequent to hardening.

Lecture35

CHEMICAL TREATMENT IN STEELS

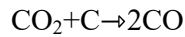
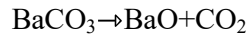
Chemical heat treatment is the process used to achieve different properties in core and steel components. There are situations in which the requirement is such that the outer surface should be hard and wear resistant and the inner core more ductile and tougher. Such a combination of properties ensures that the component has sufficient wear resistance to give long service life and at the same time has sufficient toughness to withstand shock loads.

1. Carburizing

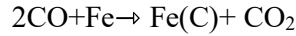
Carburizing is carried out in the temperature range 900-930°C. And the surface layer is enriched with carbon up to 0.7-0.9%. In this process, carbon diffused into steel by heating above the transformation temperature and holding the steel in contact with a carbonaceous material which may be a solid medium, a liquid or a gas. As the solubility of carbon is more in austenite state than in ferritic state, fully austenite state is essential for carburizing. The surface hardness depends on the relationship of hardness with carbon content which differs slightly for different grades of steels. carburizing is divided into three categories

- (i) **Pack carburizing:** This method of carburizing is also known as solid carburizing. It is the oldest method of carburizing steel components. In this process, steel components to be heat treated are packed with 80% granular coal and 20% $BaCO_3$ as energizer in heat resistant boxes and heated at 930°C in electric chamber furnace for a specific period of time which depends on the case depth required.

(i) Energizer decomposes to give CO gas to the steel surface:

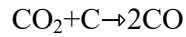


(ii) Carbon monoxide reacts with the surface of steel:



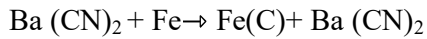
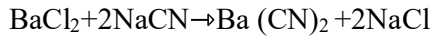
(iii) Diffusion of carbon into steel

(iv) CO_2 formed in step(ii) reacts with C in the coal:



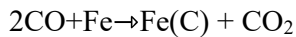
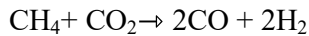
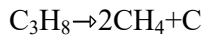
(ii) Liquid carburizing

Carburizing occurs through molten CN in low carbon steel cast pot type furnace heated by oil or gas. Bath temperature is maintained between 815 to 900°C.



(iii) Gas carburizing

It is carried out in retort type sealed quench type or continuous pusher type furnace. These furnaces are either gas fired or are heated electrically. Gas carburizing temperature varies from 870-950°C. During gas carburizing the following reactions are take place:



2. Vacuum Carburizing:

Carburizing in vacuum or reduced pressure is carried out in two stages. In the first stage carbon is made available to the steel absorption. In the second stage diffusion of the carbon takes place within the steel piece and results in appropriate concentration of carbon and depth of carburizing.

Lecture36

Thermo-mechanical treatment of steels; High temperature and low temperature Thermo-Mechanical treatment

Thermomechanical treatment is the combination of heat treatment and mechanical working in which plastic deformation occurs as a result there is a phase transformation of the material. Plastic deformation occurs due to crystal defects like vacancies, dislocations, sub-grain boundaries and stacking faults. These defects affect the phase transformation of the metals and alloys by providing nucleation sites. Hence in case of thermomechanical treatment phase transformation is an important aspect. Thermomechanical treatment is applied both to the ferrous and nonferrous materials. As major engineering applications involve the use of ferrous materials, especially to steels, which consists of producing strained austenite and its subsequent transformation to other phases.

Classification:

Depending upon the temperature of deformation of austenite, thermomechanical treatment can be broadly classified into High temperature thermomechanical processing (HTMT) and Low temperature thermomechanical processing (LTMT).

(1)HTMT:

In HTMT process deformation of austenite at a temperature above the recrystallization temperature. The austenite is immediately quenched after mechanical working. Here the obtained strength is higher than the conventional hardening and tempering process. It is a hot working process, thus recrystallization eliminates strain hardening effect. For this reason only a small reduction in area, about 20-30% is given and steel is immediately quenched. This treatment results in better ductility and impact strength.

(2)LTMT:

In this process austenite is supercooled to a temperature below the recrystallization temperature and then this supercooled austenite is deformed at this temperature. This is followed by rapid cooling immediately after the working. This process can be regarded as transformation of cold worked austenite, here deformation indicated by reduction in area which is about 80-90%. Hence the strength levels are higher than HTMT. Ductility values achieved by this treatment are comparatively lower.

Another method of classification of thermomechanical treatment is based on the deformation temperature in relation to the critical temperatures of steel. On this basis the three classes of thermomechanical treatments are the supercritical, intercritical and subcritical treatment. Supercritical thermo mechanical processing deforms the steel in an austenitic condition. Deformation is followed by rapid cooling.

Low temperature thermomechanical treatment -LTMT (Ausforming)

The process known as ausforming or low temperature thermomechanical treatment (LTMT), involves the deformation of austenite in the metastable bay between the ferrite and bainite curves of the TTT diagram. The treatment is shown schematically in Fig. 1a. Steel, with a

sufficiently developed metastable austenite bay is quenched from the austenitizing temperature to this region, where substantial deformation is carried out, without allowing transformation to take place. The deformed steel is then transformed to martensite during quenching to room temperature, and the appropriate balance of mechanical properties achieved by subsequent tempering. This ausforming treatment can be contrasted with a high temperature thermomechanical treatment (HTMT), where the deformation is carried out in the stable austenite region (Fig. 1b), usually above A_{c3} prior to quenching to form martensite. In a third process, isoforming (Fig. 1c), the steel is deformed in the metastable austenite region, but the deformation is continued until the transformation is complete at the intermediate temperature. The steel can then be slowly cooled to room temperature.

The ausforming process needs careful control to be successful and usually involves very substantial deformation. However, the attraction is that with appropriate steels dramatic increases in strength are achieved without adverse effect on ductility and toughness. Typically, a 4,7% Cr, 1.5%Mo, 0.4%V, 0.34%C steel has a tensile strength of about 2000 MPa after conventional quenching and tempering, whereas after ausforming the strength can be over 3000 MPa.

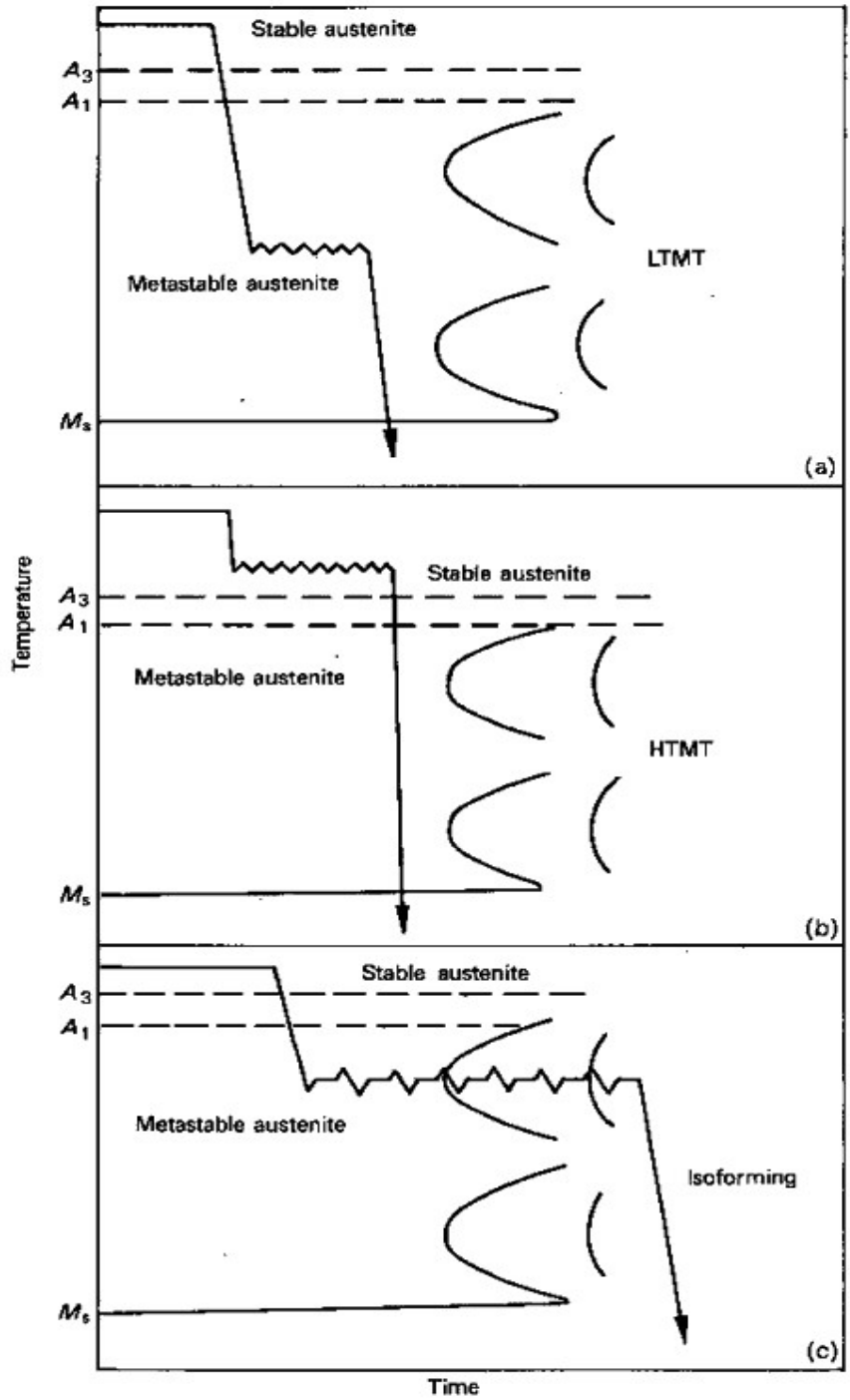


Figure 1. Schematic diagrams of thermochemical treatments:
 a) ausforming-low temperature mechanical treatment;
 b) high temperature mechanical treatment;
 c) isoforming transformation.

Steels, in which austenite transforms rapidly at subcritical temperatures, are not suitable for ausforming. It is necessary to add alloying elements which develop a deep metastable

austenite bay by displacing the TTT curve to longer transformation times. The most useful elements in this respect are chromium, molybdenum, nickel and manganese, and allowance must be made for the fact that deformation of the austenite accelerates the transformation. Consequently, it is necessary to have sufficient alloying element present to slow down the reaction and avoid the formation of ferrite during cooling to the deformation temperature.

Isoforming

The process of isoforming involves deformation of metastable austenite, but the deformation is continued until the transformation of austenite is complete at the deformation temperature (Fig. 1c). This is because the lamellar morphology of pearlite leads to low toughness in ferrite/pearlite steels, the ductile/brittle transition temperature increasing with larger volume fraction of pearlite. However, by applying deformation during the phase transformation, instead of a ferrite/pearlite aggregate, the structure produced consists of fine ferrite subgrains ($\approx 0.5\mu\text{m}$ diameter) with spheroidized cementite particles ($\approx 25\text{nm}$ diameter) mainly located at subgrain triple points.

As in the case of steels for ausforming, the chosen steel must have a suitable TTT diagram. First, it is necessary to be able to deform the austenite prior to transformation, then the transformation must be complete before deformation has ceased. Only modest increases in strength are achieved. However, there can be a very substantial improvement in toughness due to the refinement of the ferrite grain size and the replacement of lamellar cementite by spheroidized particles. However, for significant gains in toughness, deformations in excess of 70% reduction in area are needed. Finally, care must be taken to restrict deformation to temperatures at which the ferrite and pearlite reactions take place as similar deformation in the bainitic region leads to marked reductions in toughness.

High temperature thermomechanical treatments (HTMT)

In high temperature thermomechanical treatments the deformation is carried out in the stable austenite range just above A_{c3} (Fig. 1b), and so can be performed in steels, which do not possess a suitable metastable austenite bay. The steel is then quenched to the martensitic state and tempered at an appropriate temperature. The strengthening achieved arises from austenite grain size refinement, typically from 10-60 μm to 3 μm , but optimum properties are often obtained if recrystallization of the austenite is avoided. As in ausforming strong carbide forming elements are beneficial, which suggests that alloy carbide precipitation occurs in the austenite during deformation. A particular advantage of this process is that optimum

properties can be achieved at modest deformations ($\approx 40\%$) so that deformation can be carried out more readily on existing equipment. The HTMT process does not yield as high strengths as in ausforming but the ductility and fatigue properties are usually superior.

Clearly, HTMT is a variant of controlled rolling. However, it is normally applied to steels with higher alloying contents which can then be transformed to martensite and tempered.

Industrial steels subjected to thermomechanical treatments

Ausforming has provided some of the strongest, toughest steels so far produced, with the added advantage of very good fatigue resistance. However, they usually have high concentrations of expensive alloying elements and must be subjected to large deformations, which impose heavy workloads on rolling mills. Nevertheless, these steels are particularly useful where a high strength to weight ratio is required and where cost is a secondary factor. Typical applications have included parts for undercarriages of aircraft, special springs and bolts.

The 12%Cr transformable steels respond readily to ausforming to the extent that tensile strengths of over 3000MPa can be obtained in appropriate compositions. 0.4C-6Mn-3Cr-1.5Si steel has been ausformed to a tensile strength of 3400 MPa, with an improvement in ductility over the conventional heat treatment. Similar high strength levels with good ductility have been reported for 0.4C-5Cr-1.3Mo-1.0Si-0.5V steel. All of these steels are sufficiently highly alloyed to allow adequate time for substantial deformation in the austenite bay of the TTT curve prior to transformation.

Lecture 37

Heat treatment of some Cu, Al and Ti based alloys

Copper and its alloys

Homogenizing

Homogenizing is applied to dissolve and absorb segregation and coring found in some cast and hot worked materials, chiefly those containing tin and nickel.

Diffusion and homogenization are slower and more difficult in tin bronzes, silicon bronzes and copper nickels than in most other copper alloys. Therefore, these alloys usually are subjected to prolonged homogenizing treatments before hot or cold working operations.

The high-tin phosphor bronzes (above 8% Sn) are noted for extreme segregation. Although these alloys sometimes are hot worked, usual practice is to roll them cold, making it

necessary to first diffuse the brittle segregated tin phase, thereby increasing strength and ductility and decreasing hardness before rolling. These objectives are accomplished by homogenizing at about 760°C.

Annealing

For copper and brass mill alloys, grain size is the standard means of evaluating a recrystallizing anneal. Because many interreacting variables influence the annealing process, it is difficult to predict a specific combination of time and temperature that will always produce a given grain size in a given metal.

Several copper alloys have been developed in which the grain size is stabilized by the presence of a finely distributed second phase. Examples include copper-iron alloys such as and aluminum-containing brasses and bronzes. These alloys will maintain an extremely fine grain size at temperatures well beyond their recrystallization temperature, up to the temperature where the second phase finally dissolves or coarsens, which allows grain growth to proceed.

Generally, two annealed tempers are available: light anneal, which is performed at a temperature slightly above the recrystallization temperature, and soft anneal, which is performed several hundred degrees higher, at a temperature just below the point at which rapid grain growth begins.

When annealing copper that contains oxygen, the hydrogen in the atmosphere must be kept to a minimum to avoid embrittlement. For temperatures lower than about 480°C, hydrogen preferably should not exceed 1%.

Stress Relieving

Stress relieving is aimed to reduce or eliminate residual stress, thereby reducing the likelihood that the part will fail by cracking or corrosion fatigue in service. Parts are stress-relieved at temperatures below the normal annealing range that do not cause recrystallization and consequent softening of the metal.

Residual stresses contribute to this type of failure, which is frequently seen in brasses containing 15% zinc or more. Even higher-copper alloys such as aluminum bronzes and silicon bronzes may crack under critical combinations of stress and specific corroding, and all copper alloys are susceptible to more rapid corrosion attack when in the stressed condition.

Stressed phosphor bronzes and copper nickels have comparatively slight tendencies toward stress-corrosion cracking; these alloys are more susceptible to fire cracking, which is

cracking caused when stressed metal is heated too rapidly to the annealing temperature. Slow heating provides a measure of stress relief and minimizes non-uniform temperature distributions, which lead to thermal stress.

Using a high stress-relieving temperature for a short time is generally considered best for keeping processing time and cost to a practical minimum, even though there is usually some sacrifice in mechanical properties. Using a lower temperature for a longer time will provide complete stress relief with no decrease in mechanical properties. Actually, the hardness and strength of severely cold worked alloys will increase slightly when low stress-relieving temperatures are used.

An additional benefit of a thermal stress relieving is dimensional stability of cold-formed parts. Also, it is often advisable to stress relieve welded or cold formed structures. For these structures, stress-relieving temperature is 85 to 110°C above that used for mill products of the same alloy.

Precipitation Hardening

High strength in most copper alloys is achieved by cold working. Solution treating and precipitation hardening is applied to strengthen special types of copper alloys above the levels ordinarily obtained by cold working.

Examples of precipitation hardening copper alloys include the beryllium coppers, some of which also contain nickel, cobalt or chromium; the copper-chromium alloys; the copper-zirconium alloys; the copper-nickel-silicon alloys and the copper-nickel-phosphorus alloys.

All precipitation-hardening copper alloys have similar metallurgical characteristics: they can be solution treated to a soft condition by quenching from a high temperature, and then subsequently precipitation hardened by aging at a moderate temperature for a time usually not exceeding 3 h.

Beryllium Coppers. Wrought beryllium coppers, can develop wide ranges of mechanical properties, depending on solution treating and aging conditions, on the amount of cold work imparted to the alloy and on whether the alloy is cold worked after solution treating and before aging or is cold worked after aging.

Chromium coppers. Chromium coppers containing about 1% Cr, are solution treated at 950 to 1010°C and rapidly quenched. Solution treating usually is done in molten salt, but may be done in a controlled-atmosphere furnace to prevent surface scaling and internal oxidation.

Solution treated chromium copper is aged at 400 to 500°C for several hours to produce the desired mechanical and physical properties. A typical aging cycle is 455°C for 4 h or more.

Zirconium Copper. Zirconium copper (99.8Cu-0.2Zr) is solution treated at 900 to 925°C, then quenched in water. Time at the solution treating temperature should be minimized to limit grain growth and possible internal oxidation by reaction of zirconium with the furnace atmosphere. Because solution and diffusion of the zirconium occur rapidly at the solution treating temperature, holding at temperature is not required. Aging is done at 500 to 550°C (930 to 1020°F) for 1 to 4 h. If the material has been cold worked, following solution treating, aging temperature may be reduced to 375 to 475°C.

Alpha Aluminum Bronzes. The structure and consequent heat treatability of aluminum bronze varies greatly with composition. Single-phase (alpha) aluminum bronzes, which contain only copper and aluminum (up to about 10% Al), can be strengthened only by cold working. They can be softened by annealing at 425 to 760°C.

Aluminium alloys

Aluminium is a commonly foundry metal. Apart from light weight, the low melting temperature is an advantage. Aluminium-12% silicon alloy is among the most important cast alloys. The advantage is the high fluidity imparted by Si. The Al-Si phase diagram is simply eutectic, with the eutectic temperature of 577°C and the eutectic composition at 12.6% Si. Rapid cooling of the Al-Si alloy refines the eutectic structure.

Heat treating processes for aluminum are precision processes. They must be carried out in furnaces properly designed and built to provide the thermal conditions required, and adequately equipped with control instruments to insure the desired continuity and uniformity of temperature-time cycles. To insure the final desired characteristics, process details must be established and controlled carefully for each type of product.

The general types of heat treatments applied to aluminum and its alloys are:

- Preheating or homogenizing, to reduce chemical segregation of cast structures and to improve their workability
- Annealing, to soften strain-hardened (work-hardened) and heat treated alloy structures, to relieve stresses, and to stabilize properties and dimensions
- Solution heat treatments, to effect solid solution of alloying constituents and improve mechanical properties

- Precipitation heat treatments, to provide hardening by precipitation of constituents from solid solution.

Lecture 38

Heat treatment of Ti and its alloys

Titanium and titanium alloys are heat treated in order to:

- Reduce residual stresses developed during fabrication (stress relieving)
- Produce an optimum combination of ductility, machinability, and dimensional and structural stability (annealing)
- Increase strength (solution treating and aging)
- Optimize special properties such as fracture toughness, fatigue strength, and high-temperature creep strength.

Various types of annealing treatments (single, duplex, (beta), and recrystallization annealing, for example), and solution treating and aging treatments, are imposed to achieve selected mechanical properties. Stress relieving and annealing may be employed to prevent preferential chemical attack in some corrosive environments, to prevent distortion (a stabilization treatment) and to condition the metal for subsequent forming and fabricating operations.

Alloy Types and Response to Heat Treatment

The response of titanium and titanium alloys to heat treatment depends on the composition of the metal and the effects of alloying elements on the α - β crystal transformation of titanium. In addition, not all heat treating cycles are applicable to all titanium alloys, because the various alloys are designed for different purposes.

- Alloys Ti-5Al-2Sn-2Zr-4Mo-4Cr and Ti-6Al-2Sn-4Zr-6Mo are designed for strength in heavy sections.
- Alloys Ti- 6Al-2Sn-4Zr-2Mo and Ti-6Al-5Zr-0.5Mo-0.2Si for creep resistance.
- Alloys Ti-6Al-2Nb-1 Ta-1Mo and Ti-6Al-4V, for resistance to stress corrosion in aqueous salt solutions and for high fracture toughness.
- Alloys Ti-5Al-2.5Sn and Ti-2.5Cu for weldability; and
- Ti-6Al-6V-2Sn, Ti-6Al-4V and Ti-10V-2Fe-3Al for high strength at low-to-moderate temperatures.

Effects of Alloying Elements on α - β Transformation. Unalloyed titanium is allotropic. Its close-packed hexagonal structure (α phase) changes to a body-centered cubic, structure (β -phase) at 885°C (1625°F), and this structure persists at temperatures up to the melting point.

With respect to their effects on the allotropic transformation, alloying elements in titanium are classified as α stabilizers or β stabilizers. Alpha stabilizers, such as oxygen and aluminum, raise the α -to- β transformation temperature. Nitrogen and carbon are also stabilizers, but these elements usually are not added intentionally in alloy formulation. Beta stabilizers, such as manganese, chromium, iron, molybdenum, vanadium, and niobium, lower the α -to- β transformation temperature and, depending on the amount added, may result in the retention of some β phase at room temperature.

Alloy Types. Based on the types and amounts of alloying elements they contain, titanium alloys are classified as α , near- α , α - β , or β alloys. The response of these alloy types to heat treatment is briefly described below.

Alpha and near-alpha titanium alloys can be stress relieved and annealed, but high strength cannot be developed in these alloys by any type of heat treatment (such as aging after a solution beta treatment and quenching).

The commercial β alloys are, in reality, metastable β alloys. When these alloys are exposed to selected elevated temperatures, the retained β phase decomposes and strengthening occurs. For β alloys, stress-relieving and aging treatments can be combined, and annealing and solution treating may be identical operations.

Alpha-beta alloys are two-phase alloys and, as the name suggests, comprise both α and β phases at room temperature. These are the most common and the most versatile of the three types of titanium alloys.

Oxygen and iron levels have significant effects on mechanical properties after heat treatment. It should be realized that:

- Oxygen and iron must be near specified maximums to meet strength levels in certain commercially pure grades
- Oxygen must be near a specified maximum to meet strength levels in solution treated and aged Ti-6Al-4 V
- Oxygen levels must be kept as low as possible to optimize fracture toughness. However, the oxygen level must be high enough to meet tensile strength requirements

- Iron content must be kept as low as possible to optimize creep and stress-rupture properties. Most creep-resistant alloys require iron levels at or below 0.05wt%.

Stress Relieving

Titanium and titanium alloys can be stress relieved without adversely affecting strength or ductility.

Stress-relieving treatments decrease the undesirable residual stresses that result from first, nonuniform hot forging or deformation from cold forming and straightening, second, asymmetric machining of plate or forgings, and, third, welding and cooling of castings. The removal of such stresses helps maintain shape stability and eliminates unfavorable conditions, such as the loss of compressive yield strength commonly known as the Bauschinger effect.

When symmetrical shapes are machined in the annealed condition using moderate cuts and uniform stock removal, stress relieving may not be required. Compressor disks made of Ti-6Al-4V has been machined satisfactorily in this manner, conforming with dimensional requirements. In contrast, thin rings made of the same alloy could be machined at a higher production rate to more stringent dimensions by stress relieving 2 h at 540°C (1000°F) between, rough and final machining. Separate stress relieving may be omitted when the manufacturing sequence can be adjusted to use annealing or hardening as the stress-relieving process. For example, forging stresses may be relieved by annealing prior to machining.

Annealing

The annealing of titanium and titanium alloys serves primarily to increase fracture toughness, ductility at room temperature, dimensional and thermal stability, and creep resistance. Many titanium alloys are placed in service in the annealed state. Because improvement in one or more properties is generally obtained at the expense of some other property, the annealing cycle should be selected according to the objective of the treatment.

Common annealing treatments are:

- Mill annealing
- Duplex annealing
- Recrystallization annealing
- Beta annealing

Mill annealing is a general-purpose treatment given to all mill products. It is not a full anneal and may leave traces of cold or warm working in the microstructures of heavily worked products, particularly sheet.

Duplex annealing alters the shapes, sizes, and distributions of phases to those required for improved creep resistance or fracture toughness. In the duplex anneal of the Corona 5 alloy, for example, the first anneal is near the β transus to globularize the deformed α and to minimize its volume fraction. This is followed by a second, lower-temperature anneal to precipitate new lenticular (acicular) α between the globular α particles. This formation of acicular α is associated with improvements in creep strength and fracture toughness.

Recrystallization annealing and β annealing are used to improve fracture toughness. In recrystallization annealing, the alloy is heated into the upper end of the α - β range, held for a time, and then cooled very slowly. In recent years, recrystallization annealing has replaced β annealing for fracture critical airframe components.

β (Beta) Annealing. Like recrystallization annealing, β annealing improves fracture toughness. Beta annealing is done at temperatures above the β transus of the alloy being annealed. To prevent excessive grain growth, the temperature for β annealing should be only slightly higher than the β transus. Annealing times are dependent on section thickness and should be sufficient for complete transformation. Time at temperature after transformation should be held to a minimum to control β grain growth. Larger sections should be fan cooled or water quenched to prevent the formation of a phase at the β grain boundaries.

Straightening, sizing, and flattening of titanium alloys are often necessary in order to meet dimensional requirements. The straightening of bar to close tolerances and the flattening of sheet present major problems for titanium producers and fabricators.

Unlike aluminum alloys, titanium alloys are not easily straightened when cold because the high yield strength and modulus of elasticity of these alloys result in significant springback. Therefore, titanium alloys are straightened primarily by creep straightening and/or hot straightening (hand or die), with the former being considerably more prevalent than the latter.

Straightening, sizing, and flattening may be combined with annealing by the use of appropriate fixtures. The parts, in bulk or in fixtures, may be charged directly into a furnace operating at the annealing temperature. At annealing temperatures many titanium alloys have a creep resistance low enough to permit straightening during annealing.

Creep straightening may be readily accomplished during the annealing and/or aging processes of most titanium alloys. However, if the annealing/aging temperature is below about 540 to 650°C (1000 to 1200°F), depending on the alloy, the times required to accomplish the desired creep straightening can be extended. Creep straightening is accomplished with rudimentary or sophisticated fixtures and loading systems, depending on part complexity and the degree of straightening required.

Stability. In α - β titanium alloys, thermal stability is a function of β -phase transformations. During cooling from the annealing temperature, β may transform and, under certain conditions and in β alloys, may form a brittle intermediate phase known as ω .

A stabilization annealing treatment is designed to produce a stable β phase capable of resisting further transformation when exposed to elevated temperatures in service. Alpha-beta alloys that are lean in β , such as Ti-6Al-4V, can be air cooled from the annealing temperature without impairing their stability. To obtain maximum creep resistance and stability in the near- α alloys Ti-8Al-1 Mo-1 V and Ti-6Al-2Sn-4Zr-2Mo, a duplex annealing treatment is employed. This treatment begins with solution annealing at a temperature high in the α - β range, usually 25 to 55°C (50 to 100°F) below the β transus for Ti-8Al-1Mo-1V and 15 to 25°C (25 to 50°F) below the α - β transus for Ti-6Al-2Sn-4Zr-2Mo.

Solution Treating and Aging

A wide range of strength levels can be obtained in α - β or β alloys by solution treating and aging. With the exception of the unique Ti-2.5Cu alloy (which relies on strengthening from the classic age-hardening reaction of Ti₂Cu precipitation similar to the formation of Guinier-Preston zones in aluminum alloys), the origin of heat-treating responses of titanium alloys lies in the instability of the high-temperature β phase at lower temperatures.

Heating an α - β alloy to the solution-treating temperature produces a higher ratio of β phase. This partitioning of phases is maintained by quenching; on subsequent aging, decomposition of the unstable β phase occurs, providing high strength. Commercial β alloys generally supplied in the solution-treated condition, and need only to be aged.

Solution treating of titanium alloys generally involves heating to temperatures either slightly above or slightly below the β transus temperature. The solution-treating temperature selected depends on the alloy type and practical considerations briefly described below.

β (Beta) alloys are normally obtained from producers in the solution-treated condition. If reheating is required, soak times should be only as long as necessary to obtain complete

solutioning. Solution-treating temperatures for β alloys are above the β transus; because no second phase is present, grain growth can proceed rapidly.

α - β (Alpha-beta) alloys. Selection of a solution-treatment temperature for α - β alloys is based on the combination of mechanical properties desired after aging. A change in the solution-treating temperature of α - β alloys alters the amounts of β phase and consequently changes the response to aging.

To obtain high strength with adequate ductility, it is necessary to solution treat at a temperature high in the α - β field, normally 25 to 85°C (50 to 150°F) below the β transus of the alloy. If high fracture toughness or improved resistance to stress corrosion is required, β annealing or β solution treating may be desirable. However, heat treating α - β alloys in the β range causes a significant loss in ductility. These alloys are usually solution heat treated below the β transus to obtain an optimum balance of ductility, fracture toughness, creep, and stress rupture properties.

MODEL QUESTIONS

1. If an eutectoid steel is kept at 700°C what change do you expect?
2. What is the limitation of phase diagram?
3. If a piece of steel having 0.8 % carbon has martensitic structure can it be converted to fully pearlite structure by holding it at 700° C?
4. Suggest a method of getting a mixture of Pearlite, Bainite & Martensite in an eutectoid steel.
5. What are the heat treatment methods available for Ti alloys to improve its properties.

REFERENCES

1. Phase Transformations in Metals and Alloys by D. A. Porter and K. E. Easterling, CRC Press.
2. Phase Transformations in Materials by R. C. Sharma
3. Solid State Phase Transformations by Raghavan, PHI.
4. Steel and its Heat treatment by K E Thelning, Butterworth.
5. Heat Treatment by Rajan and Sharma, PHI.
6. Principles of Heat Treatment of Steels, ASM
7. Physical Metallurgy Principles by R. E. Reed-Hill, East West Press.

.....